ministerie van verkeer en waterstaat

koninklijk nederlands meteorologisch instituut

Flux-profile relationships in the nocturnal boundary layer

Pim Bouwman

Technical Reports, TR-130

technische rapporten, TR-130

de bilt, 1990

KNMI

Voorwoord

Dit onderzoek is tot stand gekomen in het kader van mijn afstudeerwerk aan de Technische Universiteit van Delft aan de Faculteit der Technische Natuurkunde. Binnen de sectie Warmtetransport van de vakgroep Transportverschijnselen bestaat de mogelijkheid af te studeren in de fysische meteorologie. Hoogleraar voor deze groep is prof.dr. J.Wieringa en het afstudeerwerk vindt in de regel plaats op het KNMI te De Bilt, waar de student dan de functie van stagiair krijgt toebedeeld.

Vanaf april 1989 tot juni 1990 heb ik dan ook met veel plezier gewerkt op het KNMI. Mijn opdracht was de experimentele bepaling van flux-profiel relaties in de nachtelijke grenslaag. Daartoe werd te Cabauw een relatief eenvoudig experiment opgezet, waardoor van 18 juli tot 11 oktober continu kon worden gemeten. De rest van de tijd werd besteed aan voorbereiding, analyse van de metingen en verslaggeving.

Aan het project werd meegewerkt door Wim Monna, Gerard van der Vliet en door Fred Bosveld, die mijn begeleider was en de in juli naar het ECMWF in Engeland vertrokken Anton Beljaars verving. Dit alles terwijl Jon Wieringa van afstand een oogje in het zeil hield. Verder was het personeel van de meetmast in Cabauw bij het project betrokken. In het bijzonder Frans Renes en Leo Schiks hebben daar veel werk verzet.

Al deze mensen, die steeds tijd voor me konden vrij maken om vragen te beantwoorden, artikelen op te zoeken, software te verstrekken of om met mij in discussie te gaan, wil ik hartelijk bedanken. Ik denk dat ik wat betreft mijn begeleiding, vergeleken met andere studenten aan de TU benijdenswaardig veel aandacht heb gekregen. Als laatste wilde ik Casper Hofman bedanken, die mij altijd bijstond in tijden van computernood.

Dit verslag is geschreven in het Engels om een groter publiek te bereiken, dat klinkt misschien pretentieus, maar de micrometeorologische wereld is, zoals het woord al zegt, klein en binnen Nederland zijn we dus snel uitgepraat.

Tot slot ben ik altijd bereid om vragen te beantwoorden naar aanleiding van dit verslag. Mijn adres is Peperstraat 4^{II}, 1011 TL Amsterdam. Verder kunnen eventueel gegevens worden verkregen bij prof. dr. J. Wieringa of bij Drs. F. Bosveld op het KNMI, Postbus 201, 3730 AE, De Bilt.

Pim Bouwman, 1 juni 1990

Abstract

For three months continuous turbulence measurements were made to obtain flux profile relationships in the nocturnal boundary layer at Cabauw, the Netherlands. A sonic anemometer and a fast thermocouple were used for flux computations by the eddy correlation technique. The routine measurements along the 213m meteorological mast of the KNMI provided profiles for windspeed and temperature as well as additional micro meteorological information. Data reduction was performed on-line. Monin-Obukhov similarity functions were obtained using the local scaling approach in the surface layer.

The results indicate that the slopes (β) of the similarity functions ($\varphi=\alpha+\beta z/L$, $\beta=3$) found are much lower than the slopes ($\beta=10$) found by Cuypers (1987) using Nieuwstadt's (1984) data.

Terrain inhomogeneities seem to cause a translation of the similarity functions along the y-axis, they do not change the slope.This is because the linear part of the similarity functions represents the smaller eddies, who have a short lifetime and are produced and dissipated locally. When using local scaling this implies that the same relation as for unperturbed measurements should be found.

Samenvatting

Gedurende drie maanden werden in Cabauw in Nederland turbulentie metingen gedaan om de empirische flux-profiel relaties in de nachtelijke grenslaag te bepalen. Om de fluxen te bepalen met de eddie correlatie techniek werden een sonische anemometer en een snel-respons thermokoppel gebruikt. Temperatuur- en windprofielen werden verkregen uit het routine bestand van de 213 meter hoge meteorologische meetmast van het KNMI. Informatie over andere micrometeorologische grootheden werd hier eveneens verkregen. Er werd aan on-line data reductie gedaan. Door lokale schaling toe te passen in de oppervlaktelaag werden de Monin-Obukhov similariteits functies bepaald.

De gevonden richtingscoëfficiënten (β) van de similariteitsfuncties ($\varphi=\alpha+\beta z/L$, $\beta=3$) zijn veel lager dan die door Cuijpers ($\beta=10$) (1987) uit Nieuwstadt's (1984) metingen zijn gevonden.

Door stroomopwaartse terrein inhomogeniteiten verandert niet de richtingscoëfficiënt van de similariteitsfuncties, maar verschuift de totale kurve. Alleen de constante verandert. Dit is omdat het lineaire gedeelte van de similariteits functies de kleinere wervels vertegenwoordigt. Deze kleinere wervels "leven" kort, ze worden lokaal geproduceerd en gedissipeerd. Als lokale schaling wordt toegepast vinden we zo voor gestoorde en ongestoorde gebieden dezelfde relatie.

摘要

为了获得在荷兰 Cabauw 地区的夜间边界层速度廓线，我们进行了3个月的连续湍流观测，利用一个声学风速仪和一个快速温度电偶的观测资料，我们用涡度相关法来计算通量值。在 Cabauw 的 KNMI 塔来的气象观测塔的常规观测资料为我们提供了风速和温度廓线及其它有关资料。观测资料是由计算机同时处理的。我们用边界层局地尺度分析法来获得相似函数。我们获得的相似函数（$\Phi = \alpha + \beta\zeta/L$）的斜率比 Cuypers (1987) 用 Nieuwstadt (1984) 的资料获得的斜率要大的多。

地表不均匀性将使相似函数有一个平行的位移，但不改变相似函数的斜率，这是由于相似函数的线性部分代表大尺度湍流，它们的时间尺度很长，并且在部高产生并消亡。所以，当我们用局地尺度分析无扰动观测资料时，相似函数的斜率保持不变。代表大尺度湍流的相似函数常数部分有了变化，这是由于局地地形及长时间尺度湍流造成的，因为它们有较长的记忆。

Contents

1. Introduction

The lowest part of our atmosphere is called the atmospheric boundary layer, abbreviated ABL. Transport processes within the ABL are dominated by turbulence. Solar heating causes thermals of warm air to rise until they are stopped by the inversion, a positive temperature gradient that causes the thermal to be accelerated downwards. Non-turbulent air from above the inversion becomes turbulent by entrainment. The boundary layer thus grows during the day. When the sun ceases to heat the surface of the earth, the radiation balance is reversed and the surface is cooled by emission of long wave radiation. This generates a shallow layer with a positive temperature gradient: the ground inversion. The layer grows during the night and is called the Nocturnal Boundary Layer (NBL). It reaches a maximum height of about 200m under clear sky conditions (strong radiative cooling). The daytime inversion weakens and slowly descends due to the decrease of entrainment. After several hours the daytime inversion is hard to distinguish from the nocturnal one. This makes it hard to define the height of the nocturnal boundary layer. The most practical definition is that the temperature gradient becomes zero. Other NBL height definitions can be found in Stull (1988, ch. 12).

The downward (positive) heat flux causes turbulence produced by wind shear to be suppressed. The balance between mechanical production and buoyancy consumption varies from case to case, creating stable boundary layers that range from being well mixed to non-turbulent with short burst of turbulent activity (intermittency). Other phenomena that complicate modelling the nighttime boundary layer are low-level jets (Thorpe, 1977), azimuthal meandering (Hanna, 1983) and gravity waves (e.g.,Finnigan et al., 1984).

Previous studies of the nocturnal boundary layer were therefore restricted to 'ideal' circumstances, e.g., stationary, horizontally homogeneous, fully turbulent stable boundary layers over flat terrain. Of course in reality these conditions are hardly ever met. Atmospheric measurements are far from ideal. Many physical processes are simultaneously at work, while the idealized models focus on the dominant processes only. In a laboratory we can repeat measurements infinitely, making sure the circumstances are exactly the same every time. This is impossible in the atmosphere, the atmosphere is non-reproducible. We thus expect our data to scatter due to the atmospheric statistics, apart from the scatter induced by the limits of equipment (as in a laboratory experiment) and by the influence of unknown parameters.

Nevertheless there is reasonable agreement about the general picture of the nocturnal boundary layer. Continuing studies seem unlikely to alter our basic picture (Mason & Derbyshire 1990). Still there was reason to perform another experiment, investigating flux-profile relationships in Cabauw.

Flux-profile or flux-gradient relationships have to be established empirically. The Monin-Obukhov similarity theory relating surface layer mean vertical gradients of wind speed, temperature and specific humidity to the corresponding surface turbulent fluxes,

determines relationships up to the specification of universal similarity functions, φ, of z/L only. (z height above the surface, L Obukhov length.) The general character of the similarity functions is known over a limited range of stability conditions, centered on neutral, but their specification for more extreme stability conditions still demands attention. For $z/L < 0.5$, φ is found to be $1+\beta(z/L)$, with β a "constant" with values between 0 and 10 (cf.§5.2.2).

The Monin-Obukhov similarity theory (Monin & Obukhov, 1954) assumes constant fluxes in the surface layer, where $z<<|h|$, h is the NBL height.. This reduces its validity to typically the lowest fifty meters of the boundary layer. Under extreme stability conditions (z/L is large) this may only be a few meters. Nieuwstadt (1984) and Sorbjan(1986) therefore propose a so-called local similarity theory to be used above the surface layer. Turbulence there scales with height and local values of the fluxes. To compute wind profiles Holtslag (1984) ignores their approach, and applies surface layer similarity theory up to two hundred meters with reasonable results. The similarity functions which Cuijpers (1987) finds from the data, upon which Nieuwstadt (1984) bases his local scaling approach, differ significantly from other literature.(§2.3) He finds $\beta=10$ for $z/L<0.5$ and $\beta=5$ for $z/L>0.5$. Apart from that the turbulent kinetic energy budget shows a loss.

Perturbations in the upstream surface conditions in Cabauw cause wind profiles in which two logarithmic parts can be distinguished. Beljaars (1982, Beljaars et al, 1983) developed a model that shows that flux-profile relationships for strongly perturbed areas will deviate from those found over uniform terrain. The rough to smooth transition for westerly winds in Cabauw causes an increase of the shear stress with height and fluxes that are not adapted to the profiles(Beljaars, 1982). The model only works for the neutral boundary layer.

The experiment performed here investigates the flux-profiles for the different sectors in Cabauw by measuring both profiles and fluxes. Moreover the dataset contains information to check the turbulent kinetic energy budget, this will be done in the future, This report is about the first subject only. The main purpose is to determine the value for β in Cabauw for disturbed and undisturbed sectors.

2 Theory

2.1 The Reynolds equations

A common approach for studying turbulence is to split variables into a mean part and a fluctuating part. The perturbation or fluctuating part represents the turbulence effect that is superimposed on the mean variable. Such variables are: wind, temperature, humidity or concentrations of pollutants. Turbulence can be visualized as consisting of irregular swirls of motion called eddies (Stull 1988). Turbulence consists of many different size eddies superimposed on each other.
The splitting technique (Reynolds decomposition) can be applied to the equations describing the flow of fluids in the atmosphere: the Navier-Stokes equation, the continuity equation for incompressible fluids, the equation for the conservation of heat and the equation of state:

$$\frac{\partial u_i}{\partial t} + u_j \frac{\partial u_i}{\partial x_j} = -\frac{1}{\rho}\frac{\partial p}{\partial x_i} + f_c \varepsilon_{ij3} u_j + \upsilon \frac{\partial^2 u_i}{\partial x_j^2} - g\delta_{i3} \qquad (2.1)$$

$$\frac{\partial u_i}{\partial x_i} = 0 \qquad (2.2)$$

$$\frac{\partial \theta}{\partial t} + u_j \frac{\partial \theta}{\partial x_j} = K \frac{\partial^2 \theta}{\partial x_j^2} - \frac{1}{\rho c_p}\frac{\partial Q_j}{\partial x_j} \qquad (2.3)$$

$$p = \rho R T \qquad (2.4)$$

Here u_i denotes the i-component of windspeed (i=1,2,3 for u,v and w in the x, y and z-direction respectively, with z vertical). We use the Einstein summation notation, ε_{ijk} is the alternating unit tensor and δ_{ij} the Kronecker Delta. ρ is the density of air, υ the kinematic viscosity, p is the pressure, g the gravitational acceleration, f_c is the coriolis parameter ($1.15\ 10^{-4} s^{-1}$). θ is the potential temperature, the temperature of an air parcel brought to a reference height adiabatically. To first order θ can be approximated by (see A.4):

$$\theta = T + \frac{g}{c_p} z \qquad (2.5)$$

Finally K is the thermal diffusivity, c_p the specific heat at constant pressure, Q the net radiation, R the gas constant and T the temperature. For a detailed derivation of this and what follows see for example Businger (1982).

We split the variables into mean and turbulent part:

$$A = \overline{A} + A' \tag{2.6}$$

For turbulence that is both homogeneous and stationary the overbar denotes either time, spatial or ensemble average. The notation in Dirac brackets $< A >$ is also used for averages. A' is the fluctuation with $\overline{A'} = 0$ by definition.

The Boussinesq approximation (Batchelor 1967) allows us to substitute temperature fluctuations in place of density fluctuations:

$$\frac{\rho'}{\overline{\rho}} = -\frac{\theta_v'}{\overline{\theta_v}} \tag{2.7}$$

with θ_V the virtual potential temperature: the potential temperature dry air must have to equal the density of moist air at the same pressure. For unsaturated air this yields:

$$\theta_v = \theta(1 + 0.61q) \tag{2.8}$$

with q the specific humidity (g/kg).

Now we can apply Reynolds decomposition and the Boussinesq approximation to equations 2.1 to 2.3 and take the average:

$$\frac{\partial \overline{u_i}}{\partial t} + \overline{u_j}\frac{\partial \overline{u_i}}{\partial x_j} = -\frac{1}{\overline{\rho}}\frac{\partial \overline{p}}{\partial x_i} + f_c \varepsilon_{ij3}\overline{u_j} - g\frac{\theta_v'}{\overline{\theta_v}}\delta_{i3} - \frac{\partial}{\partial x_j}\left(\overline{u_i' u_j'}\right) \tag{2.9}$$

$$\frac{\partial \overline{u_i}}{\partial x_i} = 0 \tag{2.10}$$

$$\frac{\partial \overline{\theta}}{\partial t} + \overline{u_j}\frac{\partial \overline{\theta}}{\partial x_j} = -\frac{\partial}{\partial x_j}\left(\overline{\theta' u_j'}\right) \tag{2.11}$$

For the mean state hydrostatic equilibrium is assumed.The radiation and diffusion terms are neglected. The diffusion terms are much smaller than the turbulent (eddy) diffusivities. The radiation term is important in the first two meters near the surface only, and very small in the surface layer.

For the horizontal pressure gradient terms we substitute the geostrophic wind definition:

$$\vec{u}_G = \left(-\frac{1}{\rho f_c}\frac{\partial p}{\partial y}, \frac{1}{\rho f_c}\frac{\partial p}{\partial x}, 0\right) = \left(U_g, V_g, 0\right) \tag{2.12}$$

to obtain the so-called Reynolds equations:

$$\frac{\partial \overline{U}}{\partial t} + \overline{u_i}\frac{\partial \overline{U}}{\partial x_i} = f_c\left(V - V_g\right) - \frac{\partial}{\partial z}\left(\overline{u'w'}\right) \qquad (2.13)$$

$$\frac{\partial \overline{V}}{\partial t} + \overline{u_i}\frac{\partial \overline{V}}{\partial x_i} = -f_c\left(U - U_g\right) - \frac{\partial}{\partial z}\left(\overline{v'w'}\right) \qquad (2.14)$$

$$\frac{\partial \overline{\theta}}{\partial t} + \overline{u_i}\frac{\partial \overline{\theta}}{\partial x_i} = -\frac{\partial}{\partial z}\left(\overline{\theta'w'}\right) \qquad (2.15)$$

The left hand terms represent storage and advection, the first right hand term in 2.13 & 2.14 represent body forcings, the correlation terms in 2.13 to 2.15 are related to the Reynolds stress, τ, and the sensible heat flux, H, in a coordinate system aligned with the mean wind as follows:

$$\tau = -\rho\left(\overline{u'w'}\right) \qquad (2.16)$$

$$H = -\rho c_p\left(\overline{\theta'w'}\right) \qquad (2.17)$$

From now on we will refer to them as the turbulent momentum flux and the turbulent heat flux, as they represent the transport of momentum and heat by turbulence. Or in short: momentum and heat flux.

The surface values of the momentum flux and the heat flux are usually defined as:

$$-\left(\overline{u'w'}\right)_s = u_*^2 \qquad (2.18)$$

$$-\left(\overline{\theta'w'}\right)_s = u_*\theta_* \qquad (2.19)$$

The friction velocity, u_*, is a surface layer velocity scale; θ_* has no special name, but is a surface layer temperature scale.

2.2 Turbulent kinetic energy budget and scaling.

Multiplying the Navier-Stokes equation with u_i gives us an equation for the kinetic energy. Averaging and subtracting it from its original yields the Turbulent Kinetic Energy (TKE) budget equation (see for example Stull,1988). To simplify the picture, we assume horizontal homogeneity and neglect subsidence, furthermore we choose the coordinate system aligned with the mean wind (<V>=0). We obtain the following equation:

$$\underset{\text{I}}{\frac{\partial \bar{e}}{\partial t}} = \underset{\text{II}}{\frac{g}{\bar{\theta}_v}\left(\overline{w'\theta_v'}\right)} \underset{\text{III}}{-\left(\overline{u'w'}\right)\frac{\partial \bar{u}}{\partial z}} \underset{\text{IV}}{-\frac{\partial}{\partial z}\left(\overline{w'e} + \frac{1}{\bar{\rho}}\overline{w'p'}\right)} \underset{\text{V}}{-\varepsilon} \qquad (2.20)$$

The turbulent kinetic energy is defined as:

$$\bar{e} \equiv 0.5\left(\overline{u'^2} + \overline{v'^2} + \overline{w'^2}\right) \qquad (2.21)$$

In equation 2.20 term I represents storage of energy, term II is the buoyant production or consumption, term III is the shear production or consumption. Term IV represents the internal redistribution of energy, it is sometimes called the flux-divergence term. Term V represents the conversion of turbulence into heat, the viscous dissipation ε, which can be approximated by (Tennekes and Lumley, 1972):

$$\varepsilon = 15\nu\overline{\left(\frac{\partial u'}{\partial z}\right)^2} \qquad (2.22)$$

for isotropic turbulence.Turbulence will be generated by shear and at daytime also by buoyancy, there is energy transfer from large eddies to small eddies, driven by vortex stretching. When the eddies reach the molecular diffusion scales, they will be dissipated by viscous friction.(Tennekes & Lumley, 1972). This process is called the energy cascade.

The ratio of terms II and III defines the flux-Richardson number:

$$Ri_f = \frac{\text{buoyant production / consumption}}{-\text{shear production / consumption}} = \frac{\frac{g}{\bar{\theta}_v}\left(\overline{w'\theta_v'}\right)}{\left(\overline{u'w'}\right)\frac{\partial \bar{u}}{\partial z}} \qquad (2.23)$$

The negative sign in term III is dropped by convention. When $Ri_f<0$ the flow is turbulent, when $Ri_f>1$ the flow *becomes* laminar. For values between zero and one the state depends on whether the flow was turbulent or laminar before Ri_f got this value.

For the situation of zero heat fluxes or neutral stability it is easy to derive the logarithmic wind profile with the mixing length theory (Stull,1988):

$$u(z) = \frac{u_*}{\kappa}\ln\left(\frac{z}{z_0}\right) \qquad (2.24a)$$

where κ is the von Karman constant (0.4) and z_0 the aerodynamic roughness length, the

height at which the windspeed becomes zero. Typical values for the roughness length in Cabauw can be found in table 3.2. The roughness length is a measure for the effectiveness of momentum destruction by the surface roughness elements.

In the neutral surface layer turbulence is mainly produced by wind shear. This gives us the idea of non-dimensionalizing the TKE equation with the value of the shear production term III under neutral conditions. With $\frac{\partial \bar{u}}{\partial z} = \frac{u_*}{\kappa z}$ and the definition for the friction velocity (2.18) we see that:

$$-\left(\overline{u'w'}\right)_s \frac{\partial \bar{u}}{\partial z} = -\frac{u_*^3}{\kappa z} \qquad (2.24b)$$

under neutral conditions.Multiplying the TKE equation with $-\frac{\kappa z}{u_*^3}$ assuming stationarity and including only the terms II, III and V yields:

$$-\frac{\kappa z}{u_*^3}\frac{g}{\bar{\theta}_v}\left(\overline{w'\theta_v'}\right) + \frac{\kappa z}{u_*^3}\left(\overline{u'w'}\right)\frac{\partial \bar{u}}{\partial z} + \frac{\kappa z}{u_*^3}\varepsilon = 0 \qquad (2.25)$$

In this nondimensional form term II is assigned the symbol ξ:

$$\xi = \frac{z}{L} \text{ with } L = \frac{-\bar{\theta}_v u_*^3}{\kappa g\left(\overline{w'\theta_v'}\right)_s} \qquad (2.26)$$

L is the Obukhov length. Obukhov (1946) showed that ξ contains all the relevant scaling parameters for the surface layer where the fluxes are constant with height. The surface layer is typically 10% of the ABL-height.

When $\xi > 0$ the surface layer is statically stable, when $\xi < 0$ the surface layer is unstable. When $L = \infty$ and thus $\xi = 0$, we have the neutral stability situation.

Term III is called the dimensionless wind shear:

$$\varphi_m = \frac{\kappa z}{u_*}\frac{\partial \bar{u}}{\partial z} \qquad (2.27)$$

In a neutral surface layer we see that $\varphi_m = 1$ by definition.

By analogy we can define a dimensionless potential temperature gradient, and a dimensionless dissipation:

$$\varphi_h = \frac{\kappa z}{\theta_*}\frac{\partial \bar{\theta}}{\partial z} \qquad (2.28)$$

$$\varphi_\varepsilon = \frac{\kappa z}{u_*^3}\varepsilon \qquad (2.29)$$

From a dimension analysis Monin and Obukhov (1954) concluded that the non dimensionalized gradients and other turbulence parameters can be functions of ξ, the dimensionless height, only:

$$\varphi_m\left(\frac{z}{L}\right)=\frac{\kappa z}{u_*}\frac{\partial \bar{u}}{\partial z} \tag{2.30}$$

$$\varphi_h\left(\frac{z}{L}\right)=\frac{\kappa z}{\theta_*}\frac{\partial \bar{\theta}}{\partial z} \tag{2.31}$$

We already mentioned the fact that $\varphi_m(0)=1$ by definition.If we assume that the exchange coefficients for heat and momentum are equal, also $\varphi_h(0)=1$[1]. The similarity functions φ_h and φ_m have to be found empirically.

The governing equations can be solved analytically only by means of closure hypotheses. A first order closure hypothesis is:

$$-\left(\overline{u'w'}\right)=K_m\frac{\partial \bar{u}}{\partial z} \tag{2.32}$$

$$-\left(\overline{w'\theta_v'}\right)=K_h\frac{\partial \bar{\theta}}{\partial z} \tag{2.33}$$

Here $K_{m,h}$ are the exchange coefficients for momentum and heat. The equations say that transport is always downward if there is a positive gradient. The closure hypothesis makes it possible to eliminate the eddy correlation terms in the Reynolds equations and thus solve them. In practice the assumptions made in closure hypotheses restrict us. The coefficients $K_{m,h}$ for example are also dependent on stability.

Therefore the similarity approach is used to gain better understanding of the physics behind the turbulent atmosphere. Dimensionless groups are formed by choosing "the right" scaling parameters. If chosen well, the similarity relations describe the problem uniquely. The relations can then be found by measuring all the parameters in an experiment. In Monin-Obukhov similarity theory we assume that turbulence scales with height, and with the turbulent surface fluxes.

The Monin-Obukhov similarity theory is now the most widely accepted approach for relating surface layer mean vertical gradients to the surface turbulent fluxes The success though didn't really ameliorate our knowledge of the governing physics. All we can say is that we have found all the relevant scaling parameters. For the rest, we can predict situations in which the same variables play the principal parts and we have a framework within which we can continue to develop our thoughts on the physics.

Monin-Obukhov similarity theory is valid in the surface layer only. Above the

[1] One of the problems here is that we have a zero heat-flux.

(nocturnal) surface layer the turbulence scales with height and the *local* fluxes. This is called local scaling, a similarity approach developed by Nieuwstadt (1984). He defines a local Obukhov length :

$$\Lambda = \frac{-\overline{\theta_v}\left(\overline{u'w'}\right)^{3/2}}{\kappa g\left(\overline{\theta_v'w'}\right)} \qquad (2.34)$$

This local Obukhov length becomes equal to L in the surface layer. To obtain useful information Nieuwstadt had to assume profiles for the shear stress and the heat flux. The assumptions are rather arbitrary, but necessary: we don't know the values for the fluxes at different heights, we can only measure them.

For large positive values of z/Λ or z/L we expect the dependence on z to disappear. The eddies no longer feel the presence of the surface, because they are smaller. This is because there is less energy input in the stable boundary layer. Negative buoyancy suppresses turbulence. The disappearance of the dependency on z is called z-less stratification. (Wyngaard 1973). If we assume:

$$\varphi_m(\xi) = 1 + \beta\xi \qquad (2.35)$$

With β the slope, then for $\beta\xi >> 1$, we expect $\varphi_m(\xi) = \beta\xi$ and thus z-less stratification; we can divide both sides by z. To obtain dimensionless functions, L or Λ is brought to the left hand side to obtain :

$$\frac{\kappa\Lambda}{u_*}\frac{\partial\bar{u}}{\partial z} = \text{constant} \text{ and } \frac{\kappa\Lambda}{\theta_*}\frac{\partial\bar{\theta}}{\partial z} = \text{constant} \qquad (2.36)$$

The large values for the stability parameter are usually found for large values of z. At lower levels, ξ-values larger than 2 hardly have significance. The turbulent fluctuations are then of the order of the noise intensity of the measuring tools. The eddies are too small to be resolved by the instruments.

Hicks (1976) found β=0.74 for ξ >10 in the surface layer from measurements performed in Hay in 1967 (Carson 1977). As z is still included in the scaling this means that the constant in (2.35) becomes 0.74 for very stable situations. But as stated before, these large values for z/L cannot be taken too seriously at lower levels.

Nieuwstadt (1984) already finds z-less stratification for z/Λ>1. This is rather low: for β between 3 and 10 the condition that $\beta\xi >> 1$ is not really satisfied.

It is clearly debatable to what extent we can adopt the Monin-Obukhov similarity hypothesis beyond the fully turbulent, slightly stable regime. The fluxes may not only be discontinuous, but also not constant with height.(This is no problem in the local scaling approach.) The importance of the radiative transfer may play an important role in the development of the stable layer under very stable conditions. In such circumstances

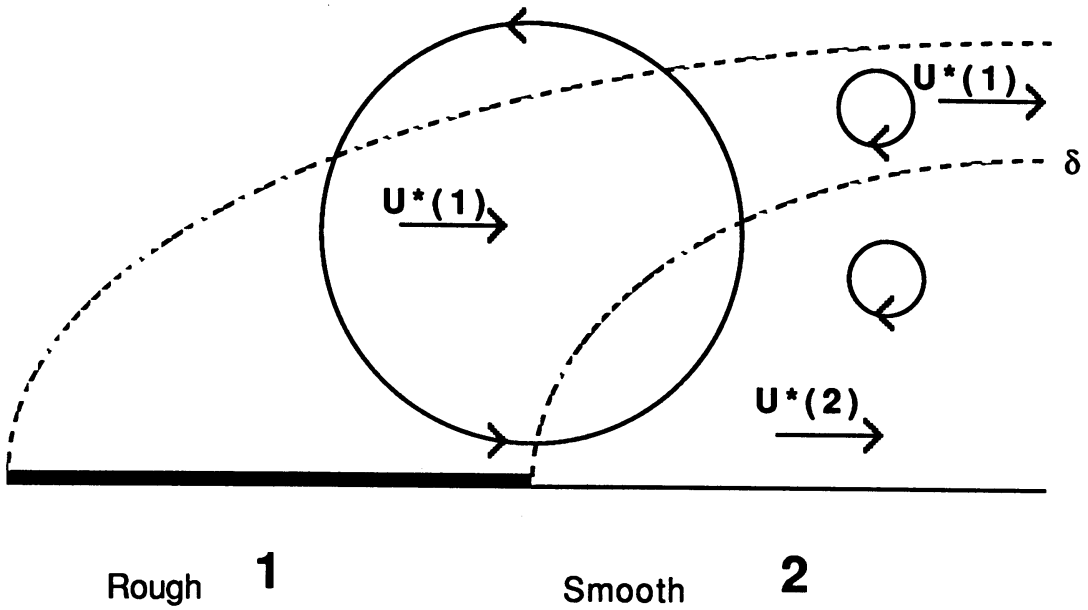

fig. 2.1 Due to a change in surface features, an internal boundary layer, with height δ, develops. Eddies of different sizes scale differently, depending on their location.

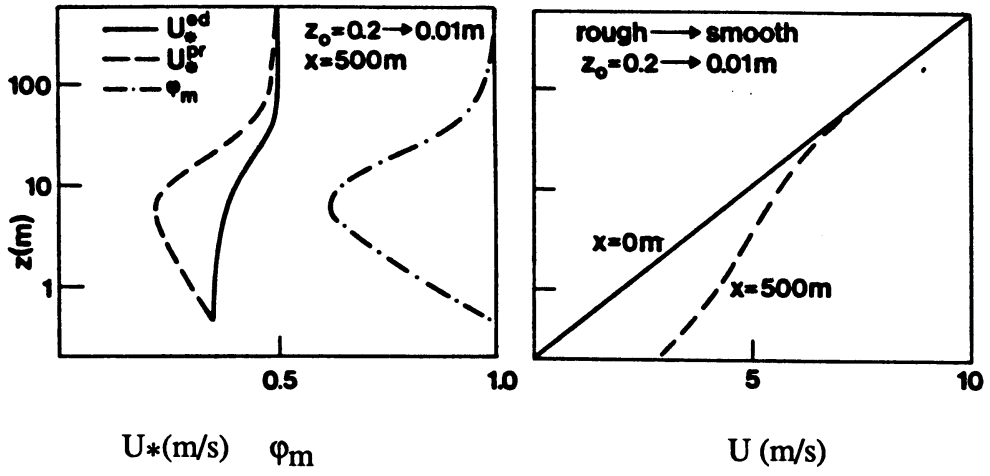

fig 2.2.a Model prediction of the dimensionless shear, the local friction velocity (U_*^{ed}) and the friction velocity derived from the profile assuming φ_m=1 at x= 500m, the fetch.

fig 2.2.b Computed velocity profiles upwind (x=0m) and downwind (x=500m) of a roughness change.(both a&b are from Bosveld & Beljaars, 1987)

scaling with the surface Obukhov length may have little or no relevance.

2.3 Terrain inhomogeneities

The air that is modified by the flow over a different surface is called an internal boundary layer. It forms due to a change in surface roughness or surface heat flux within an existing boundary layer that still has the features of the terrain upwind. The distance downwind from the change in surface features is called fetch. To make sure the profiles and fluxes are locally determined it is desirable to measure far enough downwind so that the depth of the internal boundary layer, δ, is greater than the measuring height. See fig. 2.1. Above the internal boundary layer the flow is determined by the upstream surface conditions, while below there is a gradual adjustment to the new surface roughness (as a function of fetch and stability). The layer between the adjusted layer and the external layer is called the transition layer.

Turbulent fluctuations are a result of contributions of large and small eddies. Under neutral conditions all sizes will be present. Large eddies evolve slower than small eddies. A change in surface features will therefore not influence the large eddies. Small eddies have smaller time scales and respond to the "local" roughness and scale with the local u_*, which depends on the height z above the surface.

Beljaars et al.(1987) developed a model for the neutral case that describes the downwind evolution of a flow. The model includes advective terms, resulting in a kink in the log-wind profile. They also find an increasing u_* with height for a rough to smooth transition. In the homogeneous case the fluxes are independent of height near the surface. In fig 2.2 we see the results for a rough to smooth transition of the model for the wind profile, the friction velocity u_* and the dimensionless windshear..

We see that due to the decrease in friction the windspeed increases near the surface. The profile higher up still feels the friction of the upwind terrain. The windspeed there is thus lower than the windspeed we obtain by extrapolating the surface log-wind profile upward. Consequently the matching of the two profiles (in the transition layer) results in a kink.

We also see a minimum in the dimensionless wind shear profile $\varphi_m(0) = \varphi_{m0}(z)$: $\varphi_{m0}(10) \approx 0.7$. This phenomenon is also reported by others, Schotanus (1982) finds that the ratio between the friction velocities at 20m and 3m under near neutral conditions is about 1.4 for the disturbed sectors (north-westerly and southerly winds) in Cabauw. See also Peterson (1969a): for a rough to smooth transition the flow is accelerated, due to the decreased stress. The gradient however responds much slower, so that we have a smaller dimensionless windshear in this case.

3. Measuring fluxes and profiles

3.1 Considerations

To obtain flux-profile relationships we need to know profiles of windspeed, temperature and humidity and we need to know the fluctuating components of these quantities to obtain the necessary fluxes.

The structure of the surface layer can be characterized by using averaging intervals of 30 minutes. This is because the time scale of 30 minutes roughly coincides with the spectral gap (between 30 and 90 minutes (Stull, 1984)) separating turbulence from synoptic and diurnal changes.The Kansas experiments show that 1 hour is the minimum averaging time needed for stable flux estimates between 5 and 20m (Kaimal 1975) For neutral stability the characteristic time scale for turbulent fluctuations is of the order z/U, where z is the measuring height and U the mean wind velocity.This yields a timescale that is typically several seconds. To obtain stable fluxes the averaging interval should be much larger, typically a hundred times. This yields averaging times between 10 minutes and an hour. For stable stratification, the timescales are smaller, so that the averaging intervals can even be smaller than 10 minutes For z/L=1 Kaimal (1972) shows that the peak frequency in the w-spectrum is twice the peak frequency of z/L=0. So 5 minutes is the minimum averaging time. We considered 1 hour too long, because then diurnal variations would be included too much for higher stabilities.To remove influences from trend we used 10 minute intervals and then derived 30 minute averages, resulting in 48 values for all variables per day.

To measure fluxes we need fast responding sensors. If we assume that eddies scale with the height above the surface, then we can see that there is a relation between the measuring height and the minimum wavelength we should "see". Schotanus (1982) finds a minimal wavelength:

$$\lambda_{min} = z / 3, \qquad (3.1)$$

where z is the measuring height. Spectral losses by line averaging (e.g. the sonic) can be described by the filter function F:

$$F(d,\lambda) = \frac{\sin(\pi d / \lambda)^2}{(\pi d / \lambda)^2}, \qquad (3.2)$$

where d is the line along which we average. Spectral losses become significant for $\lambda < 2\pi d$ (F=0.92). This yields a minimum height at which useful measurements can be made (Kaimal 1975):

$$z_{min} = 6\pi d. \qquad (3.3)$$

The samples used for the ten minute averages are obtained by sampling at a frequency much lower than the frequencies of the small scale structures. The sampling frequency is typically 1Hz. The actual measurement with a datalogger (section 3.2) however has an integration time of 250 microseconds per sample. Kaimal (1975) shows that 600 of these instantaneous samples (during 10 minutes) give the same averages and standard deviations as application of the statistic definitions on the analog signals.

3.2 Summary of used instruments

The instruments used are given in table 3.1:

parameter	*instrument*	*measuring height*
turbulence	sonic anemometer	11.4m
	fast thermocouple	11.4m
wind speed	propeller vane	5,10,20,40,80,120,160 200m
wind direction	propeller vane	10,20,40,80,120,160, 200m
temperature	ventilated thermocouples	0.6,2,10,20,40,80,120, 160,200m
ABL-height	acoustic sounder	

table 3.1 instruments and measurement heights

Apart from the instruments for the turbulence measurements all the instruments mentioned are provided by the Cabauw tower. The wind speed at 5m is added to the routine measurements to obtain additional surface layer information.

3.3 Instruments for profile measurements and additional information

In Cabauw a continuous measuring program provides data on the mean vertical profiles up to 200m of wind speed, wind direction, temperature, humidity and visibility. In addition various radiation components, soil heat flux, soil temperature, precipitation and mixing height are measured (Monna and van der Vliet 1987).

The temperature profile is determined by measuring temperature differences between all successive levels along the mast with Cu-Co thermocouples. At both ends of the chain the absolute temperature is measured using ice-water baths for reference. A precision of 0.06K can be obtained this way. The sensors are ventilated and double shielded (Slob 1978).

For humidity measurements wet bulb sensors, measuring a wet-bulb profile, are

positioned close to the dry sensors. The design is essentially the same for both wet and dry bulb sensors.For the water supply (constant rate) peristaltic pumps are used.

Wind speed and wind direction are measured using Gill 8002DX propeller vanes. The vanes are slightly modified by the KNMI to improve its resistance against the Dutch humid climate. The vane has a response length of 2.2m, a damping ratio of 0.40 and damped wavelength of 3.8m (Monna and Driedonks 1979). In practice a precision of 3% in wind speed and 1.5 degrees in azimuth can be reached.

All the instruments on the Cabauw tower are calibrated by the KNMI calibration laboratory.(see B.4)

The acoustic sounder scans the boundary layer with sound pulses. Acoustic waves are reflected when there is a sudden change in temperature (e.g., inversions). Echoes of sound pulses are displayed on a recorder. It gives an indication of the boundary layer height up to 500m.(For a detailed description see Parry et al, 1975) The recordings were used to check nights where strange data occurred.

3.4 Instruments for turbulence measurements

A sonic anemometer type DAT-300 with probe TR-61A, made by Kaijo Denki, is used for turbulence measurements. An electronic leveller, Kaijo Denki IC-05D, and a rotor (KNMI design) are used to determine the orientation of the sonic and to turn the sonic in the wind direction.

To determine the sensible heat flux, the temperature fluctuations measured by the sonic can be used, when corrected for windspeed and humidity. To compute the Obukhov length we need a virtual heat flux, we used the sonic heat flux, corrected for windspeed only (see A.4) A thermocouple, from now on called TFM (Temperature Fluctuation Meter) can also be mounted on the sonic probe, without disturbing the velocity field.It gave us the possibility to check the sonic temperature fluctuation measurements. The TFM is designed by the KNMI.

3.4.1 The Kaijo Denki sonic anemometer

With a sonic anemometer it is possible to measure three wind components and the temperature. The principle of operation is based on measuring the transit times for sound waves transmitted in opposite directions between two acoustic transducers. The transducers alternately act as transmitter and receiver. The wind velocity is proportional to the difference between the reciprocal transit times, and the temperature to the sum of the reciprocal transit times.

The frequency of the sound pulse is 100 kHz, the pulses are generated 20 times per second, making it possible to measure fluctuations of 10 Hz. In order to measure all three components of the wind vector, it is necessary to have three non-parallel, non-

planar sonic paths which do not interfere with each other either in transmission and reception of the sound waves or in exposure to the wind field. In figure 3.3 we can see how this is done. The W-component axis measures the vertical wind. The A and B axes measure two components of the horizontal wind, which are a 120 degrees apart.The sonic gives the horizontal orthogonal components with the bisector of A and B as Y axis.

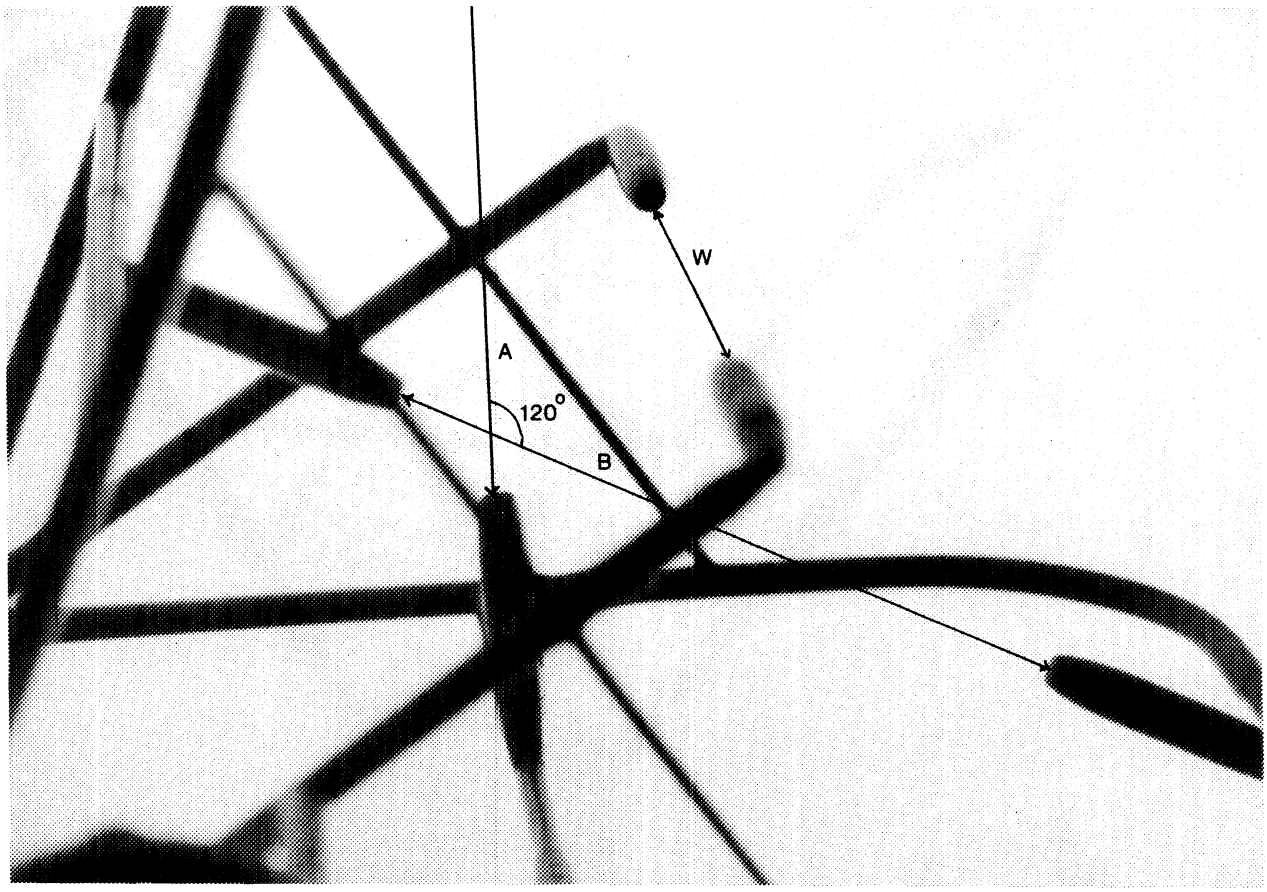

fig. 3.3 Close-up of the sonic geometry, A and B are the horizontal paths, W is the vertical path.

As the velocity of sound depends on humidity and temperature, we will measure a so-called *virtual* sonic temperature(Schotanus, 1982):

$$T_{sv} = T(1+0.51q), \qquad (3.4)$$

where T stands for temperature in K and q for specific humidity (kg/kg). In the wind components this humidity effect is eliminated, because they are computed using the difference in transit times in opposite directions (Schotanus 1982).

T is measured in the vertical direction.The acoustical paths will be bent by the horizontal wind. The correction for this in the vertical heat flux is (Schotanus, 1982):

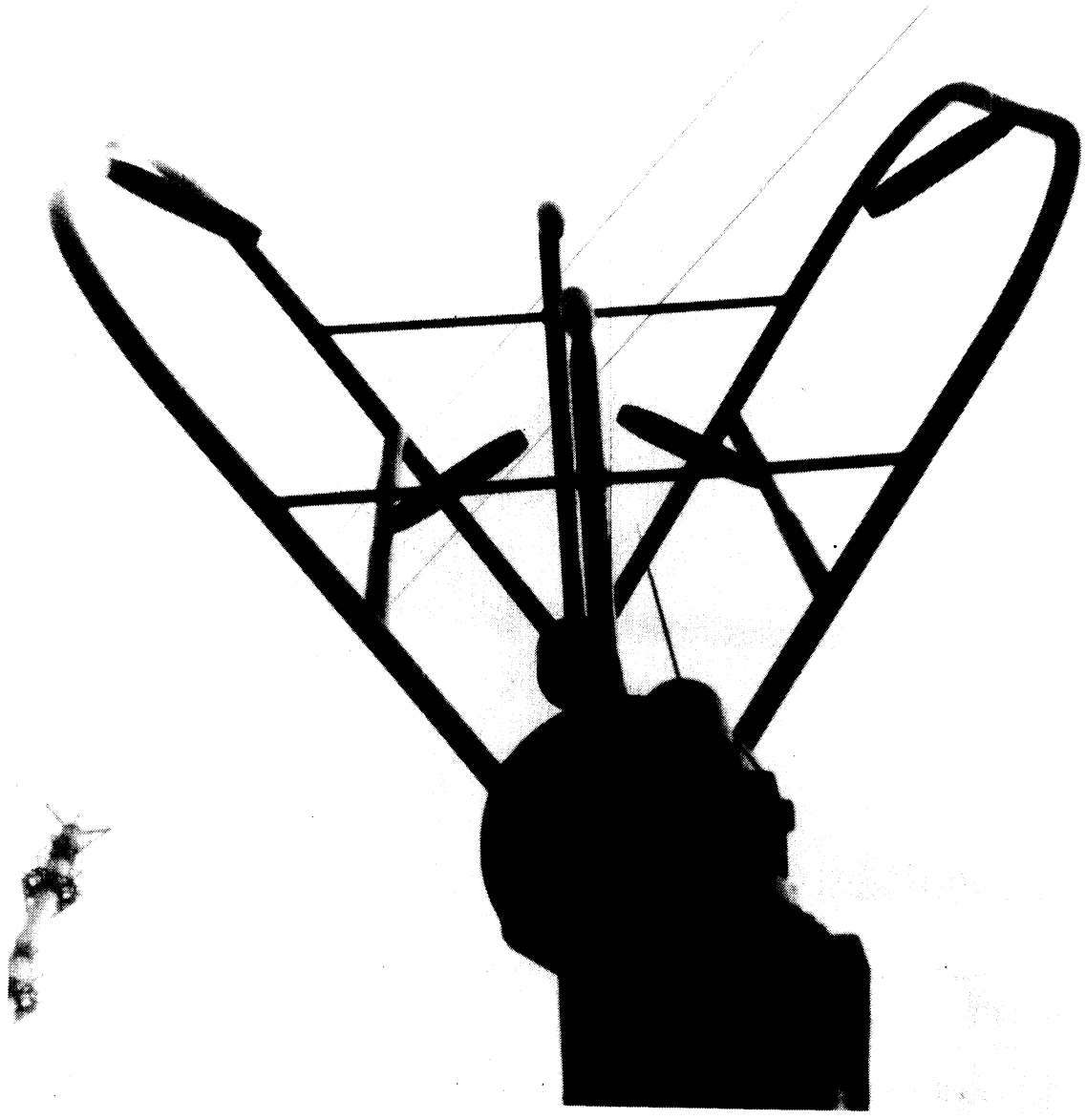

fig. 3.4. the sonic, the Cabauw mast and in the middle of the sonic frame a narrow sprit: the TFM

$$\Gamma = -\frac{2\overline{T}}{\overline{C^2}}\overline{U}\overline{(u'w')} = \frac{2}{403}\overline{U}u_*^2, \qquad (3.5)$$

where C is the velocity of sound. Again, this effect is eliminated in the wind components. Applying Reynolds' decomposition to (3.4), multiplying with w', averaging and adding the wind correction term (3.5) we obtain the virtual sonic heat flux:

$$\langle w'T_{sv}' \rangle = \langle w'T' \rangle (1+0.51q) + 0.51T\langle w'q' \rangle + \Gamma \qquad (3.6)$$

The distortion of the wind field by the frame is acceptable(<5%) when the wind direction relative to the bisector of the angle between A and B is smaller than twenty degrees(Schotanus 1982). It would be better if we could turn the sonic in the right direction; therefore the KNMI designed a rotor, which had to be operated by hand. For continuous measurements this is not very convenient. A simple electronic switch reacting on logical high or low voltages was built in. The datalogger was programmed to compute the wind direction from the horizontal components every ten minutes and turn the rotor if necessary in the right direction by means of its logical control ports.

An electronic leveller (accuracy 0.1°) was used to check that the horizontal acoustic path and the true horizontal were parallel. Misalignment can cause serious errors: Pons and Pages (1976) found that a one degree error would cause a 10% tilt error in their vertical flux.(See also Rayment and Readings, 1971) The sonic mast was guyed in three directions at two levels. Aligning proved to be very difficult. Because of the soggy soil, the guys had to be adjusted once or twice during the experiment.

An even larger error will occur if the acoustical sound path in the vertical is not exactly perpendicular to the horizontal paths. For periods when the cross correlation <uw> is small, this error is most serious.(Kaimal and Haugen, 1969). Therefore the sonic was handled very carefully to avoid bending parts of the frame.

The effects of line averaging and path separation (the distance between the horizontal sound paths A and B in the W-direction, see fig. 3.3 and Horst, 1973), become important in the lowest five meters of the surface layer (Schotanus 1982). In our experiment the center of the sonic was at 11.4m above the ground. A sound path in the Kaijo Denki is 20cm long, this makes z_{min}=3.8m in eq. 3.3.

A junction box takes care of transmitting and receiving signals. The three acoustic paths are triggered alternately. This means that the measured wind components are not measured at exactly the same time. The frequency of a full cycle is 20 Hz.

The KNMI sonic anemometers are calibrated by the Oceanographic Department in a windtunnel.At 5m/s they have a 2% precision for fluctuation measurements. During the experiment we used two sonics in succession. The seventh of August the first one was destructed by lightning.The absolute temperature measurements of the second one were of bad quality. Comparing plots of eddy correlations of the TFM and the second sonic , we concluded that the fluctuations of the sonic could be used.

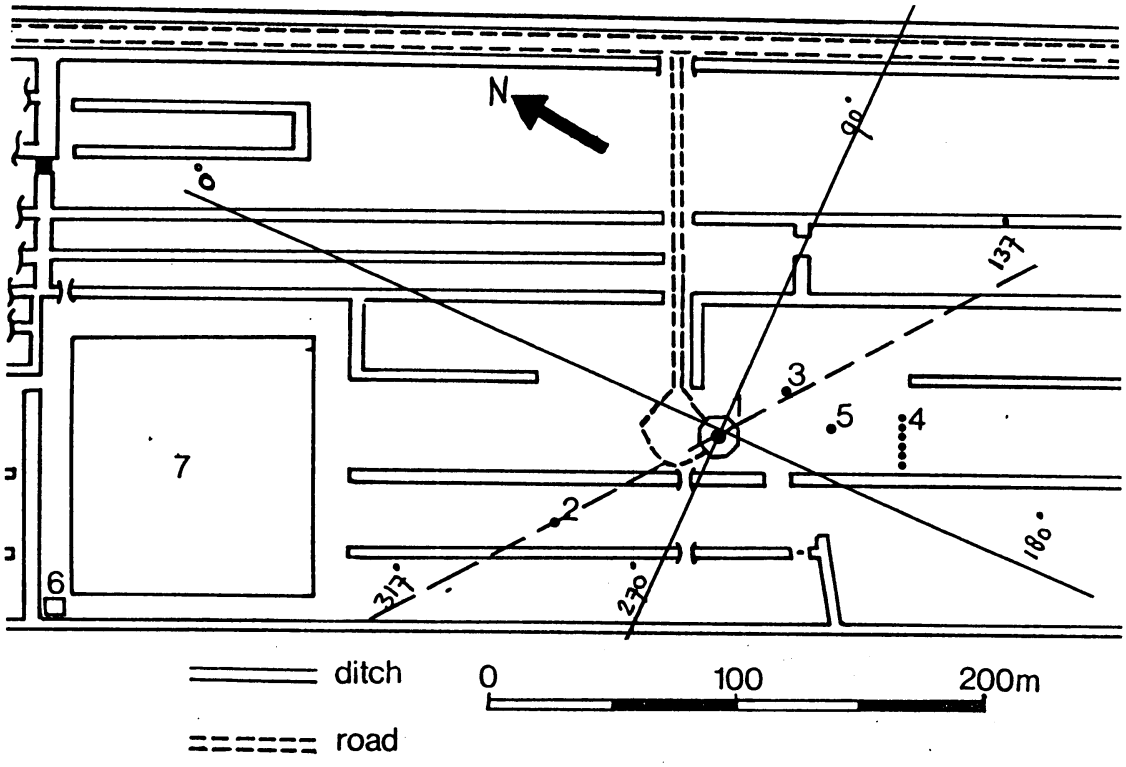

1 213m tower
2 auxiliary mast NW, sonic and TFM
3 auxiliary masts SE
4 radiation site
5 soil measurements
6 acoustic sounder
7 micro meteorological experimental site

fig 3.5 The site in detail. A North-East coordinate system is drawn across the original picture by Monna and Van der Vliet (1987). The dotted line is 137 degree line referred to in the text.

The sonic anemometer has facilities to check its electronics. Standard voltages simulate the A,B and W output. We measured the X and Y outputs.Furthermore we checked the zero by putting the sonic in a closed wooden box to obtain a no-wind situation. Most Dutch investigators perform this test is performed with covers around the measuring paths (the ones used to isolate central heating pipes), but the signals obtained in that manner show more noise. A possible reason could be reflections inside the covers. Altogether the expected values were obtained within an accuracy of 0.1%. The second sonic showed an constant offset in the w-component of 0.1 m/s.

The junction box was calibrated to assure the pulses were triggered at the right time and the right place, this was done according to the manual.(Kaijo Denki digitized ultrasonic anomometer, model DAT-300, instruction manual, for specifications see B.5)

3.4.2. The Temperature Fluctuation Meter

The TFM is a Cu-Co thermocouple, it uses a NTC-reference temperature. The NTC is encased in a block in order to provide it with a large time constant. An electronic unit containing the calibration curve for the couple converts temperatures into Volts .The TFM is calibrated by the KNMI calibration lab also. The electronic unit was calibrated by simulating the thermocouple and the NTC by a voltage source and a resistance. The amplitude of the fluctuations show an error of 0.1° at 10° amplitude at a mean temperature of 5°C.

To obtain a fast response the thermocouple consists of very thin wires (welding spot 100 μm). This makes the TFM very vulnerable. It had to be replaced half a dozen times during the experiment. Sometimes, it appeared to have broken down, but the workshop couldn't find failures, sent it back and it worked again. Maybe there is something wrong with the electronics?

3.5 The site

The profiles were obtained from the 213m meteorological mast and the surface heat and momentum fluxes from auxiliary masts at 120m north-west from the main mast.(fig.3.5) The tower is constructed as a closed cylinder of 2m diameter, with an elevator running inside. The tower is guyed at 4 levels. From 20m upwards, horizontal booms are installed every 20 meter. At each level there are three booms, extending 9 m beyond the cylinder surface, pointing in three directions: 10,130 and 250 degrees. The continuous measuring program in Cabauw selects the least disturbed boom for measurements. Due to the large size of the building at the foot of the mast, accurate measurements in the lowest 20 meters are impossible. Therefore auxiliary masts have been placed at a sufficient distance from the mast.(fig.3.5)

The Cabauw site is located in flat terrain (fig.3.6), mainly consisting of grassland interrupted by narrow ditches. Up to a distance of 200 meters from the mast there are no

obstacles or perturbations of any importance, farther on we find some scattered trees and houses for most wind directions. For easterly winds the flow is perturbed by tree rows, orchards and a village (Lopik). Although the terrain looks very uniform, some weak

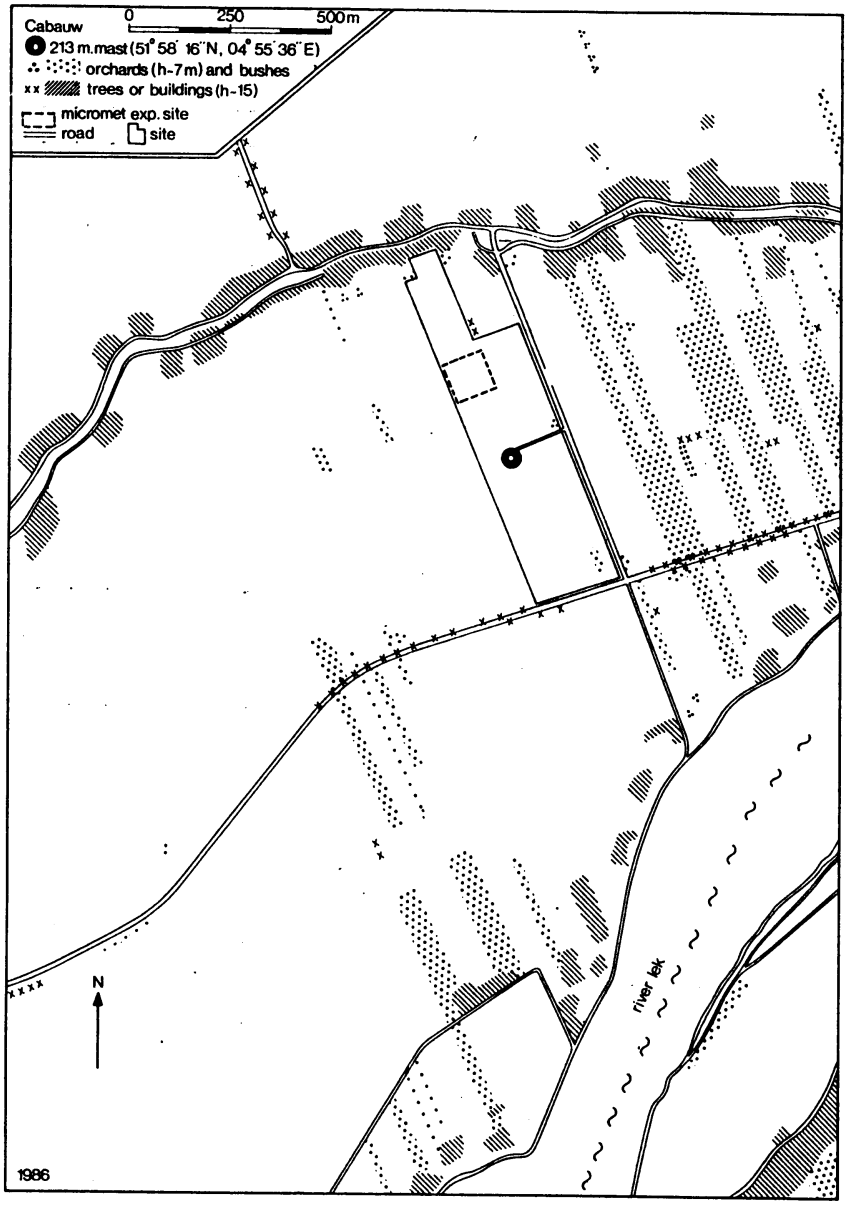

Fig. 3.6 Surroundings of the tower

inhomogeneous terrain effects have been observed, causing perturbed flux-profile relationships below 20 meters.(Beljaars1982, Beljaars et al 1983)

There are also perturbations by the main mast (Wessels, 1984, Van der Vliet, 1981) The sonic anemometer and the TFM are placed near the auxiliary masts NW (2 in fig. 3.5.) The temperature measurements for the profiles are obtained from the auxiliary mast SE (3). The dotted line from the sonic (2) via the main mast (1) to the temperature mast (3) has an angle of 137 degrees relative to the North. For wind directions of 92 to 182 degrees the sonic measures perturbed fluxes in the turbulent wake of the main mast. The electronic gap in the rotor (see A.1.5) was placed so that it looked in the direction of the main mast, so along the 137 degree line. The gap in the rotor adjusting program was 20 degrees around this line. So the frame distortion (§3.4.1) causes the sector 127 to 147 degrees to be disturbed by the sonic frame also. For wind directions of 282 to 362 (or 2) degrees the temperature profile is possibly disturbed (see § 5.2.2).

The grass in the immediate vicinity of the mast is said to be kept at 8cm height. Near the NW auxiliary masts however, the grass was mown only once during the experiment, while the south east part of the terrain was mown several times. The roughness length, estimated from gustiness measurements (Wieringa 1973), varies approximately from 0.06m in the south-west sector to 0.15m in north-east sector. The values are listed in table 3.2.

A herd of cows grazing in the immediate vicinity (50-300m)of the masts during the whole experiment may have caused perturbations.For a more detailed description of the site see Monna and van der Vliet (1987).

wind direction	*roughness length (m)*
015	0.059
045	0.100
075	0.150
105	0.150
135	0.110
165	0.041
195	0.040
225	0.037
255	0.066
285	0.061
315	0.062
345	0.045

table 3.2 Roughness length per wind direction sector, for directions in between the tabulated values a linear interpolation is used.From Beljaars (1987).

4. Data handling

4.1 Considerations

We planned to make measurements continuously for three months. If we would just store the raw data we would end up with piles of data. Analysis would then have taken lots of time. The solution to this problem is on-line data reduction. While measuring we compute mean values, standard deviations, stability parameters etc. and analyse on the spot if necessary.The disadvantage of on-line data reduction is obviously the loss of raw data! Afterwards you will always regret having thrown out data. To still have some analog information left, we recorded the TFM, the windspeed at 5m and the wind direction at 10m (D10) with a Kipp-recorder. This way people who could not handle dataloggers could still warn us if something was wrong. Especially the TFM is very vulnerable and often needed to be replaced. Discovering this one or two days after breakdown would have been a waste of precious data.

The continuous measuring program in Cabauw provides an on-line data reduction facility. The PDP11/23+ computes a data base consisting of 10 minute averages, checks on data quality and selects the best boom for the actual wind measurements. When all erroneous data have been removed from the 10 minute data base, thirty minute averages and other variables are derived and stored in files that are said to be easily accessible (Monna and van der Vliet 1987).

For recording the outputs of the additional equipment we use Campbell's 21X-micrologger, for short: the datalogger. A 192k hardware memory called storage module (SM192) serves as extended memory. The datalogger can be programmed to make calculations over time and store results for later retrieval. The datalogger has sixteen analog input channels. For more details see appendix A.1.

Eight channels are used to record the three sonic wind components, the sonic temperature, the TFM temperature and NTC reference temperature, the azimuth reading of the rotor (R) and the additional 5m propeller vane (F5).This means we have eight channels left for one very important purpose: At all times during the experiment we want to be able to check whether the instruments are still doing what they are supposed to do. Do the outputs satisfy all kinds of empirical relations? Is there output at all? Has it been raining?

Of course this information is available from the Cabauw data base, but the 30 minute files, although easily accessible, are not made on-line. They are available only a few weeks later. So it is convenient and necessary to also have some profile information to verify the empirical flux-profile relationships and information on the meteorological circumstances. Table 4.1 lists the added channels.

For all these signals we compute 10 minute averages. For U,V,W,T_{sv} and T we calculate the covariance matrix. To obtain information about the small scale structure we use the burst measurement facility of the datalogger. It takes 10 samples at a maximum rate of 1030 Hz. We used 25 Hz and computed standard deviations of the differences between the first and the third, the first and the fifth and the first and the ninth sample of

W and T_{tfm} to obtain the necessary information to obtain structure parameters. (not included in this report)

The datalogger stores all these values and derives thirty minute averages that are stored in the storage module.

All together the datalogger produces 44 outputs every half hour. If the storage module capacity had been the only concern, I could have come back three weeks later to collect the data.

instrument	*parameter*
propeller vane	F10,F20,D10
thermocouple	T06,dT2,dT10,dT20
rain sensor	RI (rain indicator)

table 4.1 Additional channel inputs for the datalogger, Fx stands for wind speed, the number x for the height in meters, T for temperature and dTx for the temperature difference between the level x and the previous level.

4.2 Processing the data

The data from the datalogger and the data from the Cabauw routine measurements had to be combined for the analysis. How this is done is described in appendix 2. The combined files are day files consisting of 57 columns and 48 rows (48 half hours from 0 am to 12pm) and are available for further analysis.

The dayfiles are imported into LOTUS, a spreadsheet program. In LOTUS we created night files (noon to noon), because we were investigating the nocturnal boundary layer.From these night files graphs of the nocturnal behaviour of wind speed, temperature and radiation were plotted. Missing values and bad quality data were replaced by special codes.

From the 57 values in each row we computed all the turbulence parameters needed to investigate the similarity functions. Values had to be corrected for humidity or flow distortions. Some values had to be estimated, because they were not available or of bad quality. In appendix A4 details of the computations are given.

Demanding that the value of signals exceeded the expected measuring error, we obtained the following selection criteria:

-The sensible heat flux should be greater than ~10 Watt, or : $|\langle w'T' \rangle| > 0.01$.[2]

-The difference in temperature between the 10 and 20m level should be greater than 0.05.

[2] Another argument to do this is that $\varphi_h(0)$ will be extremely large for small $\langle w'T' \rangle$

Demanding that the turbulence was continuous, we selected on wind speed and friction velocity:

-Wind speed at 5m should be greater than 1 m/s.

-The friction velocity should be greater than 0.1 m/s.

Of course we demanded that there was no rain or fog. At sunset and sunrise we expect instationarities, but the criterium for the heat flux excluded these half hours already, so no further selection for this phenomenon was applied.

All the criteria were implemented objectively and automatically by means of macros in Lotus. This way also data that could have been alright were thrown away. Still lots of bad data were left and some were obviously very bad and probably wrong. For these data we investigated all possible error inducing factors. This way we found for example that the sonic anemometer had a changing offset. The reason for this could not be found. The offset would remain constant for a few days and then suddenly jump to another value (from 0.1 to 0.4 m/s for example). We decided to exclude the two half hours before and after the sudden jumps.

Sectors disturbed by the main mast were not excluded in this stage.Selection on wind direction sectors is included in Ch. 5. The data were sorted on their expected upstream history. The sectors chosen are mentioned in § 5.1.

The selection criteria were applied to all data. The same criteria for the dimensionless shear and for the dimensionless temperature gradients. To save precious data it would be better to use different criteria. For example temperature differences between two levels have nothing to do with the dimensionless wind shear. Selecting on the temperature difference will eliminate windshear data that are ok. As always in experiments the best way to perform things is discovered when writing the final report!

The heat flux obtained by the sonic proved to be very useful.(see A.4) The virtual heat flux that can be obtained with the TFM temperature fluctuations needs additional humidity information. As the humidity measurements in Cabauw were often not available we used the sonic temperature fluctuations and saved about 400 half hour averages.

5. Results and discussion

Our purpose was to determine flux-profile relationships :

$$\varphi_m\left(\frac{z}{L}\right)=\frac{\kappa z}{u_*}\frac{\partial \bar{u}}{\partial z} \qquad (5.1)$$

and:

$$\varphi_h\left(\frac{z}{L}\right)=\frac{\kappa z}{\theta_*}\frac{\partial \bar{\theta}}{\partial z} \qquad (5.2)$$

where we have computed the dimensionless gradients and the stability parameter z/L according to the methods in appendix A.4.

5.1 The data after selection and division into sectors

Because each parameter has different inputs, the results after selection were not always compatible. The total dataset after selection contained 1122 half hour values. For φ_m the useful combinations with z/L values added up to 868 half hours. For φ_h we had 861 half hours left.

Analyzing the terrain surrounding the masts we chose wind direction sectors summarized in Table 5.1:

sector	φ_m	0<z/L<0.5	φ_h	0<z/L<0.5
0-360	867	-	861	-
45-92	109	28	109	28
92-182	115	-	-	-
182-230	109	17	114	17
230-260	105	12	111	16
230-330	441	69	-	-
282-362	-	-	283	-
182-92	752	117	-	-

Table 5.1 Amount of half hours left after selection in different sectors.

The half hour values for 0<z/L<0.5 are used for linear regression, these values will

be refered to as slightly stable.The sector 182-92 is the complete dataset minus the 92-182 sector.

The 45-92 degree sector shows inhomogeneities. The sector 230-260 degrees is open, (2km fetch over pasture land), or homogeneous. The 182-230 degree sector has a somewhat smaller roughness length, and is almost unperturbed. Because the number of data in these sectors were small, we also chose a sector that was larger and could be seen as very slightly disturbed: the 230-330 degree sector. This selection was done by eye from the main mast. To see whether the main mast truly disturbed our measurements, the sector disturbing fluxes (92-182 degrees) and the sector disturbing temperature profiles (282-362 degrees) were chosen. There are still some empty spots left in table 5.1, these half hours were not analysed.

5.2 Discussion.

5.2.1 Similarity functions for the stable case.

Many experiments have been performed to find similarity functions for the stable regime. A few results are listed below:

experimentator	κ-value	φ_m	φ_h	site
Zilitinkevitch (1968)	0.43	$1+9.9\xi$	$1+9.9\xi$	Tsimlyansk
Businger et al.(1971)	0.35	$1+4.7\xi$	$0.74+4.7\xi$	Kansas
Wieringa (1980)	0.41	$1+6.9\xi$	$1+9.2\xi$	Kansas*)
Dyer (1974)	0.41	$1+5\xi$	$1+5\xi$	Hay
Cuijpers (1987)	0.41	$1+10(z/\Lambda)$	$1+10(z/\Lambda)$	Cabauw
Zhang et al (1988)	0.40	$1+6.2\xi$	-	Carpenter

Table 2.1 Similarity functions found in different experiments. Cuijpers used the data from Nieuwstadt (1984).*)Wieringa corrected the Kansas measurements for flow distortion by the instrument boxes in the measuring towers.See also Wyngaard et al.(1982) for comments and the reply by Wieringa (1982).

We note that many different values for κ are being used. This leads to different similarity functions already before measurements have taken place (Högström, 1987). The value for κ is usually chosen so that $\varphi_m(0) = 1$, Högström argues that former experiments find different similarity functions due to instrumental shortcomings. In particular flow distortion has not been adequately treated. He states that κ=0.4 is always constant, leading to values φ_m=1 and φ_h=0.95 at neutrality for horizontally homogeneous conditions. Högström himself (1987) finds:

$$\varphi_m = 1.00+3.43\xi + 8.4\xi^2 \qquad |\xi| < 0.15$$
$$\varphi_m = 0.8+6.0\xi \qquad \xi > 0.15$$

$$\varphi_h = 0.95 + 5.24\xi + 6.3\xi^2 \qquad |\xi| < 0.2$$
$$\varphi_h = 0.7+7.75\xi \qquad \xi > 0.2$$

The higher slope for higher stabilities is in contradiction with others, generally speaking a decreasing slope is found. (Carson & Richards 1977).

The fact that different groups find different slopes raises questions: are we investigating similarity functions at all? Or do we miss a few parameters in our scaling? Does the constant β, that is not so constant, have parameters influencing it that are not accounted for, but may be constant in each single experiment?

Neglecting advection terms is risky too, terrain inhomogeneities cannot be taken into account. Production of turbulence is not always local, it can be advected from elsewhere.

5.2.2 The influence of terrain inhomogeneities for stable stratification.

When experimentators force their similarity functions through $\varphi_m(0) = 1$, they change the von Karman constant accordingly.The problem with this approach is that changing a "constant" also changes the slope of our similarity function. As the supporting model and measurements are valid under neutral conditions only, there is no reason why this should be true. On the contrary: when the stability increases, we expect the upwind terrain to have less influence on the fluxes and profiles.

Under stable conditions we have a so-called log-linear profile, that follows from integration of (2.35):

$$u(z) = \frac{u_*}{\kappa}\left\{\ln\left(\frac{z}{z_0}\right) + \beta\left(\frac{z}{L}\right) - \beta\left(\frac{z_0}{L}\right)\right\} \qquad (5.3)$$

We assume $\beta = 5$ (Businger 1971). At 10 meters and with typical roughness length 0.1m we have $\ln(z/z_0) \approx 4.6$. We see that the linear factor, $5(z/L)$, becomes more important for large values of (z/L), say (z/L)>1. The term $5(z_0/L)$ is small . So if β(z/L)>>1, we expect the profile to be linear, we have already seen this is called z-less stratification. From this we conclude that the terrain effect represented by z_0 vanishes for greater stabilities. So the slope of the similarity functions will be less sensitive to changes in the upstream terrain for increasing stability.

For greater stabilities the internal boundary layer will develop slower. To illustrate this Bergström (1988) gives an empirical formula for the growth of an internal boundary layer by wind:

$$z_{IBL} = 0.2x^{(0.78-0.33z/L)} \qquad (5.4)$$

Here x is the fetch.As the fetch can be seen as a time scale, it is clear that internal boundary layers develop slower under very stable conditions.

Although this means <u'w'> is a function of height, this doesn't interfere with the scaling we use. In fact we always use local scaling, because we measure locally. We measure eddies that scale with the local fluxes; the local <u'w'>. So whether we measure in the internal boundary layer or not is not of importance here.

A more serious problem is the gradient. The change in surface features causes the surface momentum flux and the surface heat flux to change almost immediately. The profile is still the profile advected from the upwind terrain. From the bottom up the profile will be adapted by the locally determined turbulence. This takes time. The time scales involved are comparable to the time scales for the growth of the internal boundary layer. So there is a time lag between the flux and corresponding gradient.

But again: in the local scaling approach we expect eddies to be generated by the local shear. And because the time scales involved are small, the turbulence will be dissipated locally too.The process of internal boundary layer growth and thus the adaption of the wind and temperature profiles takes much longer. This behaviour resembles the behaviour we expect in the z-less stratification limit, that is represented by the linear part in the log-linear profiles. Consequently the slope of the similarity functions will be the same as in the homogeneous case. It does not depend on the history of the flow.

The logarithmic part is representing the larger eddies that we have round neutral and for unstable conditions. These eddies evaluate much slower and show the upstream surface features. The behaviour in this case is already explained by the model of Beljaars above.

Peterson (1969a&b) concludes that changes in surface roughness cause the surface shear stress to react slower than the windshear. This does not agree with the expected time lag for the gradient mentioned above. He also finds that the nondimensional windshear at neutrality is less than unity for rough to smooth transitions and more than unity for smooth to rough transitions. In the first case he speaks of an accelerated flow,

in the second case of a decelerated flow. Furthermore he states that the vertical flux divergence of turbulent energy cannot be neglected, which is indeed essential in this theory.

5.3 Graphical presentation

Because the huge amount of graphs would spoil our reading appetite, we added them in the first appendix A.0. A few, smaller in size, are included in this paragraph, for illustration. They have the same number as the ones added.The graphs are made with a Macintosh application called Cricketgraph.

In the figures 5.1 and 5.2 we see the result of the complete dataset for both the dimensionless wind shear and the dimensionless temperature gradient. Only data for $0.5<z/L<1.5$ are visible, because of the choice of axis scaling. Data outside that interval on the stable side are seldom found, the unstable side is not the subject of this study. We show the unstable side to clarify the intersection at neutral stability.

There are two things to be said from these figures. First of all, we see something that looks like the general picture we expect. The form is resembling the Dyer-Hicks relations (Dyer 1974). Secondly the φ_h data look a lot worse than the φ_m data.

5.3.1 Dimensionless wind shear

If we exclude the sector supposedly distorted by the main mast, we see some improvement. (fig 5.3). It seems that the 92-182 degrees sector contains relatively more outliers. Regression analysis on the slightly stable part yields $\varphi_m=(0.89\pm0.05) + (3.1\pm0.2)\xi$. Compared to Businger (1971) the slope is rather low, it is still lower compared to Högström (1987).

Figure 5.4 shows the 182-230 degrees sector. We have relatively few data on the stable side. We see that $\varphi_m(0)\approx1$, maybe a little smaller. The regression curve on the stable side is shown in figure 5.5. Linear regression gives unrealistic results, because outliers influence the result disproportionately. The result is at least not what we see by eye in figure 5.4. If we use values round neutral (positive and negative, say $|\xi|<0.1$ and fit a second order polynomial, the result for $\varphi_m(0)$ will tend to 1. For the 230-260 degree sector we have similar results (figures 5.6 and 5.7). Therefore we choose a sector containing more data that is also relatively homogeneous in the upstream surface features.

The 230-330 degree sector is plotted in figure 5.8. An eye-fit is added to show the tendency for the slightly stable part. We see that for $z/L>0.6$ the slope decreases. This might be caused by intermittency. Suppose we have a burst of turbulent activity. The

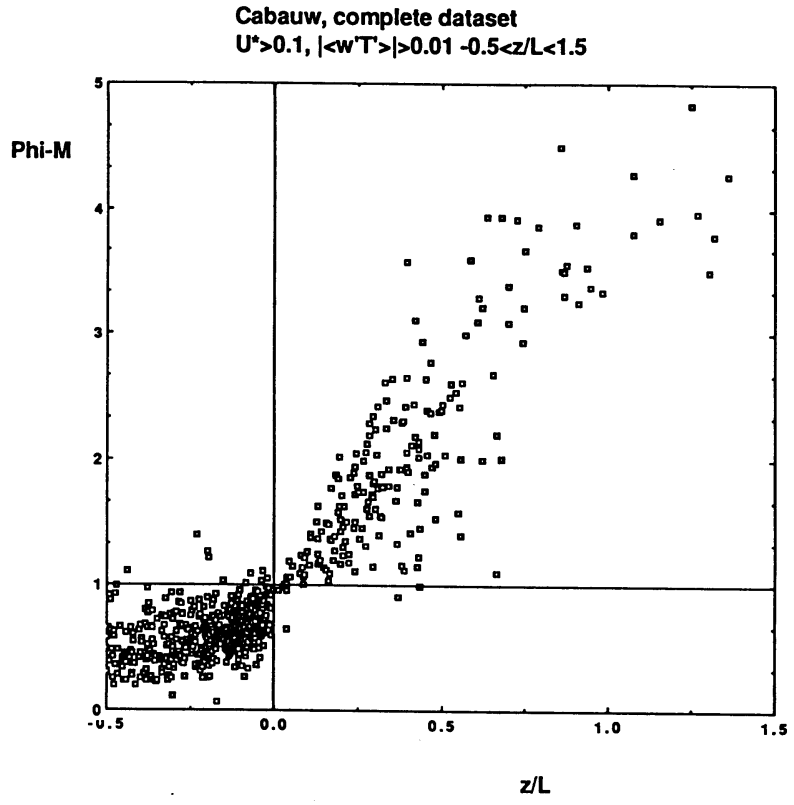

fig 5.1 φ_m versus z/L for all data

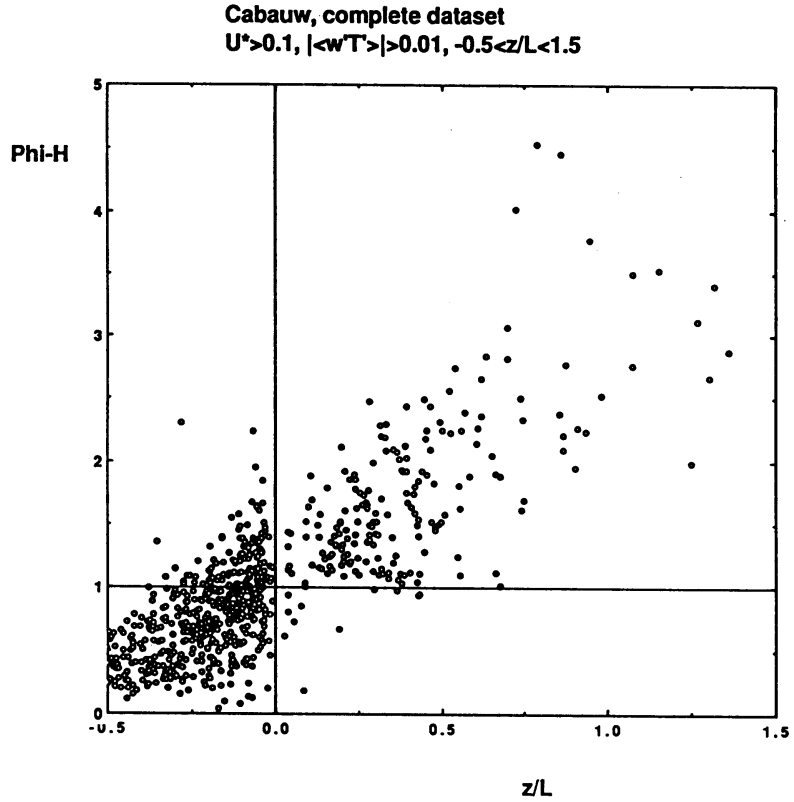

fig 5.2 φ_h versus z/L for all data

value of z/L will become smaller. Because of the rapid vertical mixing, the gradient will decrease, leading to smaller dimensionless shear values. After some time the turbulence has decayed. The next half hour we will now measure a higher z/L value. The gradient however, will adapt much slower; the increase of the gradient has to be established by molecular diffusion. The gradient shows a time lag. This is what we already concluded in paragraph 5.2.2 for changes in upstream surface conditions. Consequently the dimensionless wind shear will be lower than 1+ 3.2(z/L) for large z/L as can be seen in fig. 5.8.[3] The linear regression given by Cricketgraph is shown in figure 5.9. It confirms our eye-fit.

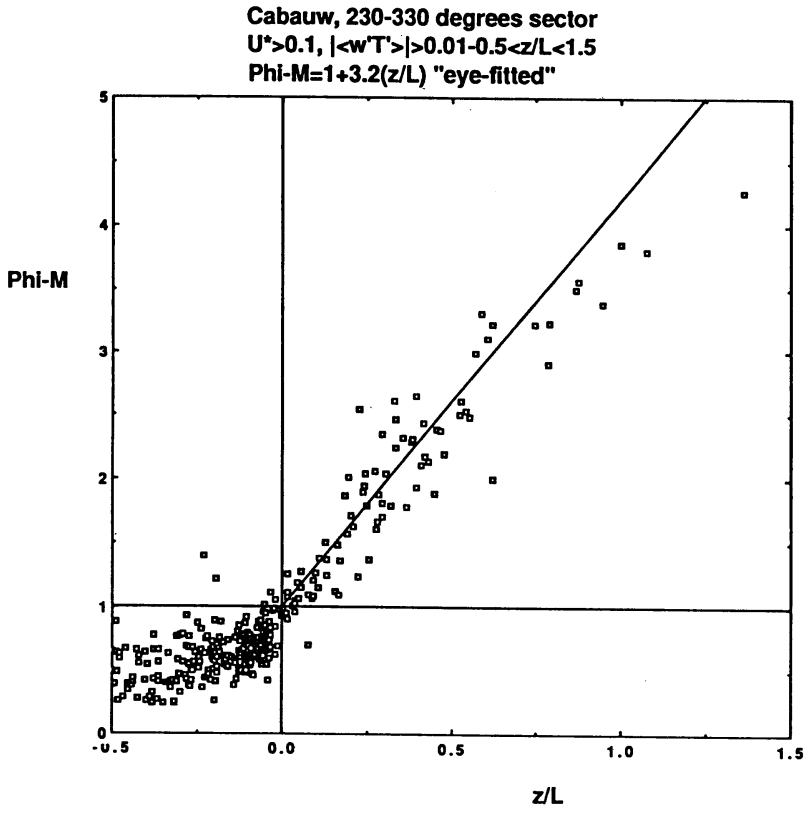

fig 5.8 The 230-330 degrees sector with an eye-fitted line for the slightly stable side.

The 45-92 degree sector is perturbed by tree rows, orchards and the village Lopik. We expect shifted profiles. In figure 5.10 we see the result. The value round neutral is clearly lower than in figure 5.8, $\varphi_m(0) \approx 0.8$. Regression on the slightly stable part also shows this (fig 5.11). The slope is also lower here, this is not what we expect. We only have 28 observations here though, while figure 5.8 contains 69 values in the same range. The exact results of the regression are given in table 5.2 at the end of this chapter. We see there that the results for the homogeneous and the inhomogeneous sector are not incompatible. We note that the error intervals given are the estimators of the variance in

3 This should be checked in the analog recordings from the Kipp-recorders.

the regression coefficients (see A.3), and are not equal to the measuring uncertainty.

Cricketgraph provides a facility that takes running averages over an odd number of values, they call it smoothing. This way we introduce a correlation between successive z/L values, statistically this is not correct. We think however, that it illustrates the tendency quite well, systematic deviations can be seen now (fig 5.12).

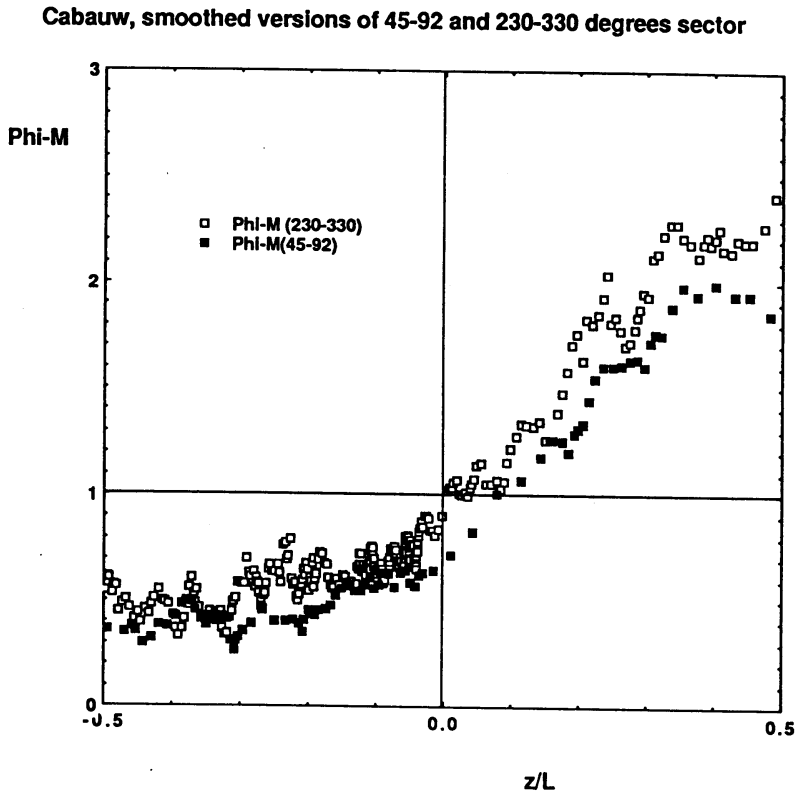

fig 5.12 smoothed versions of 5.8 and 5.10, running averages are taken over 9 and 5 values respectively. Black squares stand for 45-92 degree sector, open squares stand for the 230-330 degrees sector.

We clearly see the whole curve is shifted in the 45-92 degrees sector. The reason is given in §5.2.2. Similar results are found by F.Bosveld (not published yet) above a forest in the roughness layer. Although the roughness layer has nothing to do with upstream terrain inhomogeneities, there is an analogy: The geometry of the surface, whether it is upstream or very close to the measurements does not change the slope of the curve, at least not for stable stratification. It merely changes the value of $\varphi_m(0)$(see also § 2.3). We could say that the scaling for the neutral case, or the logarithmic part of the profiles, fails. It should include geometry or history information (such as fetch, internal boundary layer height, and some scale to account for the phaselag between fluxes and profiles).

5.2.2 The dimensionless temperature gradient.

The temperature profile may be disturbed by the main mast as well. However, in fig 5.13 we see the 282-362 degrees sector (black squares)within the plot for the complete dataset (circles). We don't see any improvement between the two.

The 182-230 degree sector is shown in figure 5.14, we see too much scatter to obtain relevant results with linear regression (see A.3). The 230-260 degrees sector (fig. 5.15) looks a little better. It appears that $\varphi_h(0)\approx 1.3$, while this is the open sector. We could not find a reason for this strange behaviour. Whenever different values for $\varphi_h(0)$ are found, they are generally lower than their $\varphi_m(0)$ counterparts. Businger(1971) for example finds $\varphi_h(0)\approx 0.74$.Adding the two graphs and ignoring the huge amount of scatter on the near neutral unstable side, we find $\varphi_h=1+2.3(z/L)$ eye-fitted.(fig 5.16)

The 45-92 degrees sector shows a systematic deviation from $\varphi_h(0)\approx 1$ for the whole curve again (fig. 5.17). To illustrate this we smoothed the 230-260 degrees and the 45-92 degrees sector to obtain figure 5.18. The result looks similar to that of φ_m (fig 5.12). This means that the high value for $\varphi_h(0)$ is not due to scatter, the deviation is systematic. If we include the 182-230 degrees sector also, we see that it lies more or less between the other two (fig 5.19), although it shows more scatter.

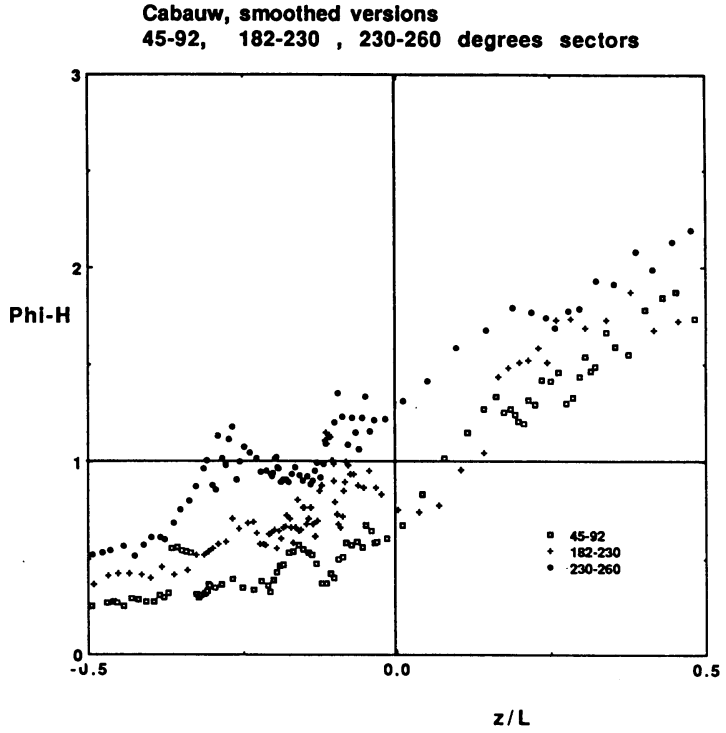

fig 5.19 Three smoothed sectors that show similar shifted curves. The running average was taken over 5 successive values.

The question remains, why is the 230-260 curve shifted upwards? We can not doubt

its validity, the curve is obtained the same way we obtained all the other curves. So it is a result of measurements, we have to accept it.

The measurement for the dimensionless wind shear seem a lot better than those for the dimensionless temperature gradients. We tried to find an explanation.

If we have a look at figure 3.5 again, we see that the distance between flux measurements and temperature profile measurement is 95m, that is a large distance. The integral scale, defined as the maximum distance at which the correlation between wind fluctuation measurements is greater than zero, should be considerably greater than the distance between the measurements to assure reasonable correlation between the measurements. Measuring at 10m height, Duchêne-Marrullaz (1977) finds that the integral scale in the longitudinal direction is 75m, and 35m in the lateral direction. Mackey (1977) finds larger values, 205m and 55m for the longitudinal and the lateral direction respectively. A distance of 95m is acceptable according to Mackey, but is too far apart according to Duchêne-Marrullaz for the longitudinal case, for the lateral case they both predict bad correlations.

To see what the effect is for the whole dataset, we compare sensible heat flux estimations computed by the Cabauw routine measurement program from the profiles with the heat flux we have measured with the sonic.The integrated Dyer-Hicks relations are used to compute the heat flux. The method is called the profile method. We also compare the result with measurements done by F. Bosveld in Fochteloërveen, computed the same way, but obtained by masts only 5m apart. The results are shown in figures 5.20 and 5.21.

If the measurements over a longer distance are poorly correlated, we expect them to show more scatter and possibly also bias due to differences in upwind terain characteristics. In figure 5.20 we see that for a positive heat flux of 100 W/m^2, the scatter is about 40%. In figure 5.21, unfortunately scaled differently, the scatter is about 20% round 100 W/m^2. We really should have done the measurements closer to each other.

5.4 Results of linear regression

In table 5.3 we present the results of the linear regression analysis performed with Lotus 123, on most of the sectors.

sector	$\varphi_m = \alpha + \beta.\xi$	$\varphi_h = \alpha + \beta.\xi$
45-92	$\alpha = 0.82 \pm 0.12$	$\alpha = 0.89 \pm 0.16$
	$\beta = 2.7 \pm 0.4$	$\beta = 2.0 \pm 0.6$
182-230	$\alpha = 0.81 \pm 0.18$	$\alpha = 0.84 \pm 0.28$
	$\beta = 3.5 \pm 0.6$	$\beta = 2.6 \pm 1.0$
230-260	$\alpha = 0.89 \pm 0.18$	$\alpha = 1.31 \pm 0.20$
	$\beta = 2.9 \pm 0.6$	$\beta = 1.8 \pm 0.6$
230-330	$\alpha = 0.95 \pm 0.06$	
	$\beta = 3.2 \pm 0.2$	
182-92	$\alpha = 0.89 \pm 0.05$	
	$\beta = 3.1 \pm 0.2$	

Table 5.3 Similarity functions in Cabauw for the different sectors

We see that the slope for φ_h is always lower than the slope for φ_m and that the error in the estimators is always larger for φ_h. We have no explanation for the lower slope. We have tried to explain the larger error in φ_h. The results do not agree with the results of the smoothed curves above. Both the linear regression and the smoothing technique cannot be relied on to draw the tentative conclusions we drew in the preceding paragraphs. For linear regression we need to know more about the scatter. When fitting by eye, we will tend to draw the line which we wish to see most. And last, but not least we have included the assumption that the relation is linear, which may not be quite right.

6. Conclusion

This report presents the results of three months of continuous measurements of fluxes and profiles at Cabauw during the summer of 1989. This paragraph is split into a part concerning the instruments and the data and a part concerning the results.

Instruments and data

Flux measurements were made with a Kaijo-Denki sonic anemometer. An additional fast thermocouple, KNMI design, provided extra information on temperature fluctuations. In the final analysis the data obtained with the thermocouple have not been used. The sonic anemometer temperature fluctuations, corrected for the bending of the vertical sound path by the horizontal windspeed, are almost equal to the virtual temperature fluctuations that can be obtained with the TFM. Using those we had much more data left after selection, because the humidity measurements required were often not available.

The routine measurement program of the 213m meteorological tower provided profiles and additional micrometeorological information, such as rainfall, humidity, visibility and radiation. On-line data reduction was performed using a Campbell 21x-micrologger.The datalogger proved to be very convenient: although we lost raw data using on-line data reduction, we had all the relevant parameters to obtain similarity functions on the spot. The storage capacity of the datalogger with an extended memory was sufficient to store three weeks of data.

In future experiments the use of more than one datalogger would be an interesting option. This way one datalogger could be used the same way we did. Except for the turning of the rotor of course; this will be done by an intelligent electronic device. The second one could be used to do a spectral analysis on the spot. This way there is still no need to store the raw data. Apart from that several filters could be programmed in the datalogger, they could for example be used to see gravity wave activity.

Situations with rain or fog were excluded from the dataset, as well as periods where the instruments gave rise to suspicion.

The data used in the results are selected to have sufficient wind speed at 5m (>1m/s) and sufficient friction velocity (>0.1m/s) to assure a continuous turbulent state. The temperature differences between the successive levels along the 213m mast were selected to be greater than 0.05°. Finally, the sensible heat flux had to be greater than ~10 W/m2.

The database consisted of 1122 half hour averages, of which 867 were useful for dimensionless windshear plots and 861 were useful for dimensionless temperature gradient plots. The selection procedure was the same for both the dimensionless windshear and the dimensionless temperature gradient. The temperature differences are not included in the windshear computations, so for the windshear we could have omitted this criterium to save data.

Suggestions for further analysis of this dataset are:

-Use different selection criteria for dimensionless temperature and dimensionless windshear computations.

-To compute the Obukhov length we used the virtual sonic heat flux as given by (3.6)(see A.4), we also scaled the dimensionless potential temperature gradient with this flux. This is wrong, we should have corrected it for humidity effects to obtain a "potential" heat flux.

-It is possible to correct for flow-blocking obstacles such as the rotor and the electronic leveller underneath the sonic frame.The obstacles cause the 30-minute-average w-component of the windspeed to be greater than zero. This effect is called tilting.

-Make graphs of the diurnal variation of all the variables measured by either sonic or TFM in order to double check whether the instruments were really doing what they ought to do. The sudden jumps in the absolute temperature of the second sonic are a good example of contaminated data that can be found this way. Especially the w-component of the sonic could be of interest. The eddy heat fluxes measured by the TFM and the sonic showed reasonable agreement, but the w-component is a shared variable and could still show irregularities we have missed.

-Another shared variable is u_*, it is included in z/L as well as in the similarity functions. This can cause cross-contamination: seeming correlations between the two dimensionless variables. Hicks (1981) suggests that, to find out whether cross-contamination plays an important role or not, we should plot the dimensionless gradient as function of the gradient Richardson number. All the information needed to do this is available.

-The same Richardson number should be plotted against z/L to see when the z-less stratification limit is reached. The gradient Richardson number should be constant then (Nieuwstadt 1984,Cuijpers 1987).

-Finally the results of the burst measurements done by the datalogger for the vertical velocity and the temperature of the TFM should be used. Standard deviations of the difference between samples with different time intervals are available, they can be used to obtain structure functions.(see for example Tatarski, 1961) From the structure functions it is possible to compute the viscous dissipation for each half hour, so that the turbulent kinetic energy budget can be checked on losses.

Results

From the selected data we obtained the dimensionless windshear and the dimensionless temperature gradient as a function of z/L. The graphs are presented for z/L between -0.5 and 1.5. For some sectors linear regression on the $0<z/L<0.5$ interval was applied. When there was too much scatter to obtain reliable results this way, we fitted a line by eye. The advantage of this method is simply that it is very convenient.

The main mast at Cabauw disturbes the flux measurements in the North-West sector

for wind directions of 92° to 182°. When this sector is excluded, the data show considerably less scatter. The main mast didn't seem to influence the temperature measurements on the SE mast. The influence of the mast can be seen in figures 5.3 and 5.13.

We saw that the dimensionless temperature gradient plot shows considerably more scatter than the dimensionless windshear plot. The reason for this could be that the distance between the measurements of the temperature profile (SE-mast) and the flux measurements (NW-mast) was too large (95m).

Eye-fits of the complete dataset yields for $\varphi_{m,h}$:

$$\varphi_m = 0.9+3.1(z/L)$$
$$\varphi_h = 1.0+2.1(z/L)$$

as can be seen from figures 5.1 and 5.2. The slopes of the similarity functions are rather low compared to what others find. (see table 2.1) When we compare our results to what Cuijpers (1987) found from Nieuwstadt's (1984) data, that are also obtained at the Cabauw site, we see an even larger difference between the values of the slopes. In figure 6.1 we can see this.

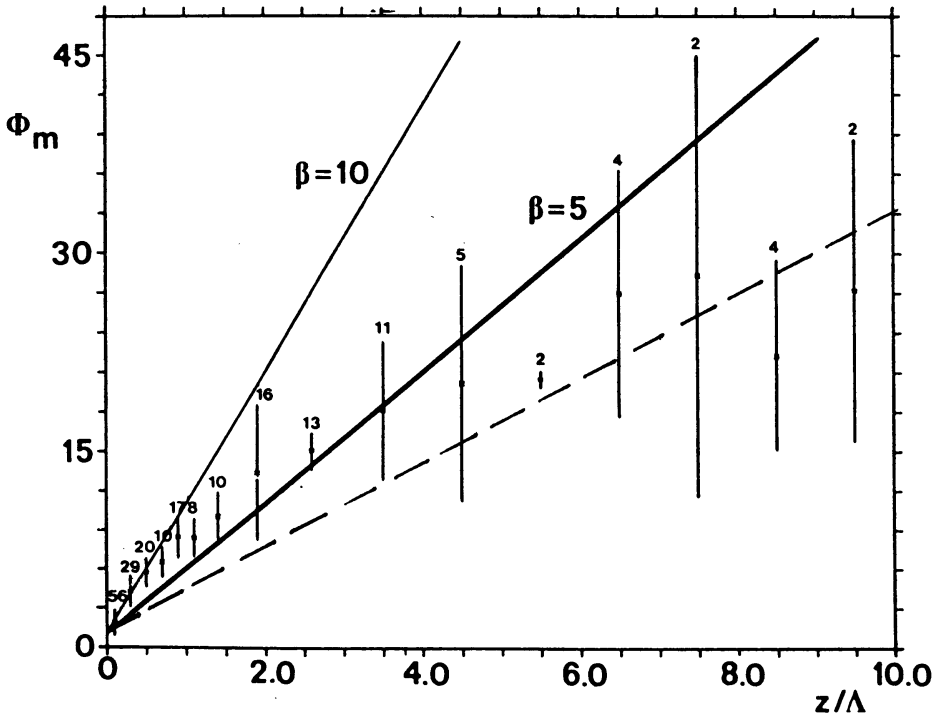

fig. 6.1 Dimensionless windshear versus stability found by Cuijpers (1987) compared to the result of this experiment (dotted line).

Cuijpers distinguished two slopes: the value $\beta=10$ should be compared to our result, $\beta=5$ is found for larger values of z/L. We didn't measure such values, because of the lower measuring height. The conclusion must be that although we find a slope that raises questions, the slope is certainly lower than 10, and does not agree with the slope from Nieuwstadt's data.

There is no good explanation for the rather low slope we find.The large distance between the temperature profile measurements and the flux measurements, as well as the omitted correction for humidity in turbulent heat flux used to scale the temperature gradient, will not improve the dimensionless windshear slope, which is also very low. The corrections for tilting won't change the turbulent fluctuations more than 10%. So further analysis is necessary to come up with better answers.

We looked at several wind direction sectors and found that for different wind directions different similarity relations are valid. The results are summarized in table 5.2. The choice of the sectors and the amount of data left in each sector are summarized in table 5.1. The difference between the different sectors is due to the different upstream surface conditions, or in other words the different histories of the flows. At the Cabauw site we distinguished the sector with westerly winds that is almost undisturbed and the sector with north-easterly winds that is disturbed by scattered trees, orchards and a village.

The theory for perturbed flows is confined to the neutral stability case. For rough to smooth transitions it predicts values lower than unity for the dimensionless windshear and the dimensionless temperature gradient, when the von Karman constant is chosen to be $\kappa=0.4$. This is indeed what we find.

For the stable regime we argued in §5.2 that the same slope for both the homogeneous and the inhomogeneous case should be found. With the results shown in figures 5.12 and 5.19 this prediction cannot be falsified.

With increasing stability we have smaller eddies, because there is less energy input. Smaller eddies, or fast turbulence, is produced and dissipated local as was already found by Nieuwstadt (1984) in his local similarity theory. Because there is a relation between the local gradient and the local flux, there is no reason why we would find another relation than the universal relation we should find under ideal circumstances, or at least we should find the same relation for undisturbed and disturbed areas at one location. This doesn't mean that the turbulence is not influenced by the changes in surface features, but the relation between local gradient and flux still holds.

For larger eddies, who evaluate much slower, the upstream surface conditions or the geometry of the surface do change the relation. This change can be seen in a shift of the whole curve and is characterized by the value of the similarity function round neutral.

Assuming that the fictional universal relation for $z/L>0$ is indeed a linear function of z/L, then the linear part representing the smaller eddies is always the same, while the constant is determined by the upstream history of the flow.

Changing the von Karman constant to obtain $\varphi_{m,h}(0)=1$ causes the slope to change

and is not correct. The von Karman constant is the value obtained for the true two dimensional flow, and is a real constant.

The results verify the local scaling approach developed by Nieuwstadt. In this case it can also be applied in the surface layer, although the term surface layer is not really appropriate here, because we don't have a so-called constant flux layer. The turbulent momentum and heat fluxes are functions of height as already argued by Beljaars (1982).Realizing this we spot another problem: the computed gradients are valid at the so-called differential height (see A.4), which is 14.4m in this experiment. The real measuring height for the fluxes is 14.4m. We thus assumed constant fluxes between 11.4 and 14.4m. Is this true? Probably not, and it could be one of the reasons for the for the slight difference in slopes between the different wind direction sectors.

In a future experiment the real measuring height has to be equal to the differential height, especially at the Cabauw site where terrain inhomogeneities play such an important role.

Concluding we state that terrain inhomogeneities do not change the slope of the similarity functions but cause a translation of the curve obtained from homogeneous terrain. The low slopes found compared to others in the literature ask for an explanation. Further analysis of the existing dataset or another experiment should give this explanation. We can conclude however, that the slope found by Cuijpers does definitely not agree with the slope we found.

APPENDICES

A.0 Figures of chapter 5

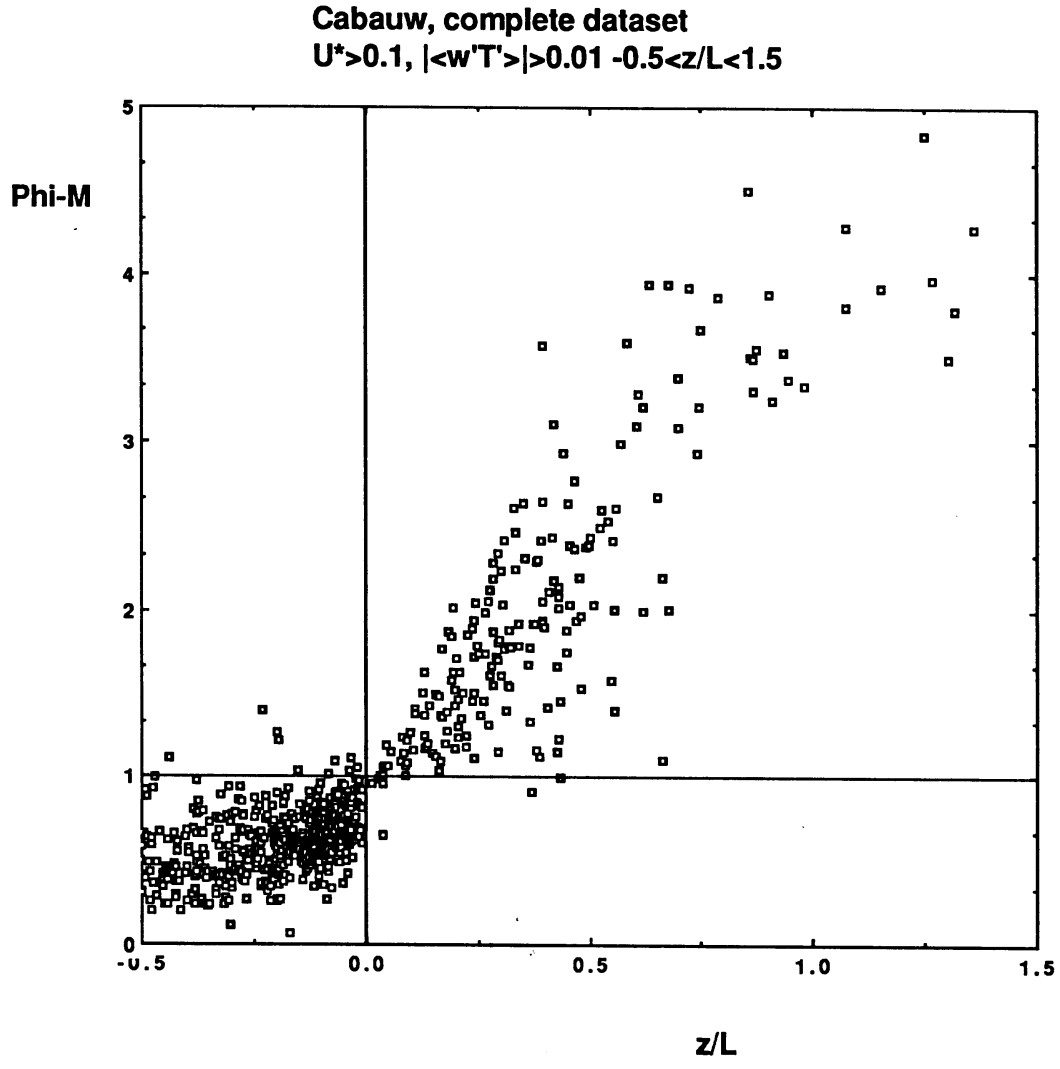

Fig. 5.1 Dimensionless windshear versus stability, completedataset for -0.5<z/L<1.5.

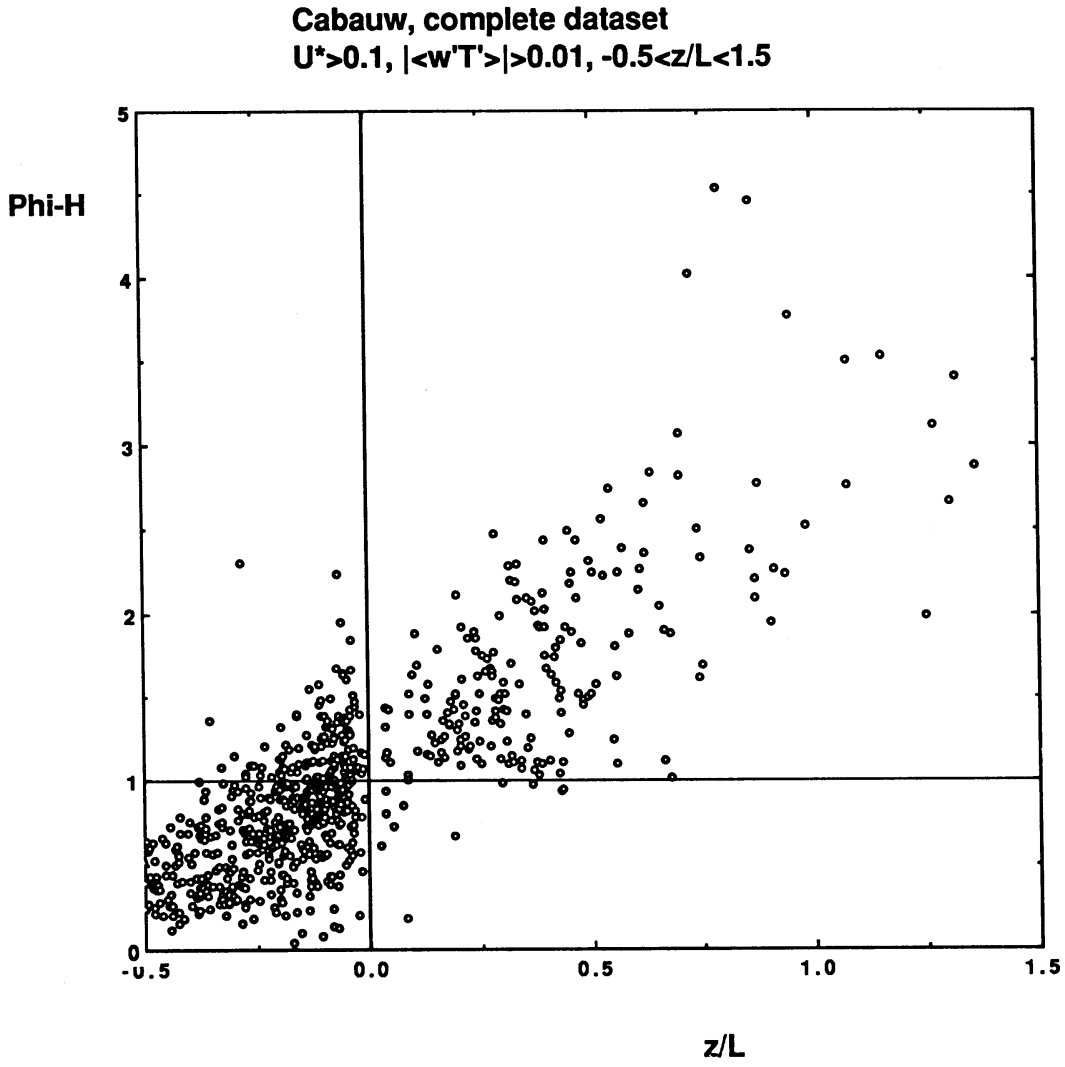

Fig 5.2 Dimensionless temperature gradient versus stability, -0.5<z/L<1.5

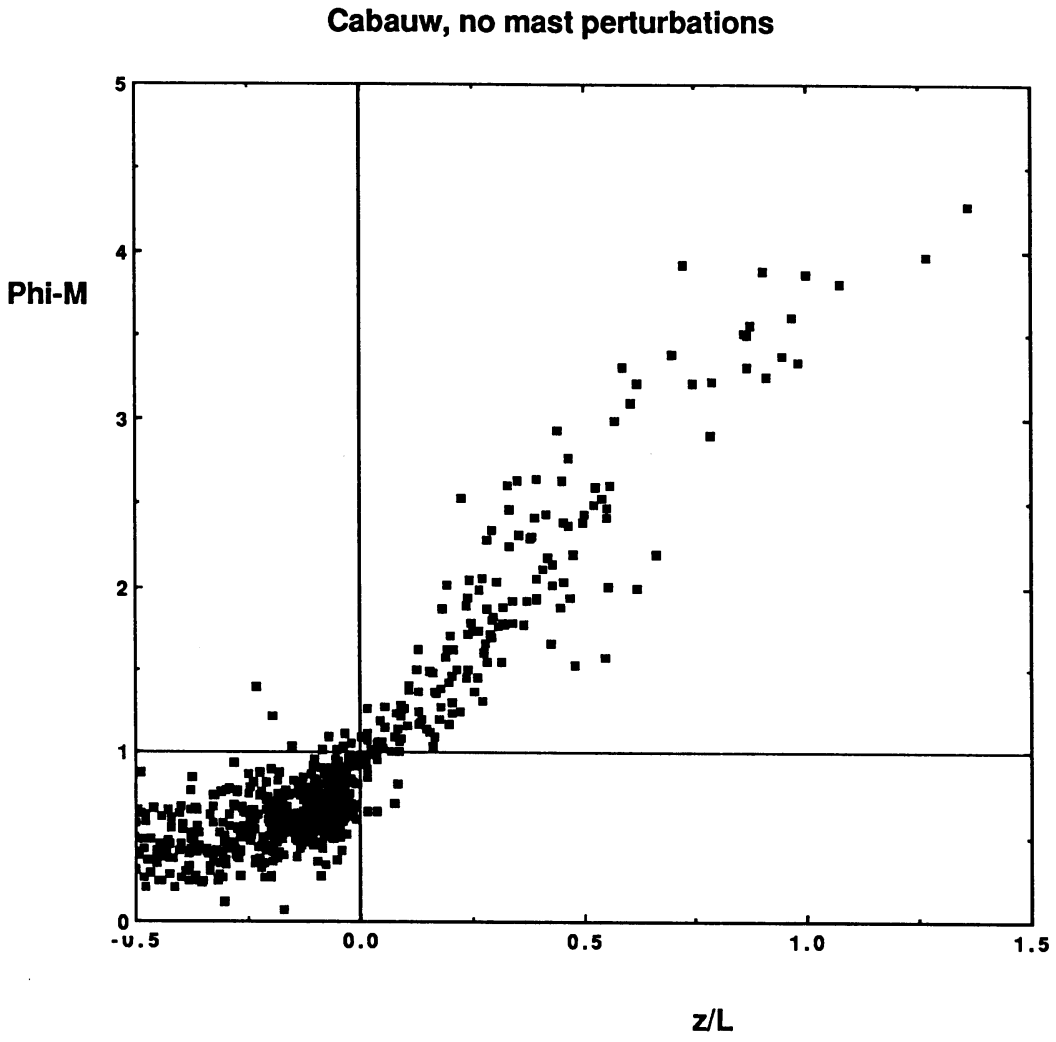

Fig 5.3 All data (φ_m)not perturbed by the main mast (182-92 degrees sector). The correction for <w'T'> > 0.01 has not been done here.

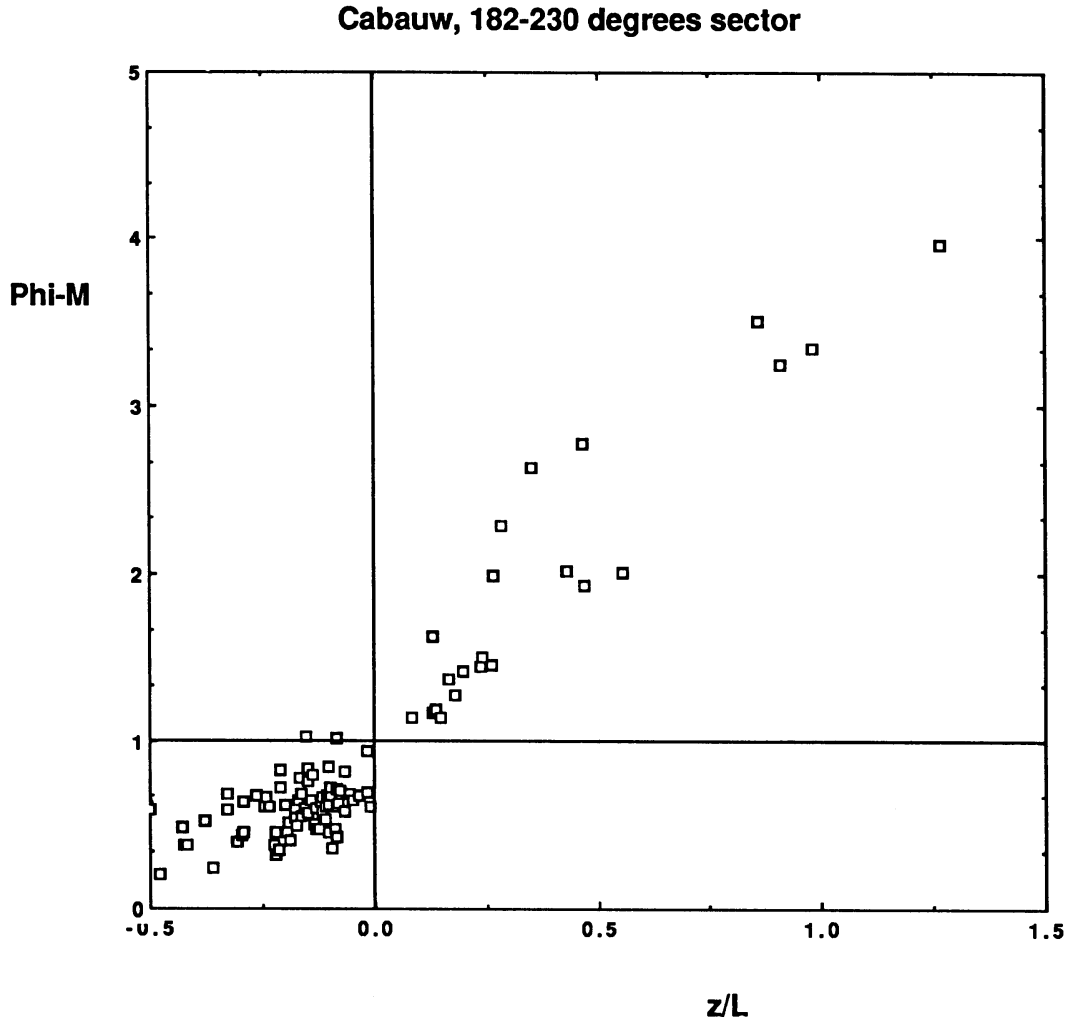

Fig. 5.4 182-230 degrees sector for φ_m, -0.5< z/L<1.5.

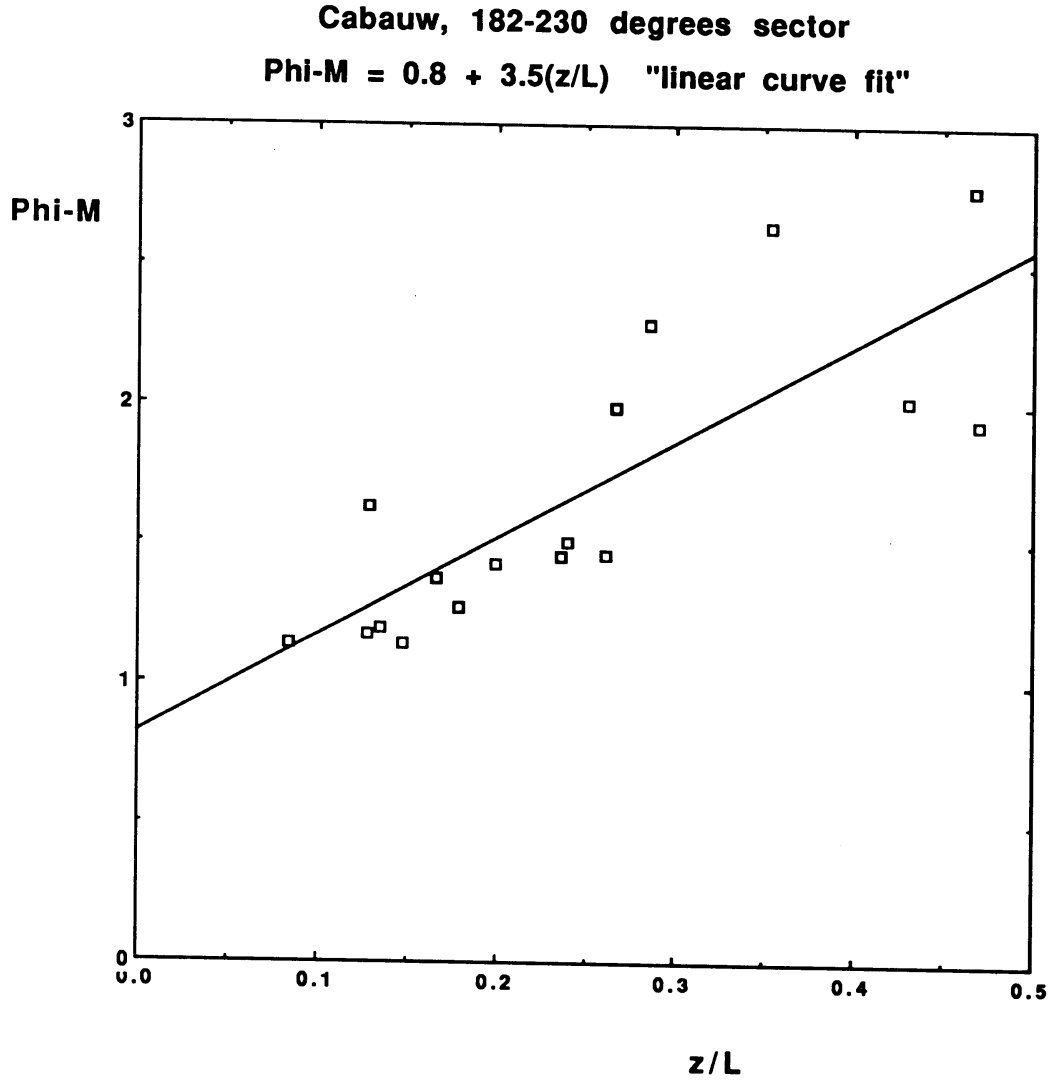

Fig 5.5 Slightly stable part of the 182-230 degrees sector with linear regression on 17 observations

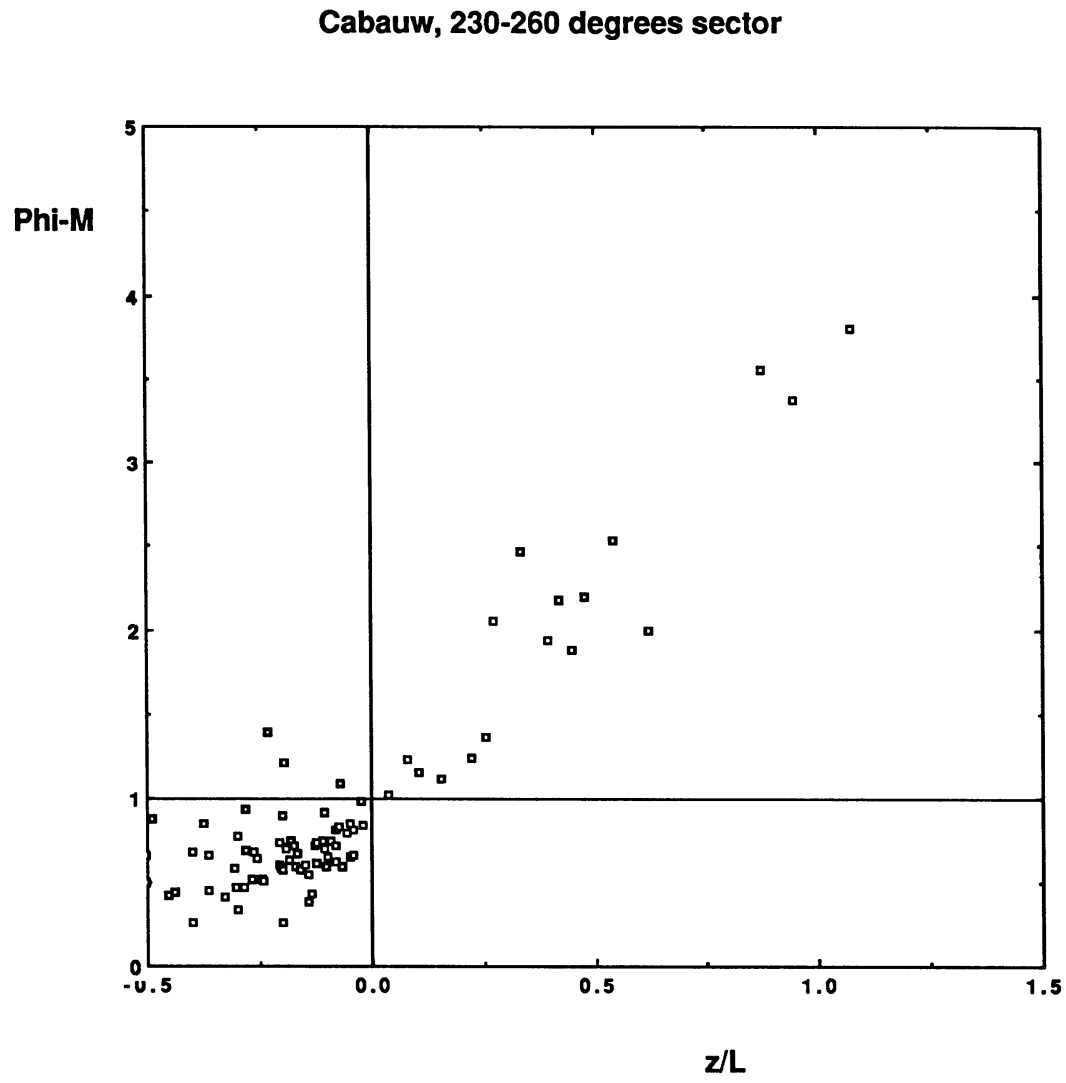

Fig. 5.6 The 230-260 degrees sector, homogeneous upstream flow conditions.

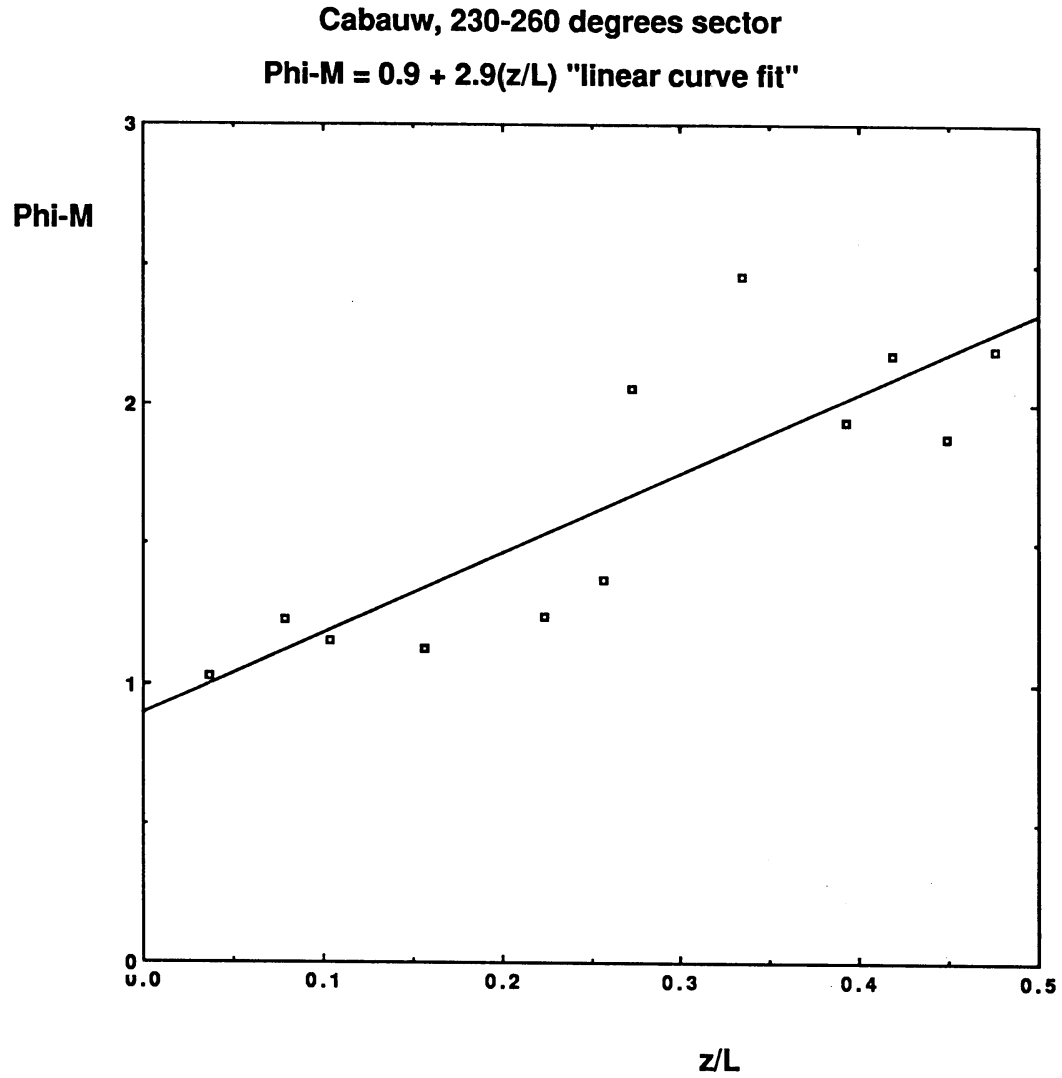

Fig. 5.7 The slightly stable part of the 230-260 degrees sector with linear regression on 12 observations.

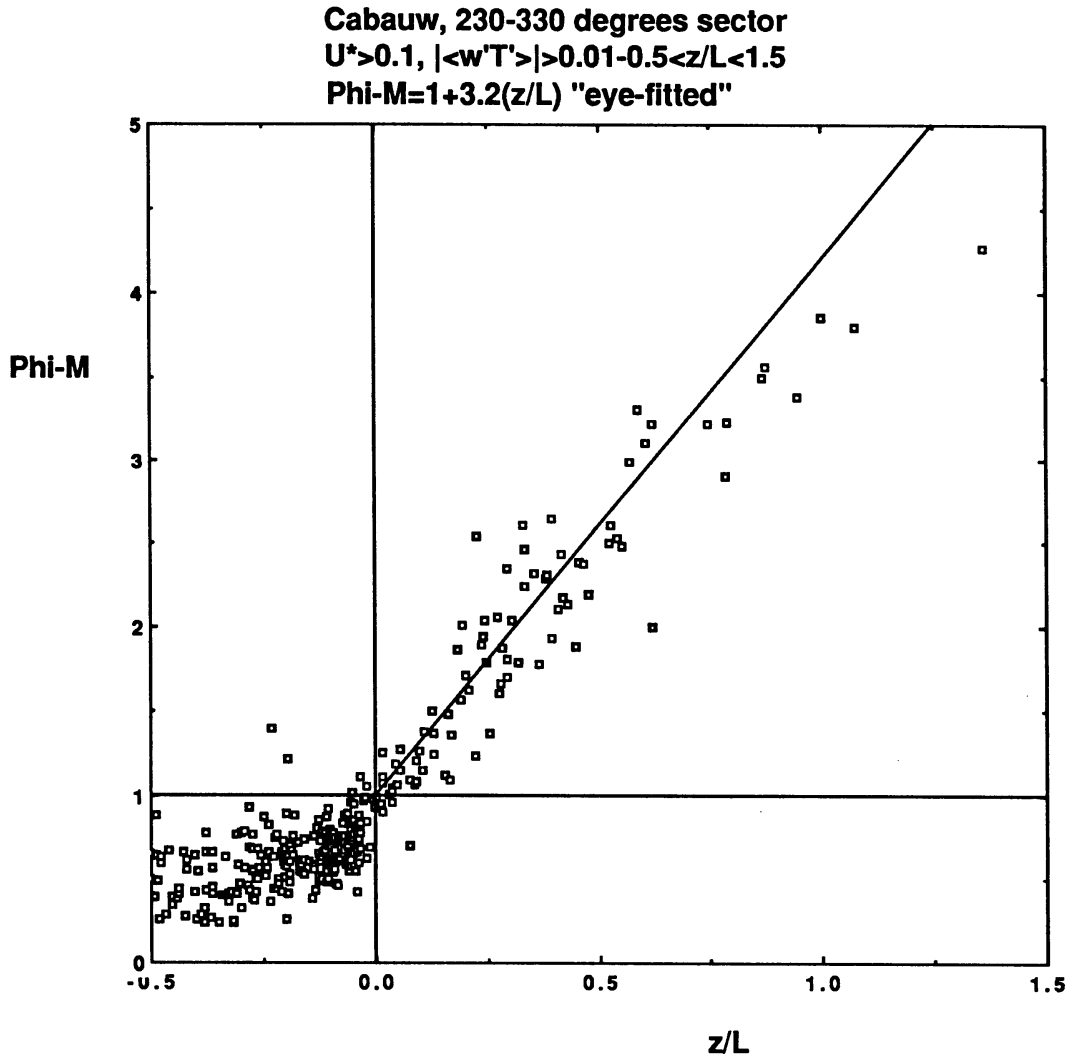

Fig. 5.8 The 230-330 degrees sector with an eye-fitted line for the slightly stable side.

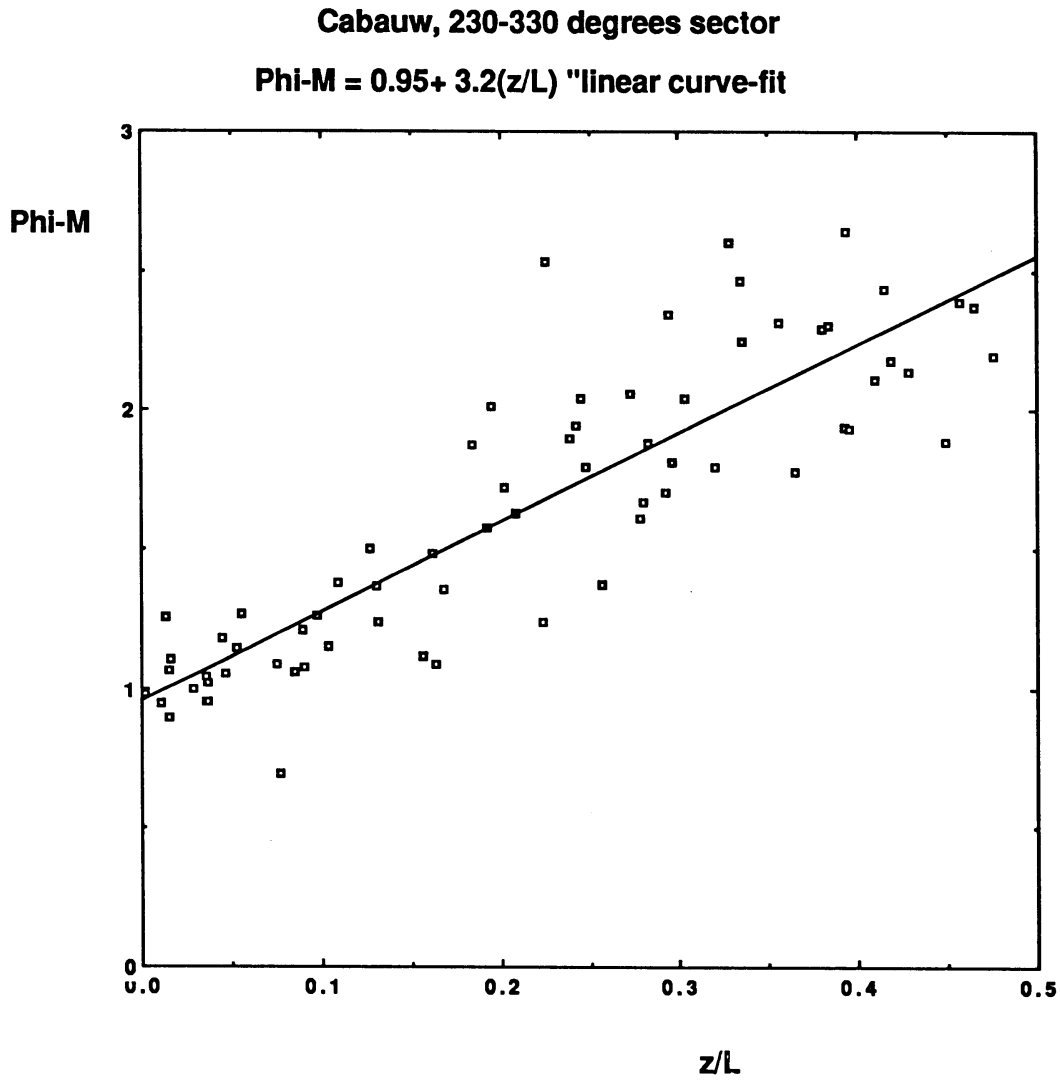

Fig. 5.9 Linear regression on 69 observations of the 230-330 degrees sector in the slightly stable range.

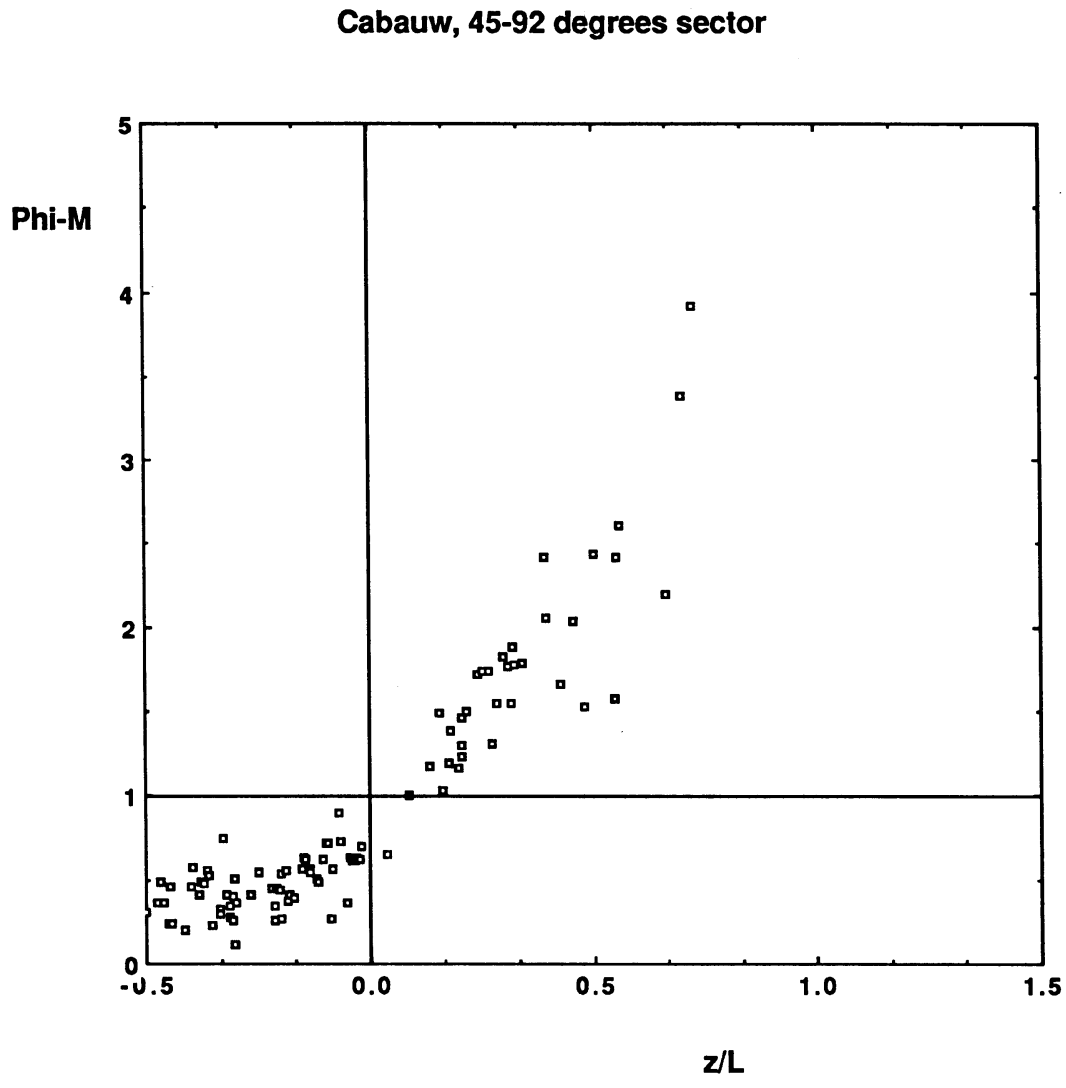

Fig. 5.10 The 45-92 degrees sector. Inhomogeneous upstream surface conditions. -0.5<z/L<1.5. The values round neutral are clearly smaller than one.

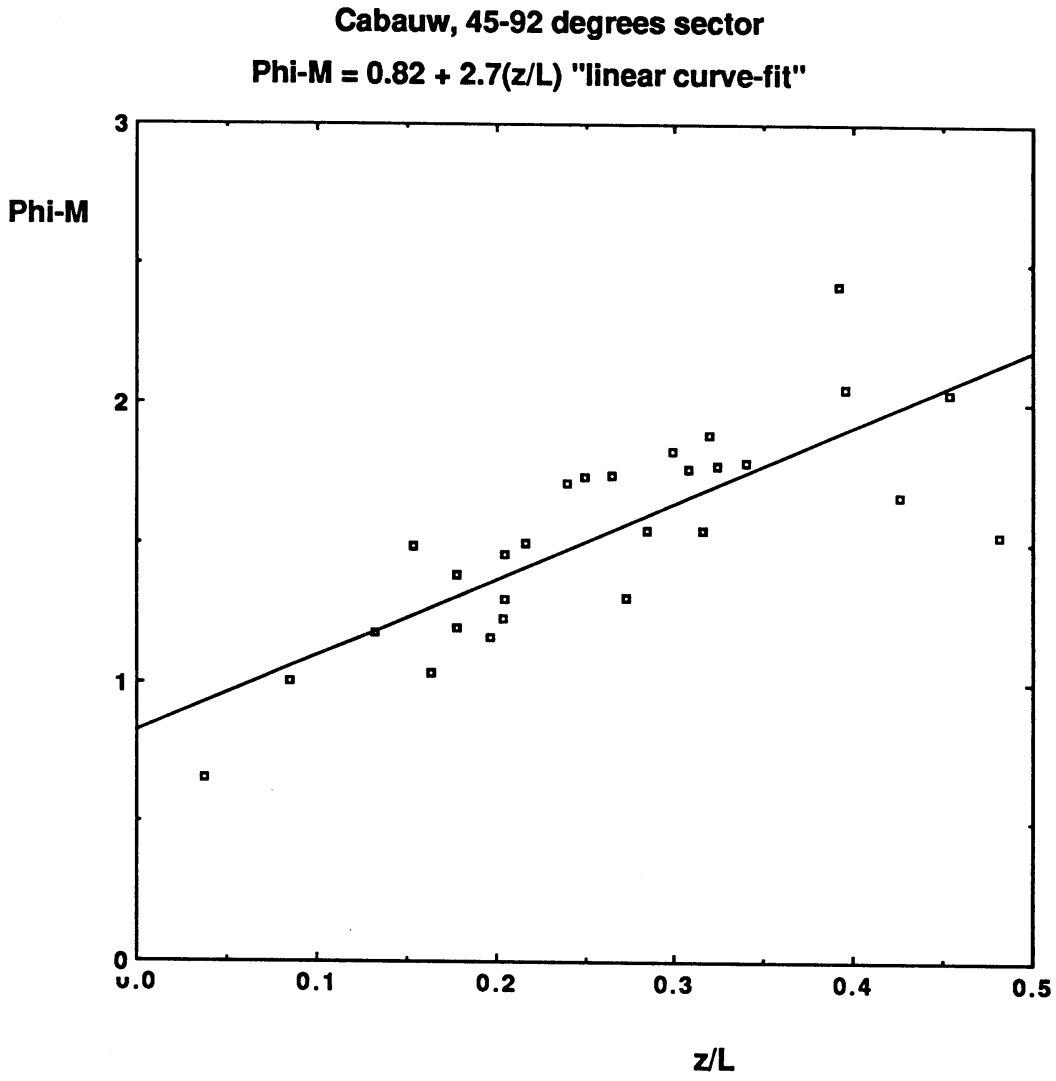

Fig. 5.11 Slightly stable part of the 45-92 degrees sector with linear regression on 28 observations.

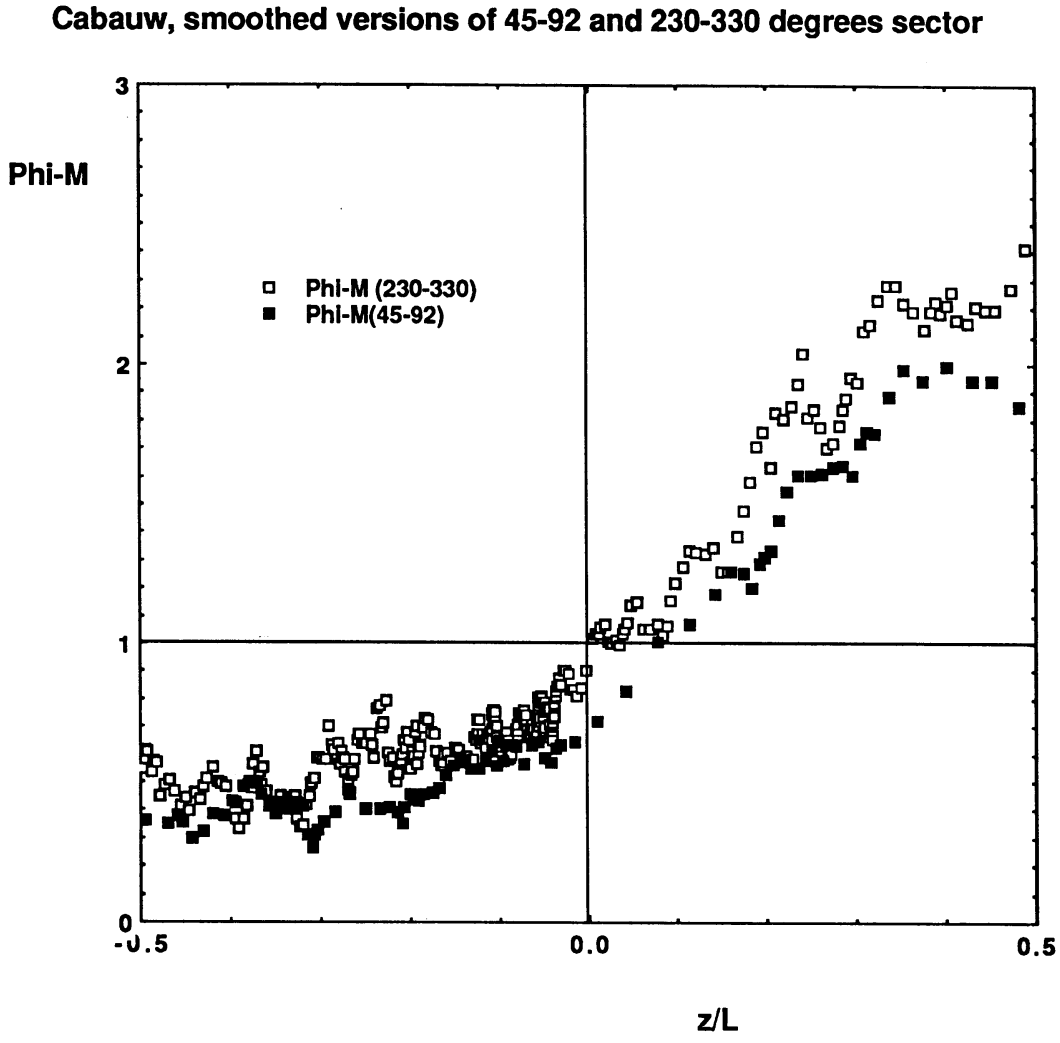

Fig. 5.12 Smoothed version of 5.8 and 5.10, running averages are taken over 9 and 5 values respectively. Black squares stand for the 45-92 degrees sector, open squares stand for the 230-330 degrees sector.

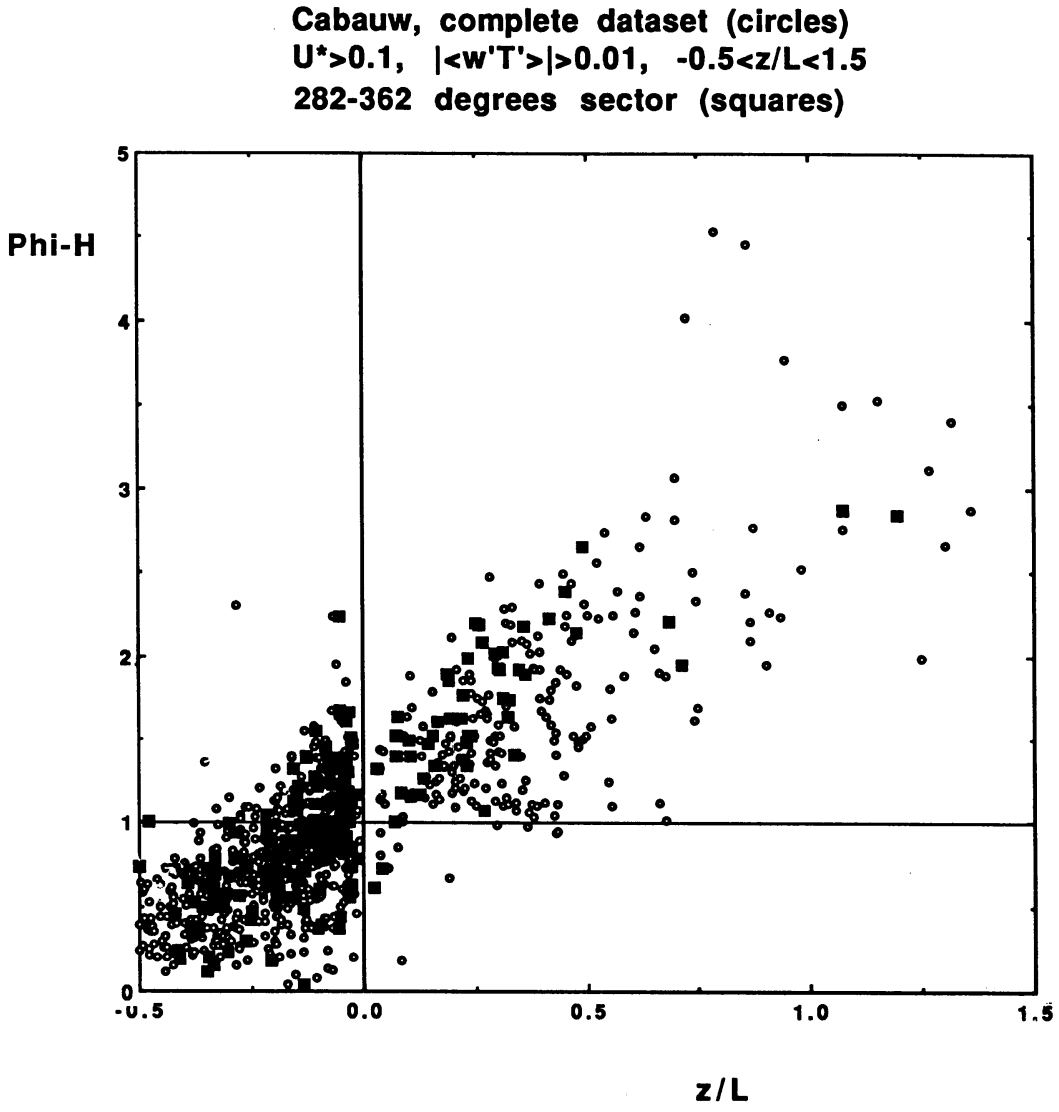

Fig 5.13 Combination of the complete φ_h dataset and the 282-362 degrees sector appearing not to disturb the temperature profiles. (circles and squares respectively)

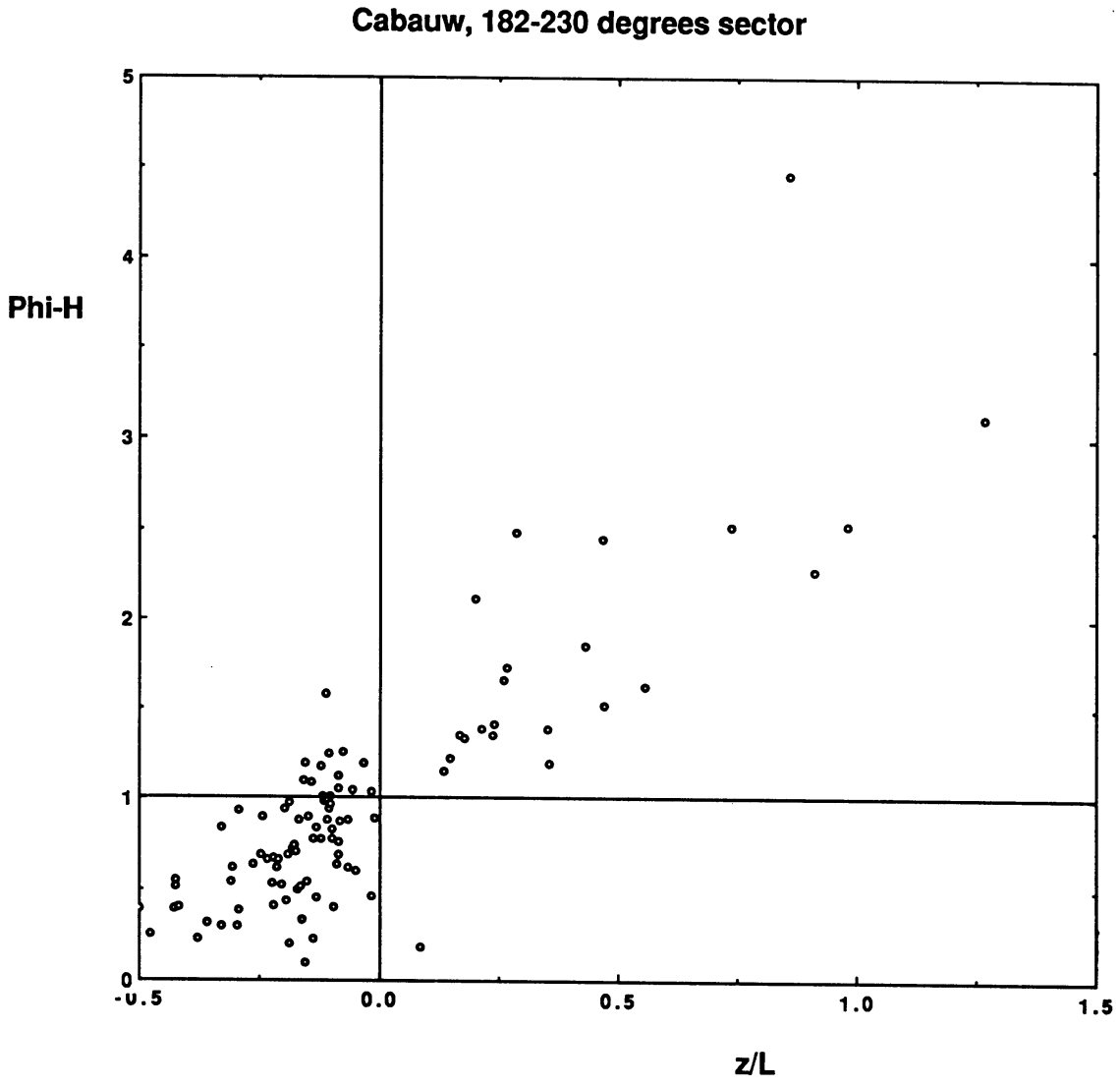

Fig. 5.14 182-230 degrees sector for φ_h, -0.5< z/L<1.5.

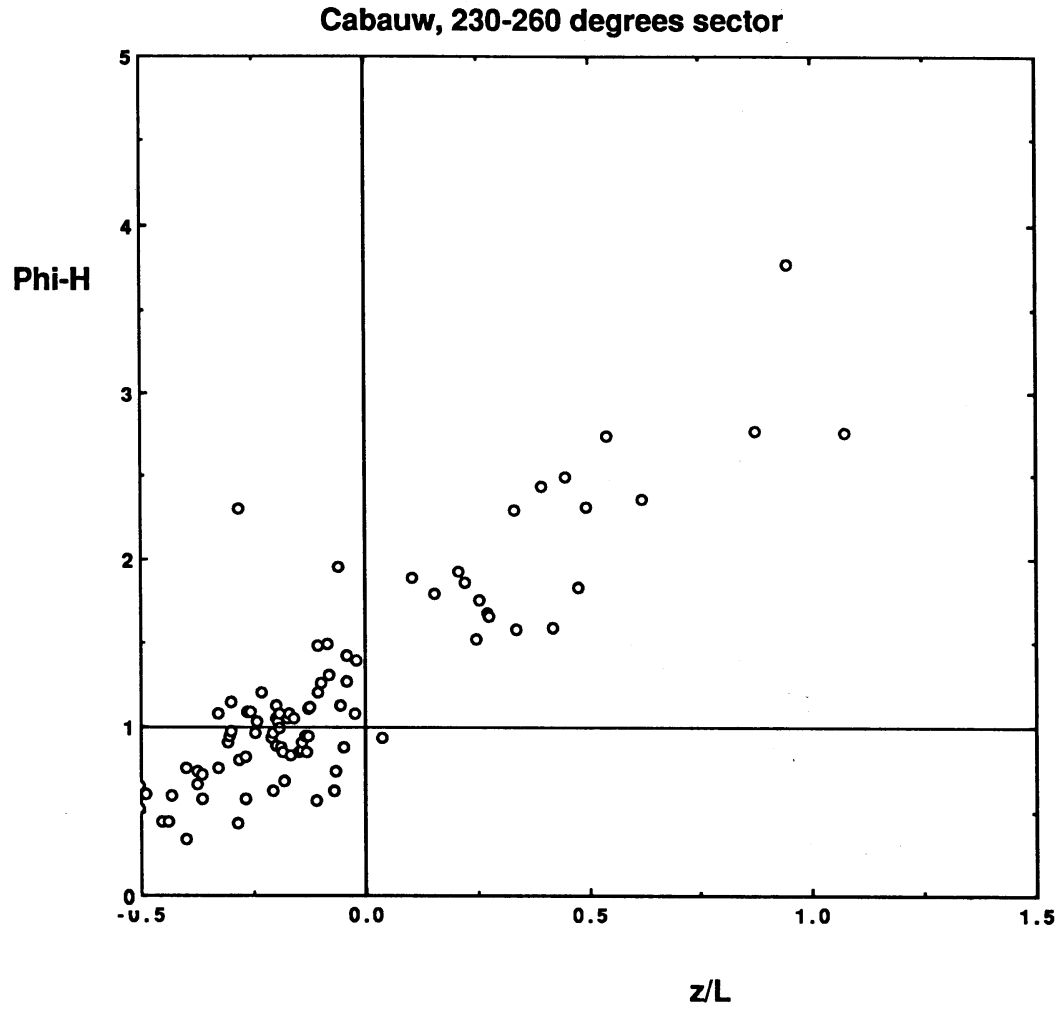

Fig. 5.15 230-260 degrees sector for φ_h, -0.5< z/L<1.5.

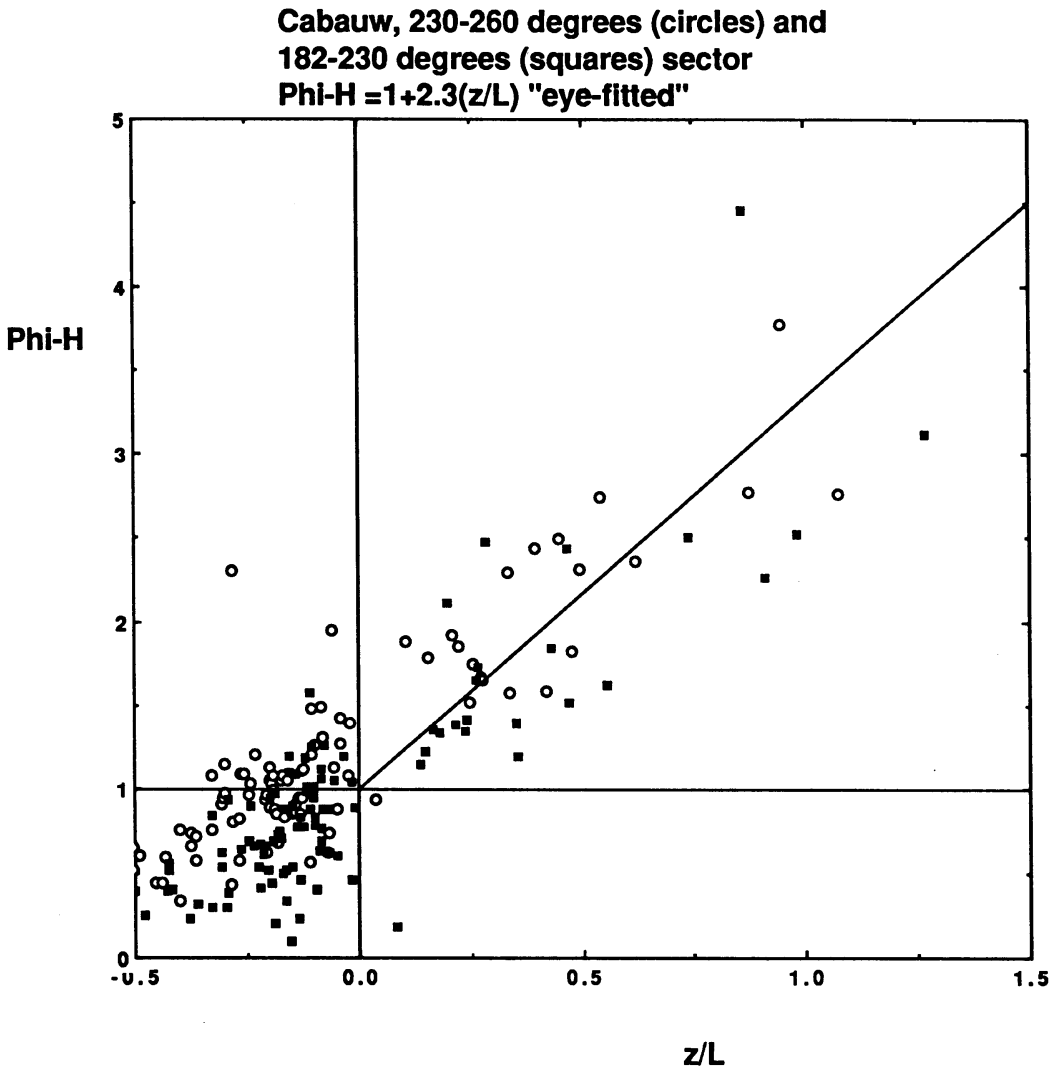

Fig. 5.16 Combination of the 182-230 and the 230-260 degrees sector for φ_h
An eye-fit was done, because linear regression seemed not useful.

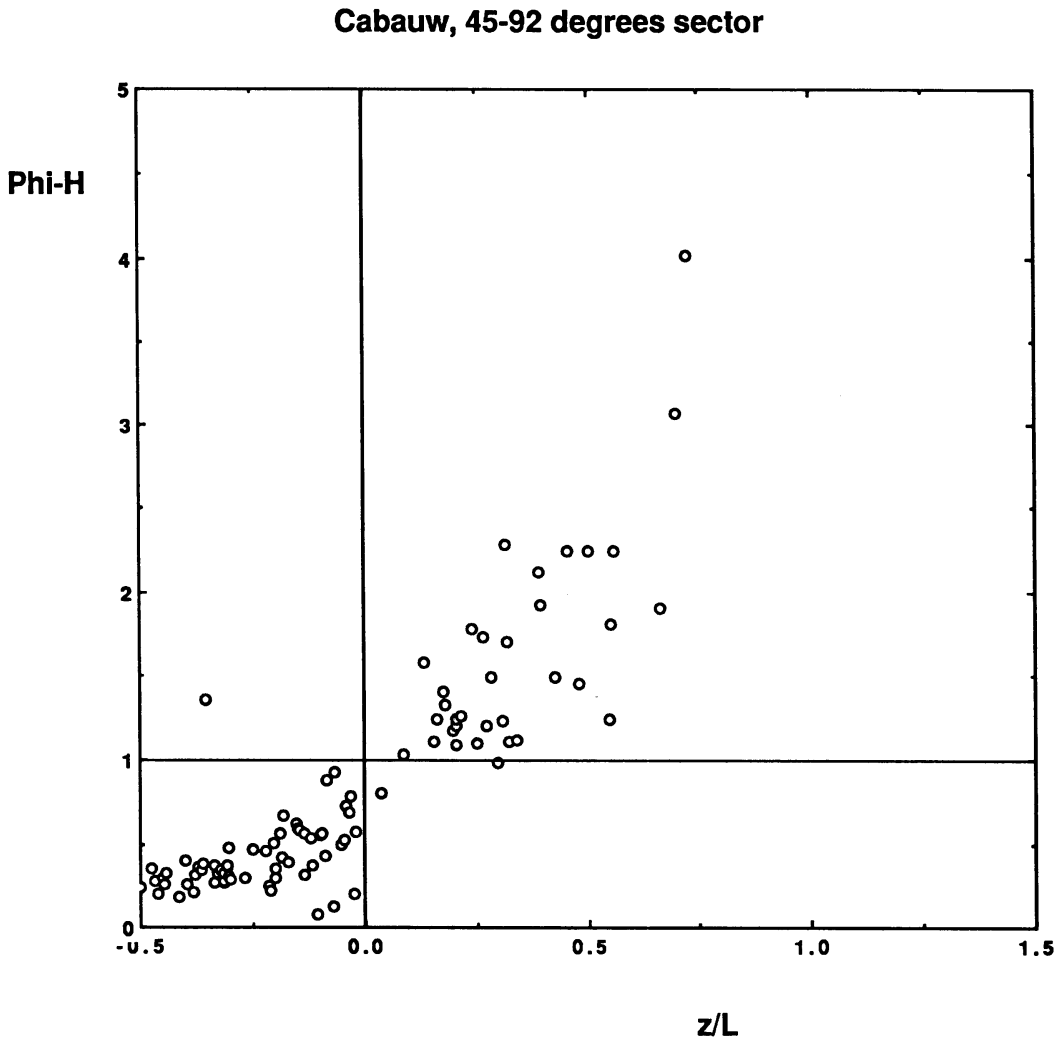

Fig. 5.17 The 45-92 degrees sector, -0.5<z/L<1.5, inhomogeneous upstream flow conditions. The value round neutral seems to be less than one.

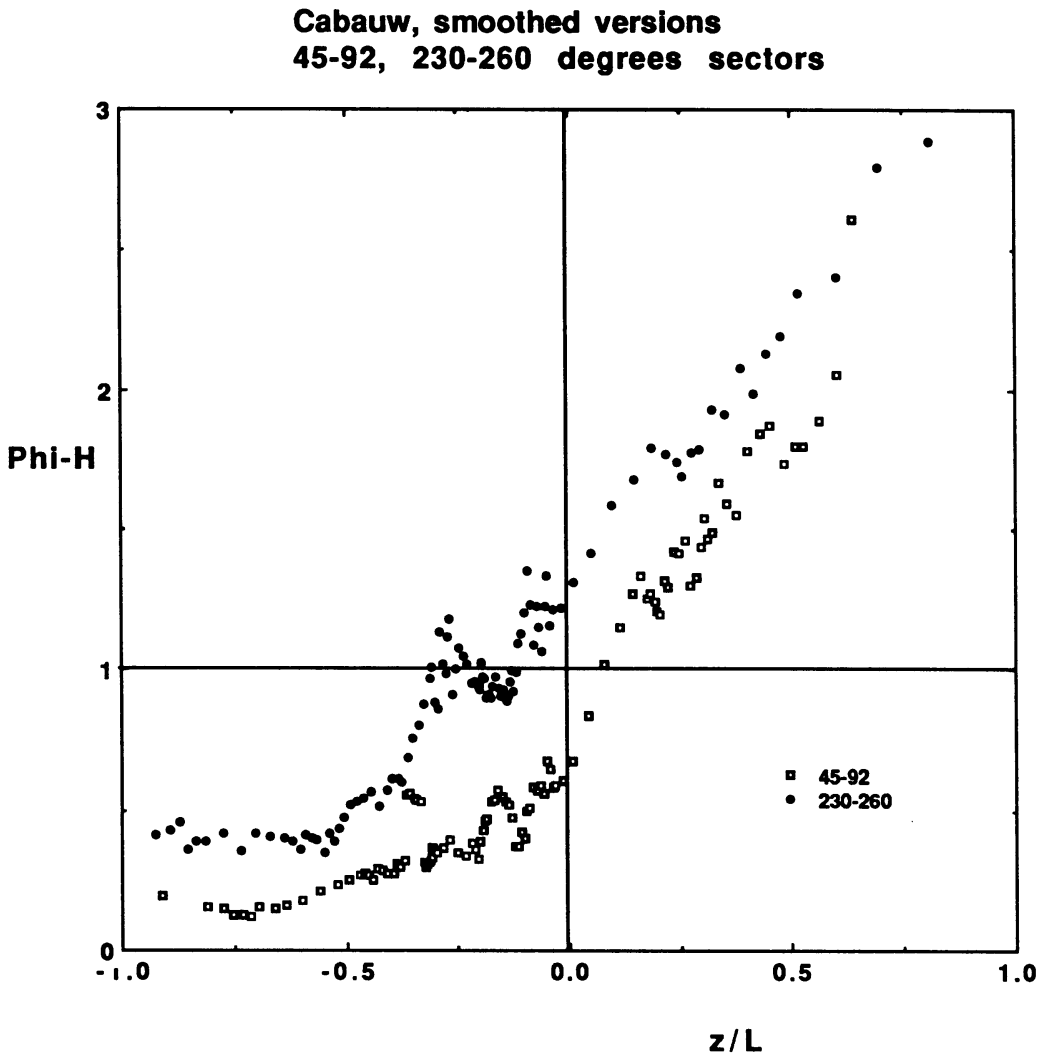

Fig 5.18 Smoothed versions of the 45-92 (squares) and the 230-260 (circles) degrees sectors, -1<z/L<1, A shift over the whole range from the inhomogeneous case (45-92) to the homogeneous case (230-260) can be seen.

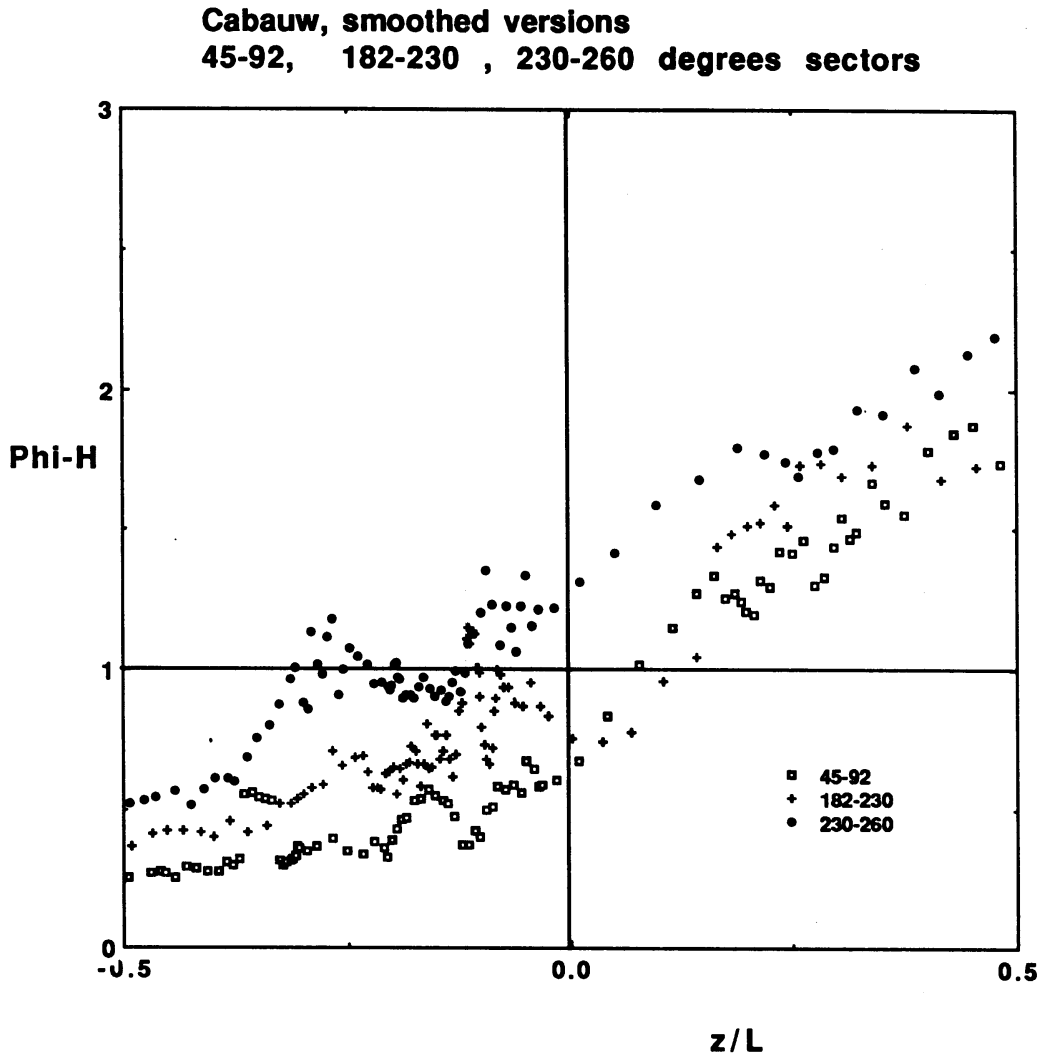

Fig. 5.19 Three smoothed sectors that show shifted curves. Compared to fig 5.18 the 182-230 degrees sector is added. It is less smooth than the other two.

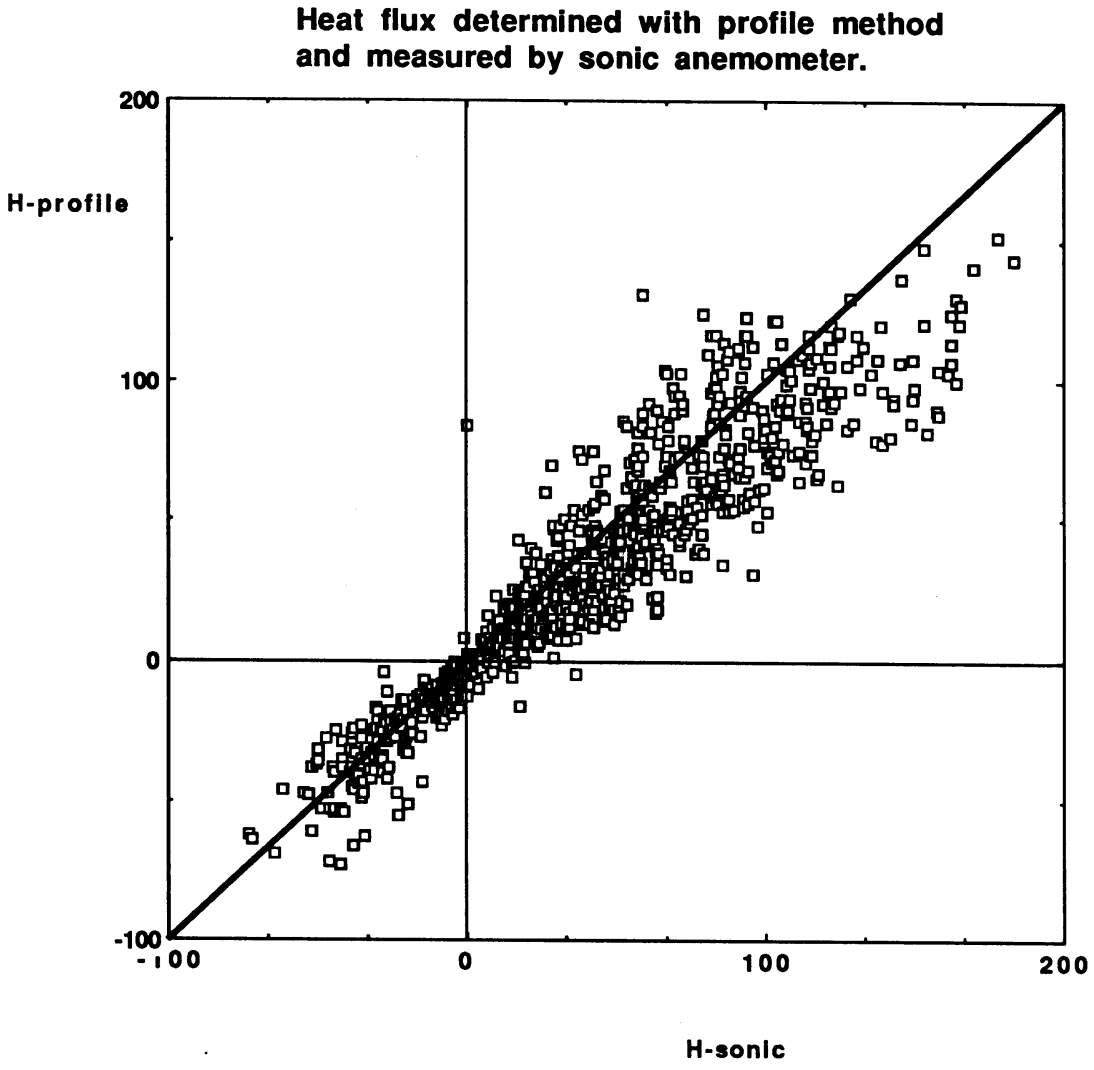

Fig. 5.20 Heat fluxes determined with profile method and eddy correlation measurements in Cabauw, while distance between profile and flux measurements was 95m.

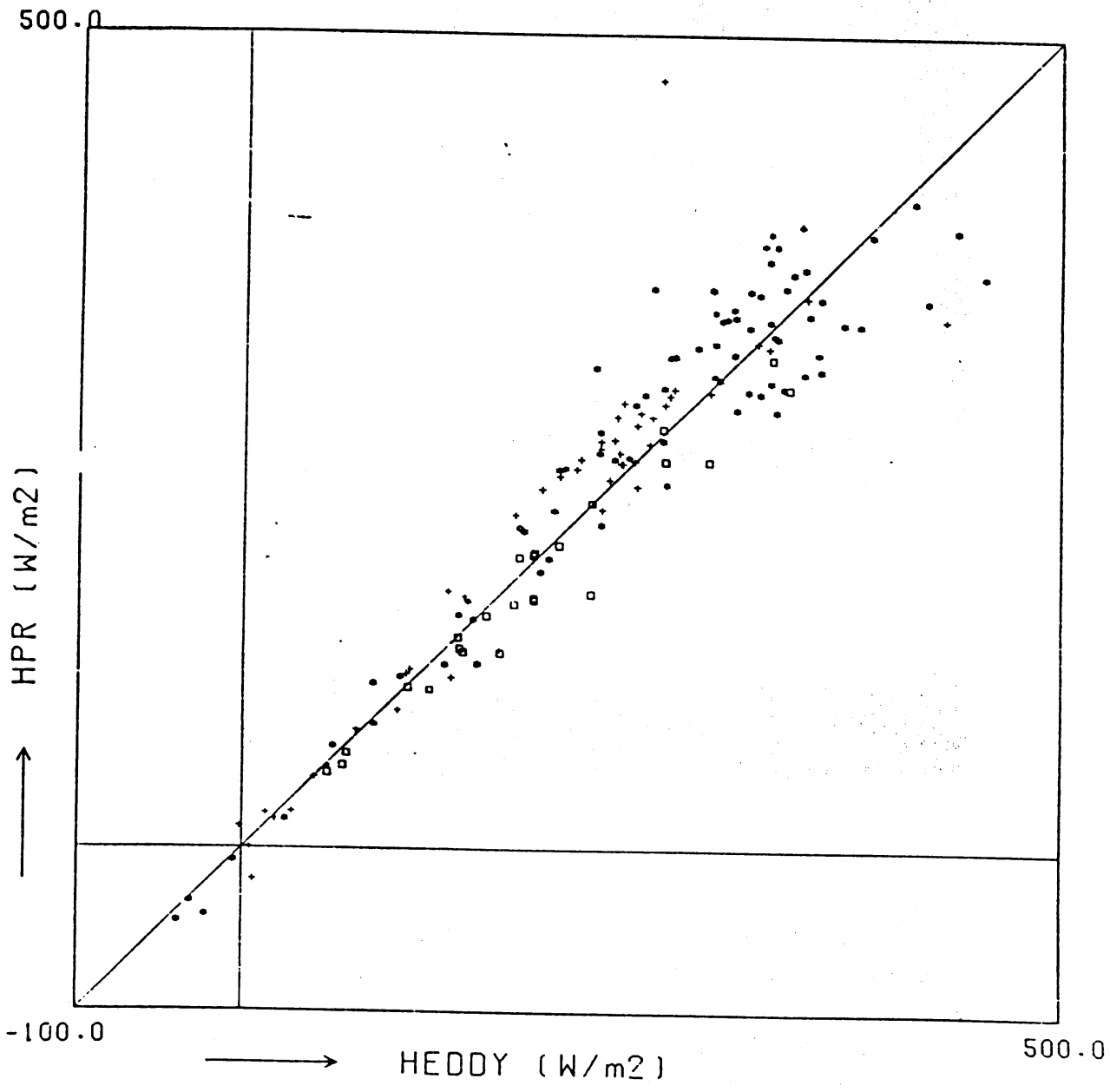

Fig 5.21 Same as fig 5.20, but the distance was 5m now, measurements done by Bosveld (1987) in Fochteloërveen.

A.1 The datalogger

A.1.1 Panel description

Fig A.1 gives an overview of the panel.

fig.A.1. the datalogger

With a Campbell 21X datalogger it is possible to convert a sensor signal into a digital value. It can process measurements over time and store the results for later retrieval. On the panel, the 16 character keyboard is used to enter programs, commands and data; these can be viewed on the 8 digit display (LCD). The 9-pin serial port provides connection to data storage peripherals, such as the SM192 storage module and provides serial communication to computer or modem devices for data transfer or remote programming. The panel also contains two terminal strips which are used for sensor inputs, excitation, control outputs etc. As the datalogger was very sensitive to high frequency noise, we designed low-pass filters (10k,100nF) and made the input channels compatible for BNC-connectors.The voltage loss by the filter was ~0.13%, which is acceptable.

A.1.2 Internal memory

The 21x has 40,960 bytes of internal Random Access Memory (RAM) divided into five areas; three of these areas are used in processing and storing measurement values. The five areas of RAM are:

-System memory: 958 bytes are required by the 21x operating system for overhead tasks such as compiling programs, transferring data etc. The user cannot obtain access to this memory.

-Program memory: 978 bytes are available for user programs entered in the two program tables or for subroutines. (see programming)

-Input storage: Input storage is the memory for storing the results of measurements or calculations. Input/output instructions place their results here, processing instructions operate on input storage values and place the result back into input storage. Input storage defaults to 28 locations, but additional locations can be assigned from Final storage.

-Intermediate storage: Some Processing instructions and most of the output instructions must maintain intermediate results calculated over time. These locations are assigned by the operating system and cannot be accessed by the the user. The default allocation is 64, but again additional space can be created at the expense of the final storage.

-Final storage: Final, processed values are stored here for transfer to printer, tape, extended memories or for retrieval via telecommunication links. Values are stored in the final storage only by the output processing instructions and only when the the output flag is set in the user's program. There are 19,328 final storage locations but this is reduced if input or intermediate storage is increased.

A.1.3 Programming

In fact programming here doesn't mean complicated algorithms and learning another language again. Single instructions mostly account for all programming problems. You can program the datalogger directly by keying in the instructions at the keyboard, but easier is the telecommunication software, which makes it possible to program on a pc and load the logger with an interface.

The datalogger has three program tables available.Tables 1 and 2 are given execution intervals which determine how often they are executed. Table 3 is used to enter subroutines which may be called from tables 1 and 2.

I already mentioned a few instruction types, I will shortly explain what they are used for, give a small programming example. For a detailed description see the manual (Campbell,21x manual)

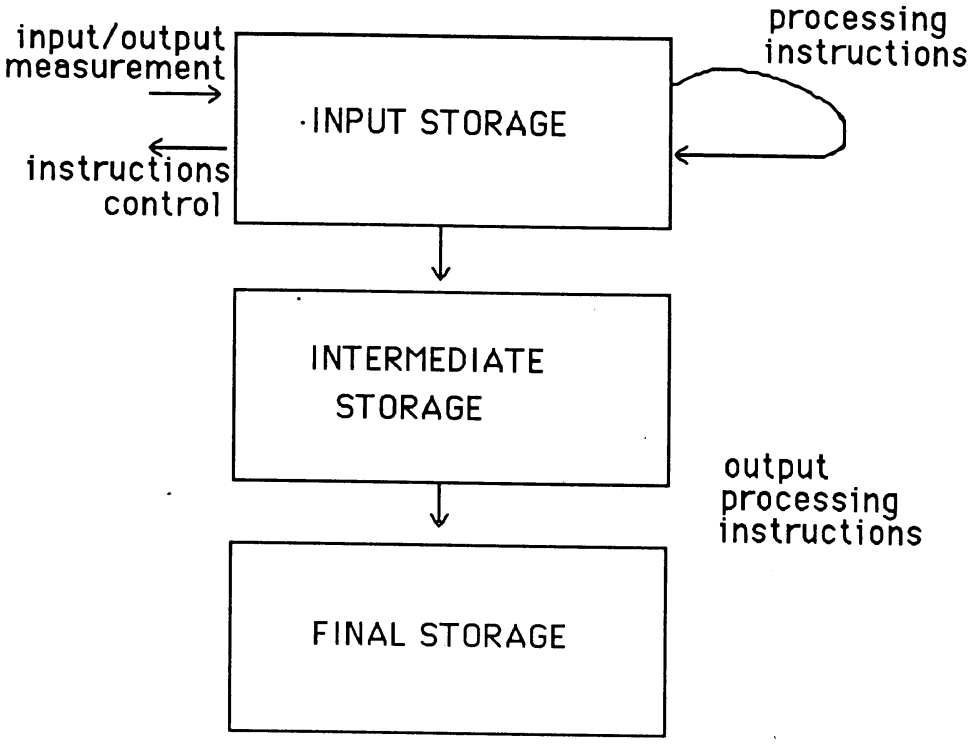

fig.A.2. schematic view of the datalogger architecture

There are input/output instructions which either tell the datalogger to measure an input channel and store the result in an input location or which tell the datalogger to generate an analogous or logical signal at one of the output ports.

Processing instructions are used to perform arithmetic operations on input locations, the results are also stored in input locations. Output processing instructions result in values being sent to Final storage or to external memory such as the the storage module, if the output flag is set.These instructions may involve some intermediate processing (e.g. averaging), the intermediate values are stored in Intermediate storage.

Finally program control instructions are used to modify flags and program execution sequence. The possibilities here are limited, but there are statements like IF THEN ELSE DO etc. There are also very intelligent instructions like a fast fourier transform, an instructions that produces a covariance matrix, and a burst measurement, which can sample a channel at a maximum rate of 1030 Hz, while the program table itself continues at a much slower rate, typically 1 Hz

A.1.4 An example

To give you an idea of the syntaxis used by the datalogger software we give a simple example.Suppose we want to measure windspeed and compute 10 minute averages and variances. The program could be made as follows:

Execution interval 0.6s

P1	single ended voltage measurement
1	repetitions
5000mV	range
1	start at input channel ..
1	store starting in input location ..
0.005	multiplier (1000mV=5m/s)
0	offset
P92	IF TIME
0	if time is ..
10	minutes into a ..
set output flag	minute interval then do:
P62	covariance matrix
1	no of input values
1	no of means
1	no of variances
1000	no of samples (10min.=600s, execution interval=0.6s)
1	first input loc. of input string
2	first input loc. to store the result
P70	sample (sends values to output if output flag is set)
1	repetitions
2	input location
P77	sends real time to output if output flag is set
code	hours,minutes
P95	END

This program measures a signal on inputchannel 1 every 0.6 seconds, stores the result in an intermediate storage location and adds the next sample until 10 minutes have past. Then it will put the results in input locations 2 and 3. The values will then be sent

to final storage by the sample instructions because the output flag is set. In every output string the time in hours and minutes will be included.

The single ended voltage measurement is made by integrating the input signal for a fixed time and then holding the integrated value for the analog to digital conversion. There is an option to choose between a fast and a slow integration time. The fast integration rate minimizes time skew between measurements and increases the throughput rate, while the slow one provides a more noise-free measurement.

The output can be retrieved with telecommunication software in the format you desire. Campbell also provides data reduction software, but I found that not so useful. For further explanation I refer to the manual.

A.1.5. The Cabauw program and problems

We want 16 input channels to be sampled. From these channels we want 10 minute averages from which we make thirty minute averages. We want to do a burst measurement of W and T and we want some standard deviations and a covariance matrix with 25 components. This doesn't seem very complicated and it isn't. We also want the datalogger to turn the rotor if necessary. Now this is complicated!

Computing the wind direction from the horizontal wind components can be done by taking the arctangent of v/u, comparing this with the azimuth R of the rotor yields the direction to turn to. Unfortunately there is no arctangent function available. There is a program instruction that calculates the wind direction, but this is an output processing instruction, which means the result is not available for the user. The solution is a polynomial for $|v/u|<1$:

$$PHI=55.91(v/u)-11.42(v/u)^3 \qquad (A.1)$$

When $|v/u|>1$ then use the relation:

$$\arctan(x)=90 - \arctan(1/x) \qquad (A.2)$$

When comparing with the azimuth do realize, that meteorological coordinates are different from goniometric ones. Apart from that the azimuth is measured with a potentiometer that has a 3 degree gap. It cannot turn 360 degrees. We situated the gap at 137 degrees from the north. This is the direction distorted by the big mast, so we made the gap even larger: 20 degrees. Summarizing: when the datalogger decides it has to adjust the rotor, it has to decide whether it is possible to take the shortest circle or not. In order not to infect the samples while turning, we have chosen to transform the U and V components to the North-East coordinate system on-line.

Now that this is solved we discover we are running out of memory. The datalogger is clearly not meant to adjust rotors. Furthermore every instruction takes processing time, thereby extending the minimum execution interval. The datalogger communication software failed to work when the datalogger was used at full capacity.

Communication apparently has a lower priority than sampling and calculating.

If the execution time of the program is longer than the execution interval, the datalogger will only execute that part of the program that fits within the interval. We reduced the program to 874 bytes of the total 978 bytes program memory. Adding up the instruction processing times in the program yielded 691.1 milliseconds. An execution interval of 0.7s however was not possible. Perhaps switching between program and subroutines costs lots of time, or sending logical signals to the control ports? We could not discover the reason and used a safe 0.8s execution interval, that is a 1.25 Hz sampling rate.

One step in reducing the program was to use only program table 1 combined with subroutines instead of using both program tables. This proved to save lots of execution time probably involved in switching between tables.

A structure diagram of the final program as well as a listing is given in appendix B1.

A.2 Description of software to join Cabauw and datalogger data

In order to work comfortably I had to make a selection and join the data made by the datalogger and the routinedata from Cabauw. The software needed to perform these tasks is written in standard Fortran77. The main program and its subroutines are:

main program:	DAGFILE.FOR
subroutines:	DATENAME.FOR
	READTKS.FOR
	READINP.FOR
	DATABASE.FOR
	SELREC.FOR
inputfiles:	DAGFILE.INP
	READ.INP
	BASENAME.INP
	CABNACHT.TKS

Listings can be found in B.2.The datafiles available are the following:

CAB89MM.DIR, with MM=07,08,09,10
CA89MMDD.B30, with MM=07 and DD=(19,....,31)
MM=08 and DD=(1,..,7),(10,..31)
MM=09 and DD=(1,..,30)
MM=10 and DD=(1,..,11)
CA89MMDD.LO3, with MM=07 and DD=(19,....,31)
MM=08 and DD=(1,..,7),(10,..31)
MM=09 and DD=(1,..,30)
MM=10 and DD=(1,..,11)

The software and datafiles are available at the KNMI for further analysis, contact person is F.Bosveld.

The Cabauw data consist of direct access monthfiles with a recordlength of 420 bytes (210 integer*2 words) named CABYYMM.DIR. The datalogger files are day files with a recordlength of 176 bytes (44 real*4 words) named CAYYMMDD.B30, where YY and MM stand for year and month respectively, DD stands for day of the month. The data are in both cases thirty minute averages, although the Cabauwfiles use the end of a thirty minute interval and the datalogger uses the beginning of a thirty minute interval as index. Several subroutines are used to create filenames that can be read by the fortran program DAGFILE.FOR and take care of all the trouble involved in shifting days, half hours etc. DAGFILE.FOR joins a CABYYMM.DIR file and the CAYYMMDD.B30 files requested. The resulting CAYYMMDD.LO3 file consists of three blocks of nineteen columns. The first two blocks, 38 columns are datalogger data. The third block, nineteen

columns are Cabauw routine data. The first record of each block consists of headers. The data are written in ASCII code, scientific notation. It is possible to choose another set of data from the Cabauw and datalogger files by changing the inputfiles to DAGFILE.FOR. These inputfiles specify the coordinates of the data in the arrays containing the complete set of data.

For the datalogger data the possibilities are listed in the file CABNACHT.TKS. This is also the file where DAGFILE.FOR gets the headers for the .LO3 files. The data are numbered: write the number of the datum you wish to see in the .LO3 file in DAGFILE.INP. It is possible to choose 38 data out of the first 44 data listed in CABNACHT.TKS: these are datalogger data.

For the Cabauw data the story is a little more complicated. The positions of the values in the records of a .DIR file have to be specified in READ.INP, while the headers are listed in CABNACHT.TKS. When DAGFILE.FOR starts reading, it first reads DAGFILE.INP to find the headers in CABNACHT.TKS (for datalogger and Cabauw data). Then it reads 38 datalogger values from a .B30 file. Next it reads the positions of the Cabauw elements in READ.INP, these are used to fill the record in the .LO3 with the last 19 values from the .DIR file. A listing of the Cabauw data is given in Engeldal (1987) table 1, from this list we can choose 19 values. A subroutine SELREC.FOR uses these values to read data from the CABYYMM.DIR file. Write the positions of the values in the file READ.INP. The headers for these values have to be written in CABNACHT.TKS. Now write the CABNACHT.TKS datanumbers of the data specified in READ.INP also in DAGFILE.INP. This results in putting the headers for the Cabauwdata at the right position, the following records will be read with the help of READ.INP by SELREC.FOR.

In the following example we wish to have U,V,W and LPHI from the datalogger dataset and F200 and F140 from the Cabauw set. Therefore we write the numbers 1,2,3,44 in DAGFILE.INP. Then we look at table 1, we need the numbers 38 and 42, we write them in READ.INP. Then we also want the headers right. We write the name of the header in CABNACHT.TKS. As we can see there is room for 36 headers apart from the datalogger headers. Finally we write the numbers of the F200 and the F140 header in DAGFILE.INP. The needed files now look as illustrated (fig A.2.1):

Note that in this example we only took four datalogger data and only two Cabauw data. We have to use 38 datalogger data and 19 Cabauw data. If another combination is desired, the program DAGFILE.FOR needs to be adjusted.

The resulting CAYYMMDD.LO3 file will be LOTUS 123 importable for further analysis and looks as follows (fig A.2.2)

We measured from the 19th of July until the 11th of October. August 8 and 9 are missing due to the destruction of the sonic anemometer by lightning.

Most of the software concerning the datalogger data are adjusted copies of Fred Bosvelds' software for the Speuld project, the subroutine SELREC.FOR is written by Anton Beljaars and described by C. Engeldal in Memorandum FM-89-11. This memorandum also contains table 1 mentioned above.

cabnacht.tks		dagfile.inp	read.inp	table 1	
nr	header	nr	nr	word	element
1	U	1	*38*	*0*	MMDD
2	V	2	*42*	*1*	UUMM
3	W	3		2	T200
.	.	44			.
.	.	*46*		*38*	F200
44	LPHI	*47*		.	
45	.			*42*	F140
46	F200			.	
47	F140			.	
.				*209*	
80					

fig A.2.1 Schematic view of the inputfiles involved. Italics are used to indicate the room used by Cabauw data.

```
[header(0),header(1), .....                    ....,header(18)]
[value(0),value(1),.....                        ....,value(18)] 000h
[value(0),                                          value(18)] 030h
[                                                       .
.                                                       .
.                                                       .
[       .....                                .....      value(18)] 2330h

[header(19)    ....                                ....   header(37)]  000h
[
.                                                           .
.                                                           .
[                                                       value(37)] 2330h

[header(38)  ....                                  ....              ] 000h
    .                                                       .
[   .                                                   value(57)] 2330h
```

fig A.2.2 Structure of the CAYYMMDD.LO3 file created.

A.3 Linear regression

The analytical relation between y and x: y=mx+c has to be verified by experiments. Here we find the statistical relation for the stochast Y:

$$Y = mx + c + \zeta, \qquad \text{(A.3.1)}$$

where ζ, the error, is independent of x and the expectation $E(\zeta)=0$. The slope m and c are constants, x is called the independent. The variance of ζ is by definition: $Var(\zeta)=\sigma^2$. Further we see that:

$$Var(Y)= Var(mx+c+\zeta)=Var(\zeta)=\sigma^2 \qquad \text{(A.3.2)}$$

This means Y is characterized by three parameters, namely m,c and σ^2. We estimate these parameters by means of the least square method for linear regression. The estimators (estimators are denoted by italic writing)for m,c and σ^2: *m*,*c* and s^2 are stochasts again and we estimate their variances to obtain information about the range they fall in:

$$Var(m) = \frac{\sigma^2}{\sum\left(x_i^2 - \bar{x}^2\right)} \qquad \text{(A.3.3)}$$

$$Var(c) = \frac{\sum\left(x_i^2\right)}{n}\frac{\sigma^2}{\sum\left(x_i^2 - \bar{x}^2\right)} \qquad \text{(A.3.4)}$$

For i = 1 to n. The overbar denotes the average.

Lotus 123 provides a facility that computes the estimate for Var(m) or σ_m^2 : s_m^2 (Eq. A.3.3) and s^2 as an estimate for σ^2. Having this information it is possible to derive the estimate for Var(c):s_c^2 by computing $\sum\left(x_i^2\right)/n$ and multiplying it with s_m^2. In our results we present our linear regression curve as follows:

$$y= (m \pm s_m)x + (c \pm s_c). \qquad \text{(A.3.5)}$$

The assumption that ζ is independent of x is essential: it means that for the whole x range, the range of the scatter has to be constant . Or in other words the stochast Y_i must approximately have the same distribution for all i.

A.4 Computations and corrections

This appendix is written to render account of the way values in the dataset are treated. Every scientist approximates, corrects or estimates his way when analyzing measurements. It is very important to know how he does that in order to be able to compare results. The derivations can be found in standard textbooks.

A.4.1 Heat and momentum fluxes

The definition for the virtual potential temperature is:

$$\theta_v = \theta(1 + 0.61q). \qquad \text{(A.4.1)}$$

Here q is the specific humidity and θ is the potential temperature, the index v denotes virtual. Because in the definition of the Obukhov length the moisture correction in the virtual temperature is small, we estimated q averagely 0.006 kg/kg. Furthermore, to obtain the absolute temperature in Kelvin 273.15 was added. Applying Reynolds decomposition, multiplying with w' and averaging yields:

$$\overline{(w'\theta_v')} = \overline{(w'\theta')}(1 + 0.61\bar{q}) + 0.61\bar{\theta}\overline{(w'q')} + 0.61\overline{(w'\theta'q')} \qquad \text{(A.4.2)}$$

The last term is small and can be neglected. The moisture flux can be approximated with the Bowen ratio method. The Bowen ratio is defined and approximated as:

$$B = \frac{c_p}{Le}\frac{\overline{(w'q')}}{\overline{(w'\theta')}} \approx \frac{c_p}{Le}\frac{\theta_{z2} - \theta_{z1}}{q_{z2} - q_{z1}}. \qquad \text{(A.4.3)}$$

Here the differences between two levels at the Cabauw mast are used, assuming first order closure as in (2.32) and (2.33) and $K_h = K_q$. This gives us an approximation for the virtual heat flux:

$$\overline{(w'\theta_v')} \approx \overline{(w'\theta')}\left[1 + 0.61\bar{q} + 0.61\bar{\theta}\frac{c_p}{Le}B^{-1}\right] \qquad \text{(A.4.4)}$$

Le is the evaporation heat for water (~2.5 . 10^6 J/kg) and c_p is the specific heat capacity at constant pressure. It depends on the humidity and can be written as follows:

$$c_p = c_{pd}(1 - q) + c_{pv}q \qquad \text{(A.4.5)}$$

The indices d and v denote dry air and vapour. Here c_{pv}=1850 J / kg.K and

c_{pd}=1004.67 J / kg.K. It is easy to derive:

$$c_p = c_{pd}(1 + q(c_{pv} / c_{pd} - 1)) = 1004.67 + 848.95q \qquad \text{(A.4.6)}$$

On the average c_p was about 1010 J / kg.K at Cabauw.

The potential temperature is defined by :

$$\theta = T(p_0/p)^{\gamma} \qquad \text{(A.4.6)}$$

where $\gamma = -\frac{R_d}{c_p} = 0.286$ and $R_d = R / M$, with R the gas constant (8134 J/kmol.K)and M the average molecular weight of atmospheric air (28.96 g). Differentiating (A.4.6) partially and using the equation of state ($p = \rho RT$) and hydrostatic equilibrium ($dp = -\rho g dz$) we obtain:

$$d\theta = \left(\frac{p_0}{p}\right)^{\gamma}(dT + \frac{g}{c_p}dz) \qquad \text{(A.4.7)}$$

We use p_0= 1000 mbar as reference pressure. Realizing that $\frac{p_0}{p} \approx 1$ in the boundary layer, and integrating from z=0 upwards (A.4.7) we finally find formula (2.5):

$$\theta(z) = T(z) + \frac{g}{c_p}z \qquad \text{(A.4.8)}$$

The ratio g/c_p is usually taken 0.01, here g=9.81 m/s^2.

In §3.3.1 we have seen that the sonic anemometer measures a sonic virtual heat flux. If we compare this to (A.4.2) we see that the difference is the constant 0.51 in (3.6) and 0.61 in (A.4.2), further there is the wind correction term Γ. The moisture correction terms are small, we assumed the difference in constants was negligible and conclude that :

$$\langle w'\theta'_v \rangle = \langle w'T'_{sv} \rangle - \Gamma \qquad \text{(A.4.9)}$$

Fluctuations in the temperature can of course be replaced by potential temperature fluctuations.

So instead of using all the moisture correction terms and Bowen ratios it is possible to use the heat flux measured by the sonic directly, corrected for the horizontal windspeed measured by the sonic. This proved to save a lot of data, because the moisture measurements in Cabauw were often of insufficient quality.

The momentum flux was computed from the the two covariances delivered by the

datalogger:

$$u_* = \sqrt[4]{\overline{(u'w')}^2 + \overline{(v'w')}^2} \qquad \text{(A.4.10)}$$

The value of κ, the Von Karman constant was chosen κ=0.4.
As argued in §2.4 in fact the Obukhov length we can calculate now is the local Obukhov length Λ as defined by Nieuwstadt (1984). If we assume constant fluxes near the surface it is equal to the surface Obukhov length L:

$$L = \frac{-\overline{\theta_v} u_*^3}{\kappa g \left(\overline{w'\theta_v'}\right)_s} \qquad \text{(A.4.10)}$$

A.4.2 Gradients

For brevity's sake we will discuss the dimensionless wind shear, the dimensionless temperature gradient is determined using the same method.

The dimensionless wind shear as given in equation 2.27 should be a function of z/L only, according to the Monin-Obukhov similarity theory. We will assume the following relation:

$$\frac{\kappa z}{u_*}\frac{\partial \bar{u}}{\partial z} = 1 + \beta\frac{z}{L} \qquad \text{(A.4.11)}$$

according to what is usually found in experiments. Integrating with respect to z, with $u(z_0)=0$ as boundary condition yields:

$$u(z) = \frac{u_*}{\kappa}\left\{\ln\left(\frac{z}{z_0}\right) + \beta\left(\frac{z}{L}\right) - \beta\left(\frac{z_0}{L}\right)\right\} \qquad \text{(A.4.12)}$$

as we have seen in (5.3) already. We have measured velocities between discrete levels only, so we need to approximate the gradient one way or another. Let us first look what happens to our log-linear wind profile (A.4.12) when we use the difference between two levels:

$$u(z_2) - u(z_1) = \frac{u_*}{\kappa}\left\{\ln\left(\frac{z_2}{z_1}\right) + \beta\left(\frac{z_2 - z_1}{L}\right)\right\} \qquad \text{(A.4.13)}$$

We see that the roughness length is eliminated this way. Rearranging (A.4.13) gives:

$$\frac{\kappa}{u_*}\frac{u(z_2)-u(z_1)}{\ln(z_2/z_1)} = 1+\beta\frac{(\tilde{z})}{L} \qquad \text{(A.4.14)}$$

with:

$$\tilde{z} = \frac{z_2 - z_1}{\ln(z_2/z_1)} \qquad \text{(A.4.15)}$$

The dimensionless wind shear can be written as:

$$\frac{\kappa z}{u_*}\frac{\partial \bar{u}}{\partial z} = \frac{\kappa}{u_*}\frac{\partial \bar{u}}{\partial \ln z} \approx \frac{\kappa}{u_*}\frac{\Delta \bar{u}}{\Delta \ln z}\bigg|_{\tilde{z}} \qquad \text{(A.4.16)}$$

If we approximate the logarithmic differential quotient by a logarithmic difference quotient we obtain the left hand side of (A.4.14). The relation is valid for $z \rightarrow \tilde{z}$. This height $\tilde{z}$, which we call the differential height, is the height at which (A.4.16) gives the best approximation for the gradient assuming that (A.4.11) is true. The dimensionless shear is thus a function of $\tilde{z}/\mathbf{L}$ if we use this way of determining the gradient.

For the z-less stratification limit this is not valid however, there we expect a linear wind profile and we can use the linear difference quotient. Of course z doesn't matter now. In practice we will not reach z-less stratification in the surface layer, so only the above mentioned method is used in our computations.

We used the windspeed and temperature differences between 10m and 20m, this makes $\tilde{z}$=14.43m, while the actual measuring height was 11.4m. This means that we need to assume constant fluxes in the first 14.43m. This condition will not always be met, because therefore we need a NBL height of 150m. The terrain inhomogeneities also cause problems, because they perturb the momentum and heat flux profiles.

B.1 Datalogger structure diagram and program

- execution interval=0.8s
- measure all inputchannels (1..16)
  - (U,V,W,T,TFM,Tn,R,F5,F10,F20,D10,T06,dT2,dT10,dT20,RI)
- scale all inputlocations (1..16)
- do a burstmeasurement for W and TFM (10samples in 40ms)
  - compute differences for timeinterval
    - 0.08s , X1-X3, take stand.dev. after 10 min.
    - 0.16s , X1-X5, take stand.dev. after 10 min.
    - 0.32s , X1-X9, take stand.dev. after 10 min.
- convert rotorangle to goniometric angle: Rg=R-270
- transform U,V to meteocoordinates (north-eastcomponents)
  - E=UsinRg+VcosRg
  - N=VsinRg-UcosRg
- read (E,N,W,T,TFM) and compute
  - means, variances and covariances after 750 samples
- measure datalogger battery status
- increment sample counter

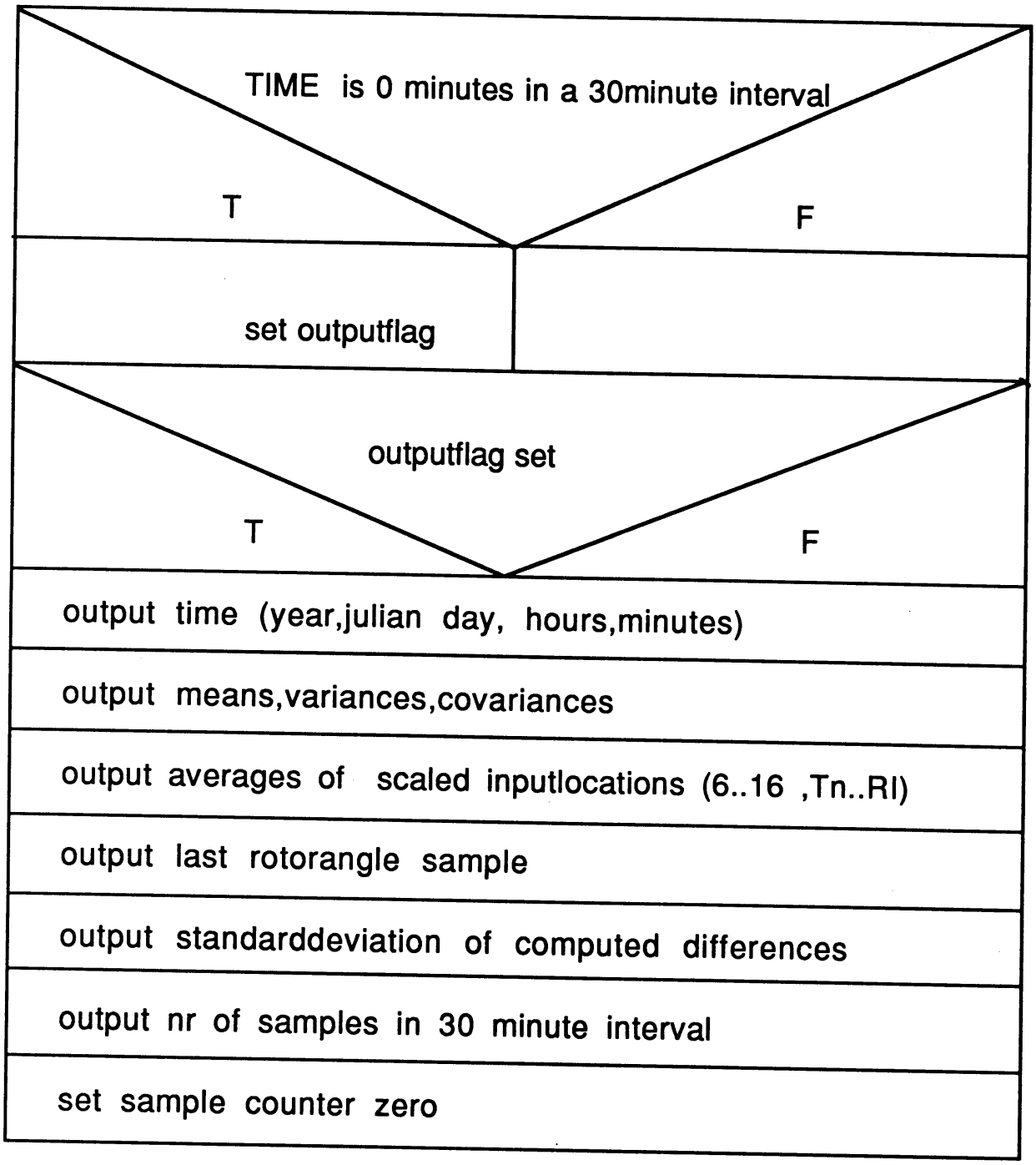

To turn the sonic anemometer in the wind direction, an electronic device was designed by the KNMI, but the automatic adjuster did not work. We decided to let the datalogger control the manual rotorangle adjuster by its logical controlports. Therefore the program continues:

SUBROUTINE 1

puts the inputvalue (location(79)) in range 0-360 degrees

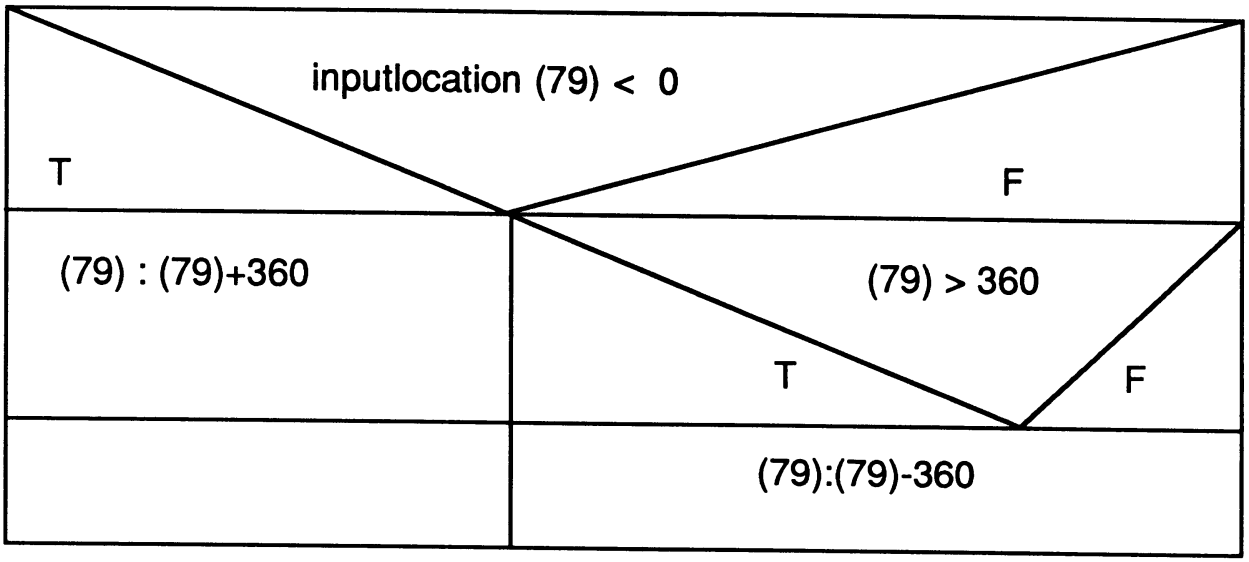

SUBROUTINE 2

computes winddirection (PHI)from north-east components compares rotorangle with PHI , if the ERROR> 5 it sets the control port for a left or a right turn high.

compute absolute value of E and N

reset flag 1

|N| < |E|

T	F
(70): E	set flag 1
(71): N	(70): N
	(71): -E

Q = (71) divided by (70)

compute arctan and convert to meteorological angle (N=0)

PHI= 270 - 55.91*Q + 11.42*Q^3 (Q<1)

E<0

T	F
PHI: PHI -180	

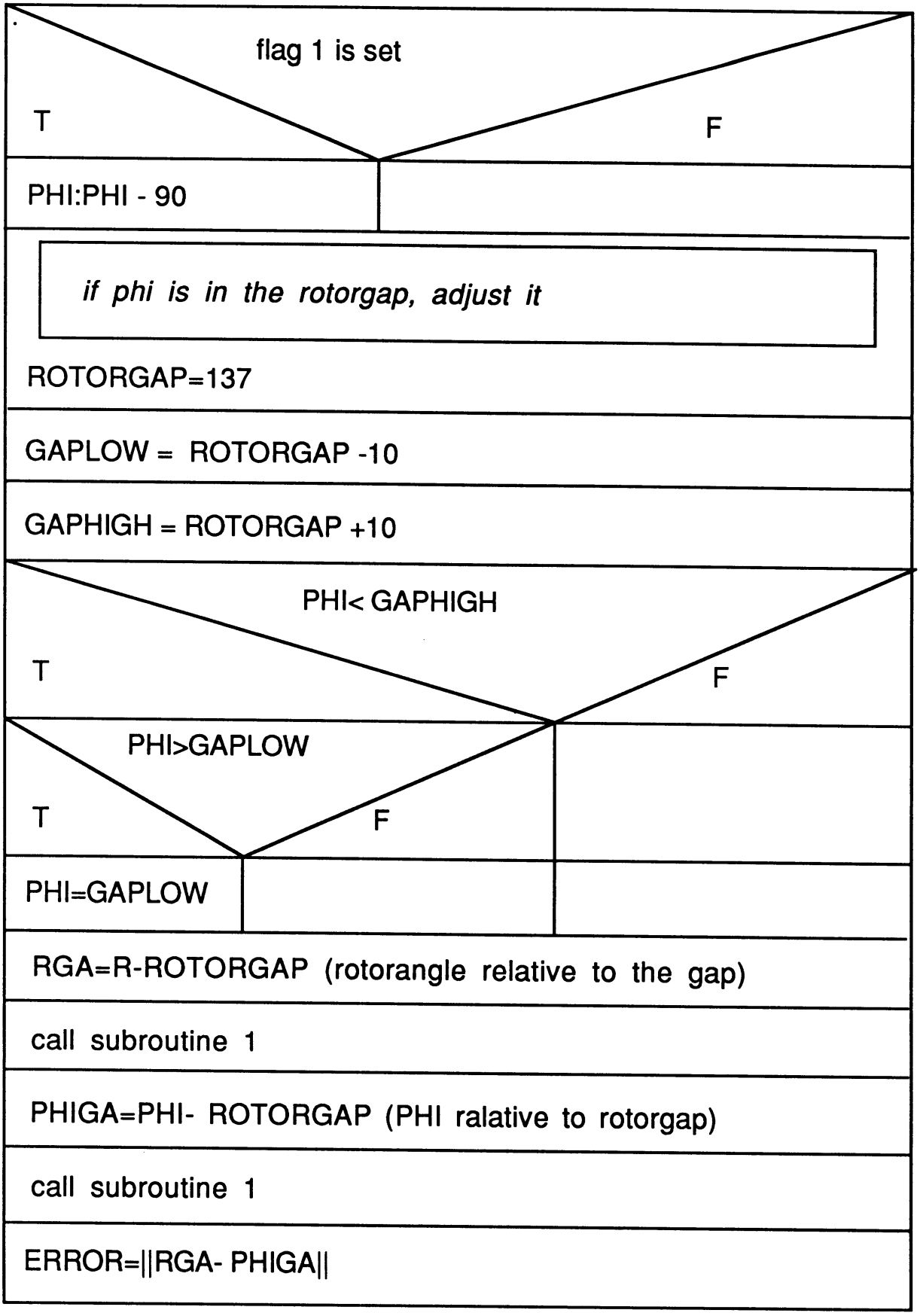
flag 1 is set
T
F
PHI:PHI - 90
if phi is in the rotorgap, adjust it
ROTORGAP=137
GAPLOW = ROTORGAP -10
GAPHIGH = ROTORGAP +10
PHI< GAPHIGH
T
F
PHI>GAPLOW
T
F
PHI=GAPLOW
RGA=R-ROTORGAP (rotorangle relative to the gap)
call subroutine 1
PHIGA=PHI- ROTORGAP (PHI ralative to rotorgap)
call subroutine 1
ERROR=||RGA- PHIGA||

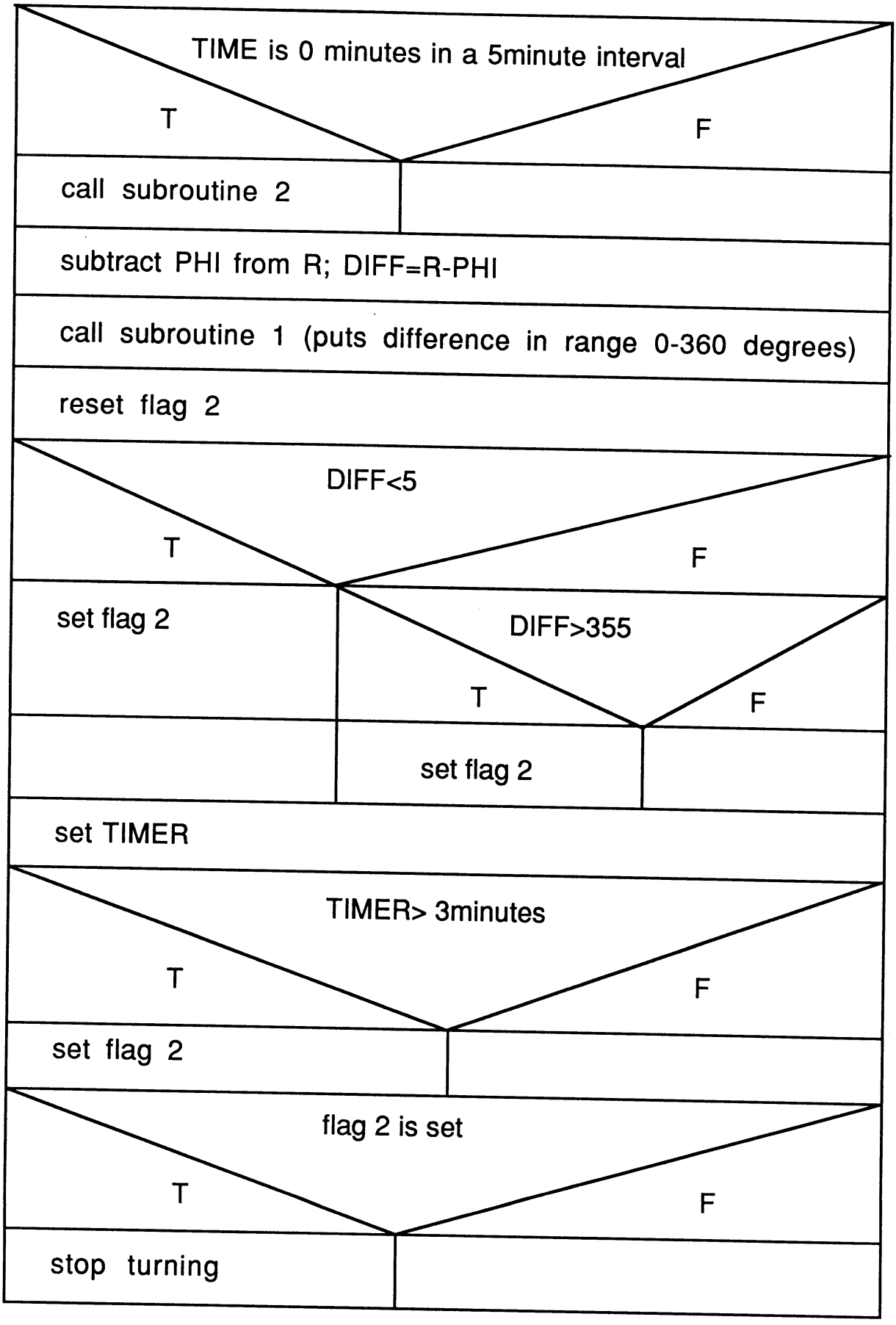
TIME is 0 minutes in a 5minute interval
T
F
call subroutine 2
subtract PHI from R; DIFF=R-PHI
call subroutine 1 (puts difference in range 0-360 degrees)
reset flag 2
DIFF<5
T
F
set flag 2
DIFF>355
T
F
set flag 2
set TIMER
TIMER> 3minutes
T
F
set flag 2
flag 2 is set
T
F
stop turning

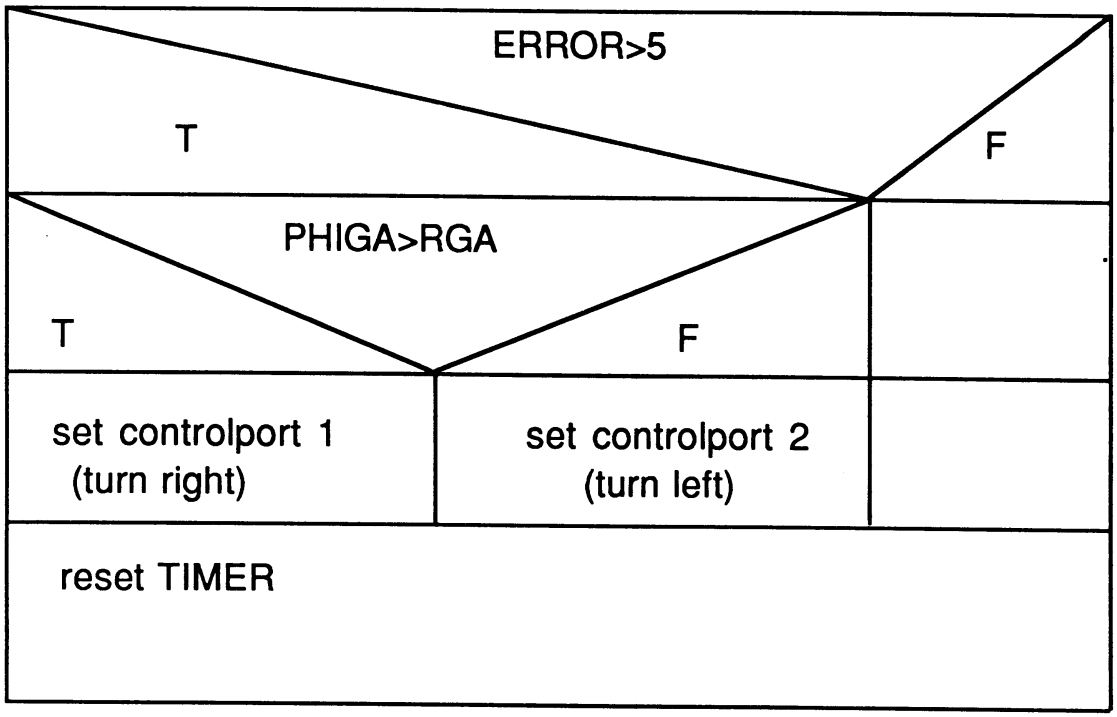
ERROR>5
T
F
PHIGA>RGA
T
F
set controlport 1
(turn right)
set controlport 2
(turn left)
reset TIMER

Program: CSONIC (13-06-89)

Input channels:

IN-Ch.	Parameter	Offset	Multipl.	Phys. Quant at 1000 mV
1	Us (sonic)	0	0.005	5 m/s
2	Vs (sonic)	0	0.005	5 m/s
3	W (sonic)	0	0.001	1 m/s
4	Tc (couple)	15	0.004	15+4 C
5	Ts (sonic)	0	0.01	10 C
6	Tn (NTC)	15	0.004	15+4 C
7	R (Rotor)	130	0.1	100 deg.
8	F5	0	0.01	10 m/s
9	F10	0	0.01	10 m/s
10	F20	0	0.01	10 m/s
11	D10	128.5	0.072	100 deg
12	T06	10.306	0.005088	5.088+10.306
13	DT2-06	2.032	0.0010136	2.032+1.0136
14	DT10-2	2.032	0.0010136	2.032+1.0136
15	DT20-10	2.032	0.0010136	2.032+1.0136
16	Rainindicator	0	1	logical 1/0

Note: The rotor direction is defined as the direction of the wind when Vs=0 and Us > 0.

: The routineprgrams measures in the range 0-10V, the routinemultipliers have been multiplied by 2 because the datalogger+circuits measure from 0-5

Input locations:

1-16 : samples of channel 1-16

17 : U (west-east)
18 : V (south-north)
19 : W
20 : Tc
21 : Ts
22 : Rg (=270-R, Rgonio)
23 : hu1; Rg+90, sin(Rg)
24 : hu2; cos(Rg)
25 : hu3; Us*sin(Rg); Mul-W
26 : hu4; Us*cos(Rg); Off-W
27 : hu5; Vs*sin(Rg); Mul-Tc
28 : hu6; Vs*cos(Rg); Off-Tc

30-39 : storage for samples of W in burst mode
40-49 : storage for samples of Tc in burst mode

50 : DW(n-2)
51 : DW(n-4)
52 : DW(n-8)
53 : DTc(n-2)
54 : DTc(n-4)
55 : DTc(n-8)

56 : s.d. DW(n-2)
57 : s.d. DW(n-4)
58 : s.d. DW(n-8)
59 : s.d. DTc(n-2)
60 : s.d. DTC(n-4)
61 : s.d. DTc(n-8)

62 : NRS (number of samples)
63 : Vbat(battery voltage)

70-79 : workspace for Table2

Page 2 Table 1

80-99 Means (5 values), variances (5 values) and covariances (10 values) of U, V, W, Ts and Tc.

The Table 1 program takes samples (including bursts for structure functions), determines variances and covariances every 10 minutes and outputs the results every 30 minutes.

```
*      1          Table 1 Programs
  01: 0.8         Sec. Execution Interval

01:   P1          Volt (SE) Us
  01: 16          Reps
  02: 15          5000 mV fast Range
  03: 1           IN Chan
  04: 1           Loc [:Us        ]
  05: 1           Mult
  06: 0           Offset
```

W and Tc in burst mode (5 samples each with dt=0.08, a multiple of 1/50 to avoid 50 Hz noise)

```
02:   P53         Scaling Array (A*loc +B)
  01: 1           Start Loc [:Us        ]
  02: 0.005       A1
  03: 0.0000      B1
  04: 0.005       A2 v
  05: 0.0000      B2
  06: 0.001       A3 w
  07: 0.0000      B3
  08: 0.004       A4 Tc
  09: 15          B4

03:   P53         Scaling Array (A*loc +B)
  01: 5           Start Loc [:Ts        ]
  02: 0.01        A1
  03: 0.0000      B1
  04: 0.004       A2 Tn
  05: 15          B2
  06: 0.1         A3 R
  07: -223        B3
  08: 0.01        A4 F5
  09: 0.0000      B4
```

Page 3 Table 1

```
04:  P53        Scaling Array (A*loc +B)
  01: 9         Start Loc [:F10       ]
  02: 0.01      A1
  03: 0.0000    B1
  04: 0.01      A2
  05: 0.0000    B2
  06: 0.072     A3
  07: 128.5     B3
  08: 5.088     A4
  09: 0         B4

05:  P53        Scaling Array (A*loc +B)
  01: 13        Start Loc [:DT2-06    ]
  02: 1.0136    A1
  03: 0         B1
  04: 1.0136    A2
  05: 0         B2
  06: 1.0136    A3
  07: 0         B3
  08: 1         A4
  09: 0         B4

06:  P53        Scaling Array (A*loc +B)
  01: 12        Start Loc [:T06       ]
  02: 0.001     A1
  03: 10.306    B1
  04: 0.001     A2
  05: 2.032     B2
  06: 0.001     A3 again scaling 12..16
  07: 2.032     B3 for more accuracy
  08: 0.001     A4
  09: 2.032     B4

07:  P23        Burst Meas. (Extented)
  01: 2         Reps
  02: 15        5000 mV fast Range
  03: 3         IN Chan
  04: 0001      Trig1stChan/Immed/InpStr/SE
  05: 40        Time per Scan (msec.)
  06: 0.01      Scans (in thousands)
  07: 0000      Samples before Trigger
  08: 0.0000    mV Limit
  09: 0000      mV Excitation
  10: 30        Loc [:Wburst    ]
  11: 0.001     Mult
  12: 0.0       Offset
convert R to Rg(goniometric angle) and transform to
North-east coordinate system

08:  P37        Z=X*F
  01: 7         X Loc :R
  02: -1        F conversion to goniometric angle
  03: 22        Z Loc [:Rg        ]
```

Page 4 Table 1

```
09:  P34        Z=X+F
  01: 22        X Loc Rg
  02: 270       F
  03: 22        Z Loc [:Rg          ] Rg=270-R

10:  P34        Z=X+F
  01: 22        X Loc Rg
  02: 90        F
  03: 23        Z Loc [:hu1         ] hu1=(90+Rg)

11:  P48        Z=SIN(X)
  01: 23        X Loc hu1
  02: 24        Z Loc [:hu2         ] hu2=cos(Rg)

12:  P48        Z=SIN(X)
  01: 22        X Loc Rg
  02: 23        Z Loc [:hu1         ] hu1=sin(Rg)

13:  P36        Z=X*Y
  01: 1         X Loc Us              Us is the X-component
  02: 23        Y Loc hu1
  03: 25        Z Loc [:hu3         ] hu3=Us*sin(Rg)

14:  P36        Z=X*Y
  01: 1         X Loc Us
  02: 24        Y Loc hu2
  03: 26        Z Loc [:hu4         ] hu4=Us*cos(Rg)

15:  P36        Z=X*Y
  01: 2         X Loc Vs              Vs is the Y-component
  02: 23        Y Loc hu1
  03: 27        Z Loc [:hu5         ] hu5=Vs*sin(Rg)

16:  P36        Z=X*Y
  01: 2         X Loc Vs
  02: 24        Y Loc hu2
  03: 28        Z Loc [:hu6         ] hu6=Vs*cos(Rg)

17:  P33        Z=X+Y
  01: 25        X Loc
  02: 28        Y Loc
  03: 17        Z Loc [:U           ] EAST=XsinRg+YcosRg

18:  P35        Z=X-Y
  01: 27        X Loc
  02: 26        Y Loc
  03: 18        Z Loc [:V           ] NORTH=YsinRg-XcosRg

Move W, Tc and Ts to loc 19, 20, and 21

19:  P31        Z=X
  01: 3         X Loc W
  02: 19        Z Loc [:W           ]

20:  P31        Z=X
  01: 4         X Loc Tc
  02: 20        Z Loc [:Tc          ]
```

```
Page 5   Table 1


21:  P31        Z=X
  01: 5         X Loc Ts
  02: 21        Z Loc [:Ts          ]

Compute differences for time intervals of 0.08, 0.16
and 0.32 s

22:  P35        Z=X-Y
  01: 30        X Loc Wburst
  02: 32        Y Loc
  03: 50        Z Loc [:DW2         ]

23:  P35        Z=X-Y
  01: 30        X Loc Wburst
  02: 34        Y Loc
  03: 51        Z Loc [:DW4         ]

24:  P35        Z=X-Y
  01: 30        X Loc Wburst
  02: 38        Y Loc
  03: 52        Z Loc [:DW8         ]

25:  P35        Z=X-Y
  01: 40        X Loc Tcburst
  02: 42        Y Loc
  03: 53        Z Loc [:DTc2        ]

26:  P35        Z=X-Y
  01: 40        X Loc Tcburst
  02: 44        Y Loc
  03: 54        Z Loc [:DTc4        ]

27:  P35        Z=X-Y
  01: 40        X Loc Tcburst
  02: 48        Y Loc
  03: 55        Z Loc [:DTc8        ]

Output every 30 minutes

28:  P92        If time is
  01: 0         minutes into a
  02: 30        minute interval
  03: 10        Set flag 0 (output)

29:  P52        Standard Deviation
  01: 6         Reps
  02: 50        Sample Loc DW2
  03: 56        SD Loc [:sdDW2      ]
  04: 750       No. of Samples
```

```
30:  P62        CV/CR (Extented)
  01: 5         No. of Input Values
  02: 5         No. of Means
  03: 5         No. of Variances
  04: 00        No. of Std. Dev.
  05: 10        No. of Covariances
  06: 00        No. of Correlations
  07: 750       Samples per Average
  08: 17        First Sample Loc U
  09: 80        Loc : means(5), variances(5), covariances(10)
```

Measure Battery voltage and increment sample counter

```
31:  P10        Battery Voltage
  01: 63        Loc [:Vbat      ]

32:  P32        Z=Z+1
  01: 62        Z Loc [:NRS     ]
```

Output time stamp

```
33:  P80        Year

34:  P77        Real Time
  01: 110       Day,Hour-Minute
```

Output means, variances and covariances (20 values)

```
35:  P70        Sample
  01: 20        Reps
  02: 80        Loc
```

Output mean value of Tn etc. (loc 6 to 16; 11 values)

```
36:  P71        Average
  01: 11        Reps
  02: 6         Loc Tn untill rainindicator
```

Output last sample of rotor (1 value)

```
37:  P70        Sample
  01: 1         Rep
  02: 7         Loc R
```

Output standard deviations of DW, DTc and NRS(7 values)

```
38:  P70        Sample
  01: 7         Reps
  02: 56        Loc sdDW2

39:  P70        Sample
  01: 1         Rep
  02: 71        Loc PHI

40:  P91        If Flag
  01: 10        0 (output) is set
  02: 30        Then Do
```

```
Page 7   Table 1


41:  P30        Z=F
  01: 0         F
  02: 62        Z Loc [:NRS       ]

42:  P95        End

43:  P92        If time is          Note: this interval may be larger
  01: 1         minutes into a      but certainly not ten minutes,
  02: 5         minute interval     because then it takes the avg of
  03: 2         Call Subroutine 2   the previous interval!!!!!!!!

If R is within 5 degrees equal to PHI or more
than 3 minutes have elapsed then stop
rotor from turning

44:  P35        Z=X-Y
  01: 7         X Loc
  02: 71        Y Loc PHI
  03: 79        Z Loc : R-phi

45:  P43        Z=ABS(X)
  01: 79        X Loc
  02: 79        Z Loc :

46:  P86        Do
  01: 1         Call Subroutine 1

47:  P86        Do
  01: 22        Reset flag 2

48:  P89        If X<=>F
  01: 79        X Loc
  02: 4         <
  03: 5         F
  04: 12        Set flag 2

49:  P89        If X<=>F
  01: 79        X Loc
  02: 3         >=
  03: 355       F
  04: 12        Set flag 2

50:  P26        Timer
  01: 77        Loc [:TIMER     ] time

51:  P89        If X<=>F
  01: 77        X Loc TIMER
  02: 3         >=
  03: 1800      F (1800 times 0.1 seconds, 3 minutes)
  04: 12        Set flag 2

52:  P91        If Flag
  01: 12        2 is set
  02: 30        Then Do
```

```
Page 8    Table 1


53:   P20         Set Port
  01: 0           Set low
  02: 1           Port Number

54:   P20         Set Port
  01: 0           Set low
  02: 2           Port Number

55:   P95         End

56:   P           End Table 1

   Input storage for subroutine 2 (locations 70-79):

 70 : HV1; abs(U); V/U
 71 : PHI (wind dir., dis. rotor direct.)
 72 : GAP (direction has to specified)
 73 : GAPL (GAP-10 lower bound of gap)
 74 : GAPH (GAP+10 upper bound of gap)
 75 : RGA=R-GAP (rotor direction relative to GAP,0-360)
 76 : PHIGA=PHI-GAP (desired w. dir. rel. to GAP,0-360)
 77 : TIMER
 78 :
 79 : DD; parameter location for subroutine 1 and 2



*      2          Table 2 Programs
  01: 0           Sec. Execution Interval

01:   P           End Table 2

outputspecification
1 arrayid.    19 vw          37 sdDW2
2 year        20 vTc         38 sdDW4
3 day         21 vTs         39 sdDW8
4 hr,min      22 wTc         40 sdDTc2
5 u-avg       23 wTs         41 sdDTc4
6 v-avg       24 TcTs        42 sdDTc8
7 w-avg       25 Tn-avg      43 #samples
8 Tc-avg      26 R-avg
9 Ts-avg      27 FF5-avg
10 var-u      28 FF10-avg
11 var-v      29 FF20-avg
12 var-w      30 DD10-avg
13 var-Tc     31 T06-avg
14 var-Ts     32 DT2-06-avg
15 uv         33 DT10-2-avg
16 uw         34 DT20-10-avg
17 uTc        35 Rainindicator
18 uTs        36 last R
```

Page 9 Table 3

```
*     3         Table 3 Subroutines

01:  P85        Beginning of Subroutine
  01: 1         Subroutine Number

   Subroutine 1 takes  direction from location 79
adds or subtracts 360 degrees to get the result in
the range of 0-360. The result is returned in
location 79

02:  P89        If X<=>F
  01: 79        X Loc
  02: 4         <
  03: 0         F
  04: 30        Then Do

03:  P34        Z=X+F
  01: 79        X Loc
  02: 360       F
  03: 79        Z Loc : phi or rotorangle

04:  P95        End

05:  P89        If X<=>F
  01: 79        X Loc
  02: 3         >=
  03: 360       F
  04: 30        Then Do

06:  P34        Z=X+F
  01: 79        X Loc
  02: -360      F
  03: 79        Z Loc :

07:  P95        End

08:  P95        End

09:  P85        Beginning of Subroutine
  01: 2         Subroutine Number

Subroutine 2 computes the angle PHI from U and V and
starts turning the rotor in the correct direction
PHI should be interpreted as the desired rotor angle


10:  P43        Z=ABS(X)
  01: 80        X Loc
  02; 70        Z Loc [:HV1        ] abs(U)

11:  P43        Z=ABS(X)
  01: 81        X Loc
  02: 71        Z Loc [:PHI        ] abs(V)

12:  P86        Do
  01: 21        Reset flag 1
```

Page 10 Table 3

```
13:  P88       If X<=>Y
  01: 71       X Loc PHI
  02: 4        <
  03: 70       Y Loc HV1
  04: 30       Then Do

14:  P31       Z=X
  01: 80       X Loc
  02: 70       Z Loc [:HV1          ]

15:  P31       Z=X
  01: 81       X Loc
  02: 71       Z Loc [:PHI          ]

16:  P94       Else

17:  P86       Do
  01: 11       Set flag 1

18:  P31       Z=X
  01: 81       X Loc
  02: 70       Z Loc [:HV1          ]

19:  P37       Z=X*F
  01: 80       X Loc
  02: -1       F
  03: 71       Z Loc [:PHI          ]

20:  P95       End

21:  P38       Z=X/Y
  01: 71       X Loc PHI
  02: 70       Y Loc HV1
  03: 71       Z Loc [:PHI          ] v/u

22:  P55       Polynomial ARCTAN; abs(V/U) < 1
  01: 1        Rep
  02: 71       X Loc PHI
  03: 71       F(X) Loc [:PHI          ] PHI
  04: 270      C0
  05: -55.91   C1
  06: 0        C2
  07: 11.42    C3
  08: 0        C4
  09: 0        C5

23:  P89       If X<=>F
  01: 70       X Loc HV1
  02: 4        <
  03: 0        F
  04: 30       Then Do

24:  P34       Z=X+F
  01: 71       X Loc PHI
  02: -180     F
  03: 71       Z Loc [:PHI          ]
```

```
25:  P95       End

26:  P91       If Flag
  01: 11       1 is set
  02: 30       Then Do

27:  P34       Z=X+F
  01: 71       X Loc PHI
  02: -90      F
  03: 71       Z Loc [:PHI        ] phi meteo

28:  P95       End

29:  P30       Z=F
  01: 137      F   to be measured at the location
  02: 72       Z Loc [:GAP        ] gapangle

30:  P34       Z=X+F
  01: 72       X Loc GAP
  02: -10      F
  03: 73       Z Loc [:GAPL       ] Gap low

31:  P34       Z=X+F
  01: 72       X Loc GAP
  02: 10       F
  03: 74       Z Loc [:GAPH       ] Gap high

If phi happens to be in rotor gap adjust it

32:  P88       If X<=>Y
  01: 71       X Loc PHI
  02: 3        >=
  03: 73       Y Loc GAPL
  04: 30       Then Do

33:  P88       If X<=>Y
  01: 71       X Loc PHI
  02: 4        <
  03: 74       Y Loc GAPH
  04: 30       Then Do

34:  P31       Z=X
  01: 73       X Loc GAPL
  02: 71       Z Loc [:PHI        ] Gap low

35:  P95       End

36:  P95       End

Compute R-direction and PHI-direction
relative  to the gap and make sure that the results
are within the range of 0 to 360 degrees

37:  P35       Z=X-Y
  01: 7        X Loc
  02: 72       Y Loc GAP
  03: 79       Z Loc : RGA (rotor-gap)
```

Page 12 Table 3

```
38:  P86        Do
  01: 1         Call Subroutine 1

39:  P31        Z=X
  01: 79        X Loc
  02: 75        Z Loc [:RGA       ] RGA

40:  P35        Z=X-Y
  01: 71        X Loc PHI
  02: 72        Y Loc GAP
  03: 79        Z Loc : PHIGA

41:  P86        Do
  01: 1         Call Subroutine 1

42:  P31        Z=X
  01: 79        X Loc
  02: 76        Z Loc [:PHIGA     ] PHIGA

43:  P35        Z=X-Y
  01: 75        X Loc
  02: 76        Y Loc
  03: 79        Z Loc : R-phi

44:  P43        Z=ABS(X)
  01: 79        X Loc
  02: 79        Z Loc :

If abs(R-PHI) near 360 or -360 then the rotor has to
turn to the other side of the gap anyway

45:  P89        If X<=>F
  01: 79        X Loc
  02: 3         >=
  03: 5         F
  04: 30        Then Do

Begin1

46:  P88        If X<=>Y
  01: 76        X Loc PHIGA
  02: 3         >=
  03: 75        Y Loc RGA
  04: 30        Then Do

Begin2

47:  P20        Set Port turn right(control port 1, green)
  01: 1         Set high
  02: 1         Port Number

48:  P94        Else

49:  P20        Set Port turn left(control port2, red)
  01: 1         Set high
  02: 2         Port Number

End 2
```

```
Page 13   Table 3


50:  P95        End

51:  P26        Timer
  01: 0         Reset Timer

End 1

52:  P95        End

End subroutine 2

53:  P95        End

54:  P          End Table 3


*      4        Mode 4 Output Options
  01: 1         (Tape OFF) (Printer ON)
  02: 2         Printer 9600 Baud


*      A        Mode 10 Memory Allocation
  01: 100       Input Locations
  02: 100       Intermediate Locations


*      C        Mode 12 Security
  01: 00        Security Option
  02: 0         Security Code
```

Page 14 Input Location Assignments (with comments):

```
Key:
T=Table Number
E=Entry Number
L=Location Number

T:   E:   L:
1:    1:   1:   Loc [:Us          ]
1:    2:   1:   Start Loc [:Us          ]
1:    3:   5:   Start Loc [:Ts          ]
1:    4:   9:   Start Loc [:F10         ]
1:    6:  12:   Start Loc [:T06         ]
1:    5:  13:   Start Loc [:DT2-06      ]
1:   17:  17:   Z Loc [:U             ] EAST=XsinRg+YcosRg
1:   18:  18:   Z Loc [:V             ] NORTH=YsinRg-XcosRg
1:   19:  19:   Z Loc [:W             ]
1:   20:  20:   Z Loc [:Tc            ]
1:   21:  21:   Z Loc [:Ts            ]
1:    8:  22:   Z Loc [:Rg            ]
1:    9:  22:   Z Loc [:Rg            ] Rg=270-R
1:   10:  23:   Z Loc [:hu1           ] hu1=(90+Rg)
1:   12:  23:   Z Loc [:hu1           ] hu1=sin(Rg)
1:   11:  24:   Z Loc [:hu2           ] hu2=cos(Rg)
1:   13:  25:   Z Loc [:hu3           ] hu3=Us*sin(Rg)
1:   14:  26:   Z Loc [:hu4           ] hu4=Us*cos(Rg)
1:   15:  27:   Z Loc [:hu5           ] hu5=Vs*sin(Rg)
1:   16:  28:   Z Loc [:hu6           ] hu6=Vs*cos(Rg)
1:    7:  30:   Loc [:Wburst     ]
1:   22:  50:   Z Loc [:DW2           ]
1:   23:  51:   Z Loc [:DW4           ]
1:   24:  52:   Z Loc [:DW8           ]
1:   25:  53:   Z Loc [:DTc2          ]
1:   26:  54:   Z Loc [:DTc4          ]
1:   27:  55:   Z Loc [:DTc8          ]
1:   29:  56:   SD Loc [:sdDW2       ]
1:   32:  62:   Z Loc [:NRS           ]
1:   41:  62:   Z Loc [:NRS           ]
1:   31:  63:   Loc [:Vbat       ]
3:   10:  70:   Z Loc [:HV1           ] abs(U)
3:   14:  70:   Z Loc [:HV1           ]
3:   18:  70:   Z Loc [:HV1           ]
3:   11:  71:   Z Loc [:PHI           ] abs(V)
3:   15:  71:   Z Loc [:PHI           ]
3:   19:  71:   Z Loc [:PHI           ]
3:   21:  71:   Z Loc [:PHI           ] v/u
3:   22:  71:   F(X) Loc [:PHI          ] PHI
3:   24:  71:   Z Loc [:PHI           ]
3:   27:  71:   Z Loc [:PHI           ] phi meteo
3:   34:  71:   Z Loc [:PHI           ] Gap low
3:   29:  72:   Z Loc [:GAP           ] gapangle
3:   30:  73:   Z Loc [:GAPL          ] Gap low
3:   31:  74:   Z Loc [:GAPH          ] Gap high
3:   39:  75:   Z Loc [:RGA           ] RGA
3:   42:  76:   Z Loc [:PHIGA         ] PHIGA
1:   50:  77:   Loc [:TIMER       ] time
1:   44:  79:   Z Loc : R-phi
```

Page 15 Input Location Assignments (cont.):

```
 1: 45: 79:   Z Loc :
 3:  3: 79:   Z Loc : phi or rotorangle
 3:  6: 79:   Z Loc :
 3: 37: 79:   Z Loc : RGA (rotor-gap)
 3: 40: 79:   Z Loc : PHIGA
 3: 43: 79:   Z Loc : R-phi
 3: 44: 79:   Z Loc :
 1: 30: 80:  Loc : means(5), variances(5), covariances(10)
```

B.2 Program listings A.2

Main program A2

```
C
      PROGRAM DAGFILE
C
      INTEGER*4     KOLOM(0:49),IDIG(0:199),H(0:20)
      REAL          Q(0:199,1:144)
      REAL          BUF(210)
      CHARACTER*2   MONTH
      CHARACTER*3   EXT
      CHARACTER*6   NAAM(0:199),UNIT(0:199)
      CHARACTER*8   BASENAME,DATEFILE
      CHARACTER*20  FILEIN,FILETEKST
C     toevoegingen sinds fred
      CHARACTER*4   EXT1
      CHARACTER*15  TIT1
      CHARACTER*21  TITLE
      INTEGER       IDATE,AAPJE,NOOTJE,DD,MM,YY,MIN,LUI,IFAIL,IQL,TOTAAL
      INTEGER       HH,X,NDATE
      CALL DATABASE(1,BASENAME)
      CALL READINP(1,BASENAME,NKOL,MINUUT,F)
      CALL READTKS(1,BASENAME,NKOL,NAAM,UNIT,IDIG)
      LREC=4*NKOL
      PRINT 999
999   FORMAT(' Geef extensie (bijv B30) : ')
      READ(5,998) EXT
998   FORMAT(A3)
C                                  -------> inlezen kolomnummers
      KOLOM(0)=0
      KOLOM(1)=1
      I=2
C
      OPEN(UNIT=4,FILE='DAGFILE.INP')
20    READ(4,*,END=30) KOLOM(I)
      I=I+1
      GOTO 20
30    CLOSE(4)
      NKOLOM=I-1
C
C--------> Datafiles openen en lezen
C
      PRINT 991
991   FORMAT(' Geef begin- en einddag (yymmdd) : ')
      READ(5,*) IDATE,NDATE

C
40    CALL DATENAME(IDATE,BASENAME,DATEFILE)
      FILEIN=DATEFILE//'.'//EXT
      PRINT 995,FILEIN
995   FORMAT(' ',A20)
```

```
      OPEN(UNIT=1,FILE=FILEIN,ACCESS='DIRECT',RECL=LREC)
      OPEN(UNIT=2,FILE=DATEFILE//'.LO'//EXT(2:2))
C
      IREC=1
50    READ(1,REC=IREC,ERR=60) (Q(I,IREC),I=0,NKOL-1)
      IREC=IREC+1
      GOTO 50
C
60    NREC=IREC-1
      CLOSE(1)
C
      WRITE(2,994) (NAAM(KOLOM(J)),J=0,18)
994   FORMAT(21(' "',A6,'"'))
C
      DO 210 IREC=1,NREC
        Q(1,IREC)=Q(1,IREC)/100.
        WRITE(2,993) (Q(KOLOM(J),IREC),J=0,18)
210   CONTINUE
C
      WRITE(2,994) (NAAM(KOLOM(J)),J=19,37)
C
      DO 220 IREC=1,NREC
        WRITE(2,992) (Q(KOLOM(J),IREC),J=19,37)
220   CONTINUE
      YY=89
      KDATE=IDATE*100
      KDATE=IBKUPD(KDATE)
      KDATE=KDATE/100
      PRINT *,'IDATE=',IDATE
      PRINT *,'KDATE=',KDATE
      AAPJE=KDATE/100
      NOOTJE=AAPJE*100
      DD=KDATE-NOOTJE
      MM=AAPJE-8900
      TIT1='C:\SELCAB\CAB89'
      EXT1='.DIR'
      WRITE(MONTH(1:2),'(I2.2)') MM
      TITLE=TIT1//MONTH//EXT1
      LUI=3
      WRITE(2,994) (NAAM(KOLOM(J)),J=38,56)
      OPEN (UNIT=LUI,FILE=TITLE,STATUS='OLD',ACCESS='DIRECT'
     *    ,FORM='UNFORMATTED',RECL=420)
            OPEN(UNIT=4,FILE='READ.INP')
            K=0
101         READ(4,*,END=201) H(K)
            K=K+1
            GOTO 101
```

```
201             TOTAAL=K-1
                CLOSE(4)
          DO 73 HH=0,24
                DO 74 MIN=0,30,30
                IF (HH.EQ.0.AND.MIN.EQ.0) GOTO 74
                IF (HH.EQ.24.AND.MIN.EQ.30) GOTO 73
                CALL SELREC(BUF,YY,MM,DD,HH,MIN,LUI,IFAIL,2)
                WRITE (2,992)(BUF(H(K)),K=0,TOTAAL)
74        CONTINUE
73        CONTINUE
          CLOSE(2)
C
993       FORMAT(F11.0,F11.2,19(' ',E10.5E1))
992       FORMAT(19(' ',E10.5E1))
C
          IF (IDATE.LE.NDATE) GOTO 40
          END
```

Subroutines A2

```
C
      SUBROUTINE DATENAME(DATUM,LOCATIE,FILENAAM)
C
      INTEGER*2 NDAG(1:12),NUMMER(1:6)
      INTEGER*4 DATUM
      CHARACTER*8 LOCATIE,FILENAAM
C
      DATA NDAG/31,28,31,30,31,30,31,31,30,31,30,31/
      N=DATUM
      FILENAAM=LOCATIE(1:2)
      DO 10 I=1,6
        NUMMER(I)=MOD(N,10)
        N=N/10
        FILENAAM(9-I:9-I)=CHAR(48+NUMMER(I))
10    CONTINUE
C
      IDAG =NUMMER(1)+10*NUMMER(2)
      MAAND=NUMMER(3)+10*NUMMER(4)
      JAAR =NUMMER(5)+10*NUMMER(6)
C
      IF (MOD(JAAR,4).EQ.0) NDAG(2)=29
      IDAG=IDAG+1
      IF (IDAG.GT.NDAG(MAAND)) THEN
        IDAG=1
        MAAND=MAAND+1
      END IF




      IF (MAAND.EQ.13) THEN
        MAAND=1
        JAAR=JAAR+1
      END IF
      DATUM=10000*JAAR+100*MAAND+IDAG
C
      RETURN
      END
```

```
      SUBROUTINE READTKS(LUN,BASENAME,NKOL,NAAM,UNIT,IDIG)

      INTEGER*4    IDIG(0:199)
      CHARACTER*8 BASENAME
      CHARACTER*6 NAAM(0:199),UNIT(0:199)

      OPEN(UNIT=LUN,FILE=BASENAME//'.TKS')
      READ(LUN,999)
999   FORMAT(//)
      DO 10 I=0,NKOL-1
        READ(LUN,998) NAAM(I),UNIT(I),IDIG(I)
998   FORMAT(5X,A6,1X,A6,1X,I2)
10    CONTINUE
      CLOSE(LUN)

      RETURN
      END



      SUBROUTINE READINP(LUN,BASENAME,NKOLOM,MINUUT,F)

      CHARACTER*8 BASENAME

      OPEN(UNIT=LUN,FILE=BASENAME//'.INP')
      READ(LUN,999) NKOLOM,MINUUT,F
999   FORMAT(///1X,I9/1X,I9/1X,F9.3)
      CLOSE(LUN)

      RETURN
      END


      SUBROUTINE DATABASE(LUN,BASENAME)

      CHARACTER*8 BASENAME

      OPEN(UNIT=LUN,FILE='BASENAME.INP')
      READ(LUN,999) BASENAME
999   FORMAT(/1X,A8)
      CLOSE(LUN)

      RETURN
      END
```

```
      SUBROUTINE SELREC(BUF, YY, MM, DD, HH, MN, LUI, IFAIL, IQL)
      IMPLICIT CHARACTER*1 (A-Z)
      REAL BUF(1)
      INTEGER YY, MM, DD, HH, MN, LUI, IFAIL, IQL

       INTEGER*2 INDEX(210), IBUF(209), ISCL(209), IST(209)
       INTEGER*2 IP, I, J, JST, IREC, IFRST, IERRC
       INTEGER*2 MMDD, ISTEP
       REAL ERRC
       SAVE IREC, IFRST, INDEX, IP
C
C      Data statements: ERRC  - errorcode
C                       ISCL  - scaling for S.I. units
C                       IST   - status locator; -1 if unused or status

       DATA ERRC /-9999./
       DATA IERRC/-9999/
       DATA IP   /1/
C
       DATA (ISCL(I), I=1, 99)
      *          /      1,100,  1,100,  1,100,  1,100,  1,
      1           100,  1,100,  1,100,  1,100,  1,  1,  1,
      2           100,  1,100,  1,100,  1,100,  1,100,  1,
      3           100,  1,100,  1,100,  1,  1,  1, 10,100,
      4            10,  1, 10,100, 10,  1, 10,100, 10,  1,
      5            10,100, 10,  1, 10,100, 10,  1, 10,100,
      6            10,  1,  1,  1,  1, 10,  1,  1, 10,  1,
      7             1, 10,  1,  1, 10,  1,  1, 10,  1,  1,
      8            10,  1,  1,  1,  1,  1,  1,  1,  1,  1,
      9             1,  1,  1,  1,  1,  1,  1,  1,  1,  1/
       DATA (ISCL(I), I=100, 199)
      *          /  1,  1,  1,  1,  1,  1,  1,  1,  1,  1,
      1             1,  1,  1,  1,  1,  1,  1,  1,  1,  1,
      2             1,  1,  1,  1,  1,  1,  1,  1,  1,  1,
      3             1,  1,  1,  1,  1,  1,  1,  1,  1, 10,
      4             1, 10,  1,  1,  1,  1,  1,  1,  1, 10,
      5             1,  1,  1, 10,  1,  1,  1,1000,  1,  1,
      6             1,  1,  1,  1,  1,  1,  1,  1,  1,100,
      7             1,  1,  1,  1,  1,  1,  1,  1,  1,  1,
      8            1,1000,  1,  1,  1,  1,  1,  1,  1,  1,
      9             1,  1,  1,  1,  1,  1,  1,  1,  1,  1/
       DATA (ISCL(I), I=200, 209)
      *          /  1,  1,  1,  1,  1,  1,  1,  1,  1,  1/
C
```

```
      DATA (IST(I), I=1, 99)
     *     /      -1,  3, -1,  5, -1,  7, -1,  9, -1,
     1        11, -1, 13, -1, 15, -1, 17, -1, -1, -1,
     2        21, -1, 23, -1, 25, -1, 27, -1, 29, -1,
     3        31, -1, 33, -1, 35, -1, -1, -1, 41, 41,
     4        41, -1, 45, 45, 45, -1, 49, 49, 49, -1,
     5        53, 53, 53, -1, 57, 57, 57, -1, 61, 61,
     6        61, -1, -1, -1, 66, 66, -1, 69, 69, -1,
     7        72, 72, -1, 75, 75, -1, 78, 78, -1, 81,
     8        81, -1, -1, 88, 88, 88, 88, 88, -1, 94,
     9        94, 94, 94, 94, -1,100,100,100,100,100/
      DATA (IST(I), I=100, 199)
     *     / -1,106,106,106,106,106, -1,112,112,112,
     1       112,112, -1,118,118,118,118,118, -1,124,
     2       124,124,124,124, -1, -1, -1,128, -1,130,
     3        -1,132, -1,134, -1,136, -1,138, -1,140,
     4        -1,142, -1,144, -1,146, -1,148, -1,150,
     5        -1,152, -1,154, -1,156, -1,158, -1,162,
     6       162,162, -1,166,166,166, -1, -1, -1,170,
     7        -1,172, -1,174, -1,176, -1,178, -1,180,
     8        -1,182, -1, -1, -1, -1, -1, -1, -1, -1,
     9        -1, -1, -1, -1, -1, -1, -1, -1, -1, -1/
      DATA (IST(I), I=200, 209)
     *     / -1, -1, -1, -1, -1, -1, -1, -1, -1, -1/
C
C       DATA IST
C
C      1. INITIALIZE BUFFER ARRAY
C
      DO 10 I=1,209
         BUF(I)=ERRC
   10 CONTINUE
      ISTEP=1
      IF (MN .LT. 0 .AND. HH .LT. 0) ISTEP=-HH
C
C      2. CHECK INPUT PARAMETERS
C
      IF (MN .NE. -1 .AND. MN .NE. -2) THEN
         IF ( (MM .LT.  1 .OR.  MM .GT. 12) .OR.
     *        (DD .LT.  1 .OR.  DD .GT. 31) .OR.
     *        (YY .LT. 70 .OR.  YY .GT. 99) )     THEN
            IFAIL=-1
            GOTO 100
         ENDIF
         IF ( (HH .LT.  0 .OR.  HH .GT. 24) .OR.
     *        (MN .NE.  0 .AND. MN .NE. 30) .OR.
     *        (HH .EQ.  0 .AND. MN .EQ.  0) )     THEN
            IFAIL=-2
            GOTO 100

         ENDIF
      ENDIF
C
C      3.1 IF MN=-2: CLEAR INDEX AND INITIALIZE
C
      IF (MN .EQ. -2) THEN
         DO 11 I=1, 210
            INDEX(I)=0
   11    CONTINUE
```

```
         IFRST=0
      ENDIF
C
C     3.2 CHECK INDEX AND READ INDEX IF NECESSARY
C

      IF ( INDEX(3) .LE. 0 ) THEN
         READ(LUI,REC=1) INDEX
         IF ( INDEX(3) .LE. 0) THEN
            IFAIL=-3
            GOTO 100
         ENDIF
      ENDIF
C
C     4. NEXT RECORD OPTION (MN=-1 OR MN=-2)
C
      IF (MN .EQ. -1 .OR. MN .EQ. -2) THEN
         IF (IFRST .EQ. -1) THEN
            IREC=IREC+ISTEP
         ELSE
            IREC=2
         ENDIF
C        Check wether present indexpointer IP is still applicable
         IF (IREC .GE. INDEX(IP+2)     .AND.
     *       IREC .LT. INDEX(IP+2)+48 .AND.
     *                 INDEX(IP+2)     .NE. -1) GOTO 13
C        Search index
         DO 12 IP=1, 207, 3
            IF (IREC .GE. INDEX(IP+2)     .AND.
     *          IREC .LT. INDEX(IP+2)+48 .AND.
     *                    INDEX(IP+2)     .NE. -1) GOTO 13
  12     CONTINUE
         IFAIL=-6
         GOTO 100
  13     YY=INDEX(IP)
         READ(LUI, REC=IREC) MMDD, IBUF
         MM=MMDD/100
         DD=MMDD-100*MM
         HH=IBUF(1)/100
         MN=IBUF(1)-100*HH
      ELSE
C
C        4.1 SCAN INDEX FOR REQUESTED DATE
C

         MMDD=MM*100+DD
         Check wether present indexpointer IP is still applicable
         IF (INDEX(IP) .EQ. YY .AND. INDEX(IP+1) .EQ. MMDD) GOTO 30
         Search index
         DO 20 IP=1, 207, 3
            IF (INDEX(IP) .EQ. YY .AND. INDEX(IP+1) .EQ. MMDD) GOTO 30
            IF (INDEX(IP) .LT. 0) THEN
               IFAIL=-4
               GOTO 100
            ENDIF
  20     CONTINUE
```

```
  30      CONTINUE
C
C
C         4.1.1 COMPUTE RECORD NUMBER AN READ RECORD
C
          IREC=INDEX(IP+2) + HH*2 + MN/30 - 1
          READ(LUI,REC=IREC) MMDD, IBUF
C         CHECK FOR TIME CONSISTENCY
          IF ( IBUF(1) .NE. HH*100+MN  .OR.  MMDD .NE. MM*100+DD ) THEN
             IFAIL=-5
             GOTO 100
          ENDIF
       ENDIF
C
C      5. INTEGER TO REAL CONVERSION WITH CONVERSION TO S.I. UNITS
C            AND ERROR TREATMENT DEPENDENT ON VALUE OF IQL
C
       DO 60 I=1, 209
          J=IBUF(I)     ,
          IF (J .EQ. IERRC) THEN
             BUF(I)=ERRC
             GOTO 50
          ELSE
             BUF(I)=FLOAT(J)
             IF(ISCL(I) .NE. 1) BUF(I)=BUF(I) / ISCL(I)
          ENDIF
          J=IST(I)
C         FOR IST=-1 WE HAVE TO DO WITH AN UNUSED ADRESS OR A STAUS WORD
          IF (J .EQ. -1) GOTO 50
C
          JST=IBUF(J)
          GOTO (40, 41, 42, 43) IQL+1
  40      GOTO 50
C
  41      IF ( JST .NE. 00 )  BUF(I)=ERRC
          GOTO 50
C
  42      IF ( JST .NE. 00 .AND. JST .NE. 02) BUF(I)=ERRC
          GOTO 50
C
  43      IF ( JST .NE. 00 .AND. JST .NE. 02 .AND.
     *         JST .NE. 20 .AND. JST .NE. 22) BUF(I)=ERRC
          GOTO 50
C
  50      CONTINUE
  60   CONTINUE
       IFAIL=1
C
 100   CONTINUE
       IFRST=-1
       RETURN
       END
```

Inputfiles A2

DATABOEL: READ.INP

```
1
28
30
32
34
38
133
149
153
155
163
169
171
173
175
177
179
181
1
```

DATABOEL: DAGFILE.INP

```
5
6
7
8
9
10
11
12
13
14
15
16
17
18
19
20
21
22
23
26
27
28
29
30
31
32
33
34
35
37
38
39
40
41
42
44
2
45
46
47
48
49
50
51
52
53
54
57
58
59
60
61
62
63
2
```

DATABOEL: CABNACHT.TKS

COLOMN DISCRIPTION OF DATA-BASE CABNACHT				
0	DAG	dag	0	-
1	BTYD	min	0	-
2	ETYD	min	0	-
3	-	-	0	-
4	-	-	0	-
5	USON	m/s	0	-
6	VSON	m/s	0	-
7	WSON	m/s	0	-
8	TFM	K	0	-
9	TSON	oC	0	-
10	<UU>	m/s2	0	-
11	<VV>	m/s2	0	-
12	<WW>	m/s2	0	-
13	<TT>	K2	0	-
14	<SS>	K2	0	-
15	<UV>	m/s2	0	-
16	<UW>	m/s2	0	-
17	<UT>	Km/s	0	-
18	<US>	Km/s	0	-
19	<VW>	m/s2	0	-
20	<VT>	Km/s	0	-
21	<VS>	Km/s	0	-
22	<WT>	Km/s	0	-
23	<WS>	Km/s	0	-
24	<TS>	K2	0	-
25	TNTC	oC	0	-
26	ROTR	o	0	-
27	FF05	m/s	0	-
28	FF10	m/s	0	-
29	FF20	m/s	0	-
30	DD10	o	0	-
31	TD1	oC	0	-
32	TD21	K	0	-
33	TD32	K	0	-
34	TD43	K	0	-
35	RAIN	0	0	-
36	ROTE	o	0	-
37	CWW1	-	0	-
38	CWW2	-	0	-
39	CWW4	-	0	-
40	CTT1	-	0	-
41	CTT2	-	0	-
42	CTT4	-	0	-
43	NSAMP	0	0	-
44	LPHI	o	0	-
45	SH20	g/kg	0	-
46	SH10	g/kg	0	-
47	SH02	g/kg	0	-
48	SH06	g/kg	0	
49	F200	m/s	0	-

50	QNET	W/m2	0	-
51	RM	mm	0	-
52	PP	mbar	0	-
53	zon	aanthu	0	-
54	WOL1	-	0	-
55	WOL2	-	0	-
56	WOL3	-	0	-
57	Uster	m/s	0	-
58	HPR	W/m2	0	-
59	HBOW	W/m2	0	-
60	LEPR	W/m2	0	-
61	LEBOW	W/m2	0	-
62	LEBAL	W/m2	0	-
63	Znul	m	0	-
64	-	-	0	-
65	-	-	0	-
66	-	-	0	-
67	-	-	0	-
68	-	-	0	-
69	-	-	0	-
70	-	-	0	-
71	-	-	0	-
72	-	-	0	-
73	-	-	0	-
74	-	-	0	-
75	-	-	0	-
76	-	-	0	-
77	-	-	0	-
78	-	-	0	-
79	-	-	0	-
80	-	-	0	-

DATABOEL: CABNACHT.INP

DATASET CABNACHT, INVOER PARAMETERS	
80	NUMBER OF COLOMNS IN DATAFILE
30	AVERAGING TIME (MIN.) IN BASIC DATA-SET
-9999.000	MISSING VALUE CODE

DATABOEL: BASENAME.INP

CABNACHT	DATA-BASE NAME

TABEL I

FILEBESCHRIJVING
CABJJMM.DIR
Recordlengte 420 bytes (210 words integer*2)

woord	element	eenheid	schaal factor in ASCII files	woord	element		eenheid	schaal factor ASCII files
0	MMDD			50	F40		M/S	10
1	UUMN			51	SD		M/S	100
2	T200	C	100	52	FMAX		M/S	10
3	KW			53	KW			
4	T140	C	100	54	F20		M/S	10
5	KW			55	SD		M/S	100
6	T80	C	100	56	FMAX		M/S	10
7	KW			57	KW			
8	T40	C	100	58	F10		M/S	10
9	KW			59	SD		M/S	100
10	T20	C	100	60	FMAX		M/S	10
11	KW			61	KW			
12	T10	C	100	62	-			
13	KW			63	-			
14	T2	C	100	64	D200		DEG	1
15	KW			65	SD		DEG	10
16	T06	C	100	66	KW			
17	KW			67	D140		DEG	1
18	-			68	SD		DEG	10
19	-			69	KW			
20	SH200	G/KG	100	70	D80		DEG	1
21	KW			71	SD		DEG	10
22	SH140	G/KG	100	72	KW			
23	KW			73	D40		DEG	1
24	SH80	G/KG	100	74	SD		DEG	10
25	KW			75	KW			
26	SH40	G/KG	100	76	D20		DEG	1
27	KW			77	SD		DEG	10
28	SH20	G/KG	100	78	KW			
29	KW			79	D10		DEG	1
30	SH10	G/KG	100	80	SD		DEG	10
31	KW			81	KW			
32	SH2	G/KG	100	82	-			
33	KW			83	V180	k1	AANT.	
34	SH06	G/KG	100	84		k2		
35	KW			85		k3		
36	-			86		k4		
37	-			87		k5		
38	F200	M/S	10	88	KW			
39	SD	M/S	100	89	V140	k1	AANT.	
40	FMAX	M/S	10	90		k2		
41	KW			91		k3		
42	F140	M/S	10	92		k4		
43	SD	M/S	100	93		k5		
44	FMAX	M/S	10	94	KW			
45	KW			95	V100	k1	AANT.	
46	F80	M/S	10	96		k2		
47	SD	M/S	100	97		k3		
48	FMAX	M/S	10	98		k4		
49	KW			99		k5		

100	KW			
101	V60	k1	AANT.	
102		k2		
103		k3		
104		k4		
105		k5		
106	KW			
107	V20	k1	AANT.	
108		k2		
109		k3		
110		k4		
111		k5		
112	KW			
113	V10	k1	AANT.	
114		k2		
115		k3		
116		k4		
117		k5		
118	KW			
119	V2	k1	AANT.	
120		k2		
121		k3		
122		k4		
123		k5		
124	KW			
125	-			
126	-			
127	K214		W/M2	
128	KW			
129	K06		W/M2	
130	KW			
131	KDIF		W/M2	
132	KW			
133	QN		W/M2	
134	KW			
135	LIN		W/M2	
136	KW			
137	LOUT		W/M2	
138	KW			
139	TS0		C	10
140	KW			
141	TS2		C	10
142	KW			
143	GSO		W/M2	1
144	KW			
145	GS5		W/M2	
146	KW			
147	GS10		W/M2	1
148	KW			
149	RR		MM	10
150	KW			
151	NM		AANT.	1
152	KW			
153	PP		MBAR	10
154	KW			
155	ZON		AANT.	1
156	KW			
157	LAMBDA			1000
158	KW			
159	SODAR	I1		1
160	SODAR	I2		1
161	SODAR	I3		1
162	KW			
163	wolken-hoogte	I1		1
164		I2		1
165		I3		1
166	KW			
167	-			
168	-			
169	UST		M/S	100
170	KW			
171	HPR		W/M2	1
172	KW			
173	HBOW		W/M2	1
174	KW			
175	LEPR		W/M2	1
176	KW			
177	LEBOW		W/M2	1
178	KW		W/M2	1
179	LEBAL			1
180	KW			
181	Z0		M	1000
182	KW			
183 t/m 209	NVT			

*Wanneer m.b.v. SELREC gelezen wordt, komt dit element niet meer in het buffer array voor. Array BUF (met een index van 1 t/m 209) bevat woord 1 t/m 209 na aanroep.

Verklaring v/d afkortingen

UST	:	wrijvingssnelheid
HPR	:	warmteflux (berekend uit profielen)
HBOW	:	warmteflux (BOWEN-RATIO methode)
LEPR	:	vochtflux (berekend uit profielen)
LEBOW	:	vochtflux (BOWEN-RATIO methode)
LEBAL	:	vochtflux (BALANS-methode)
Z0	:	ruwheidslengte (MEMO FM-88-05)
KW	:	kwaliteitscode
		k = 1 : enige samples ontbreken
		k = 2, 3 en/of w = 1 : verdachte waarden
		k = 9 en/of w = 9 : ontbrekende waarden
K214	:	inkomende kortgolvige straling (214 m)
K06	:	" " " (2 m)
kDIF	:	diffuse kortgolvige straling
QN	:	nettostraling
LIN	:	inkomende langgolvige straling
LOUT	:	uitgaande langgolvige straling
TSO	:	bodemtemperatuur - 0 cm
TS2	:	" " - 2 cm
GSO	:	bodem warmtestroom 0 cm
GS5	:	" " " - 5 cm
GS10	:	" " " -10 cm
RR	:	neerslaghoeveelheid
NM	:	regenindicator
PP	:	luchtdruk op zeeniveau

	day	time (UT)	U* (m/s)	FF5 (m/s)	FF10 (m/s)	FF20 (m/s)	D10 (degrees)	T0.6 (Celc.)
1	890721	18.3	0.275	3.192	3.562	4.186	85.3	22.61
2	890721	19	0.307	3.23	3.664	4.357	76.9	22.13
3	890721	19.3	0.224	2.15	2.516	3.163	71.6	20.88
4	890721	20	0.231	2.211	2.58	3.547	66.9	19.94
5	890721	20.3	0.285	2.842	3.267	4.15	69	20.14
6	890721	21	0.270	2.742	3.186	4.012	69.3	19.65
7	890721	21.3	0.280	3.061	3.399	4.26	68.1	19.12
8	890721	22	0.291	3.191	3.604	4.481	71.9	18.9
9	890721	22.3	0.254	2.91	3.353	4.157	75.4	18.57
10	890721	23	0.294	3.217	3.635	4.379	77.7	18.29
11	890721	23.3	0.305	3.233	3.56	4.176	78.2	18.03
12	890722	0	0.286	2.788	3.141	3.734	81.8	17.78
13	890722	0.3	0.230	2.471	2.804	3.422	83.8	17.57
14	890722	1	0.285	2.404	2.853	3.461	82.2	17.63
15	890722	1.3	0.289	2.795	3.14	3.656	83.5	17.59
16	890722	3	0.290	3.209	3.635	4.228	86.3	17.33
17	890722	18	0.217	2.355	2.687	3.27	84.2	27.32
18	890722	18.3	0.217	2.704	3.155	3.926	91	26.51
19	890722	19	0.220	2.91	3.367	4.141	94.4	25.77
20	890722	19.3	0.242	2.942	3.386	4.182	92.4	25.15
21	890722	20	0.222	2.837	3.307	4.237	90	24.23
22	890722	20.3	0.316	3.507	3.93	4.871	88.8	24.46
23	890722	21	0.276	2.989	3.4	4.3	86.8	23.86
24	890722	21.3	0.217	2.622	3.103	3.867	86.9	22.82
25	890722	22	0.193	2.457	2.864	3.735	89.9	22.09
26	890722	22.3	0.203	2.335	2.819	3.675	90.5	21.73
27	890722	23	0.118	2.034	2.253	2.882	289.5	19.83
28	890730	19.3	0.678	7.85	8.63	9.75	270.3	14.91
29	890730	20.3	0.600	8.01	8.75	9.85	270.6	15.14
30	890730	21	0.565	7.31	7.97	9.13	273.5	14.96
31	890730	21.3	0.584	7.25	7.85	8.91	276.7	14.99
32	890731	0	0.465	5.983	6.455	7.31	291.4	14.28
33	890731	3	0.361	4.245	4.713	5.49	295.6	13.94
34	890731	3.3	0.419	4.789	5.213	5.995	295.8	13.7
35	890731	4	0.311	4.372	4.728	5.459	287.3	13.35
36	890731	4.3	0.324	3.777	4.099	4.866	292.1	13.4
37	890801	19	0.348	4.413	4.795	5.556	309	12.83
38	890801	19.3	0.381	4.306	4.789	5.588	304.2	13.07
39	890801	20	0.237	3.205	3.592	4.428	301.4	12.57
40	890801	21	0.226	2.66	2.996	3.626	291.2	11.51
41	890801	22.3	0.206	2.847	3.206	3.99	258.9	10.84
42	890802	0.3	0.219	2.33	2.666	3.347	289.9	11.9
43	890802	2	0.240	3.355	3.74	4.432	292.8	12.37
44	890802	4.3	0.261	3.123	3.505	4.239	295.1	12.34
45	890806	5.3	0.249	2.755	3.134	3.828	93.1	14.99
46	890814	20.3	0.175	3.072	3.721	4.912	151.4	19.97
47	890814	21	0.294	4.109	4.856	5.975	159.8	20.51
48	890814	21.3	0.327	4.801	5.424	6.471	159.5	20.93
49	890814	22	0.262	4.013	4.606	5.619	158.4	20.35
50	890814	22.3	0.269	3.895	4.474	5.6	157.7	20.21
51	890814	23	0.314	4.782	5.44	6.446	161.6	20.42
52	890814	23.3	0.320	4.958	5.645	6.485	166.7	20.28
53	890815	0	0.347	4.918	5.62	6.68	161.6	20.25
54	890815	0.3	0.362	5.337	6.019	6.913	168.1	20.24
55	890815	1	0.297	4.834	5.39	6.085	179.1	19.95
56	890815	1.3	0.322	4.552	5.133	5.787	181.9	20.02
57	890815	2	0.395	4.977	5.548	6.363	188	20.19
58	890815	2.3	0.342	4.754	5.233	5.907	194.8	20.09
59	890815	3	0.305	3.661	4.068	4.792	192.8	19.66
60	890815	3.3	0.310	3.772	4.238	4.92	189.3	19.5
61	890815	4	0.282	3.958	4.471	5.178	188.2	19.24
62	890816	22	0.230	3.464	3.954	4.775	234.9	17.34
63	890816	22.3	0.312	4.193	4.626	5.25	248.1	17.37
64	890816	23	0.211	3.754	4.368	5.267	237.9	16.55
65	890817	0	0.211	3.549	4.207	5.172	222.9	16.05
66	890817	1	0.215	3.191	0.249	4.785	227.5	15.35
67	890817	2	0.210	3.1	0.014	4.15	213.7	14.83
68	890817	2.3	0.231	3.606	0.014	5.242	227.8	14.62
69	890817	3	0.257	3.961	0.013	5.627	224.3	14.73
70	890817	3.3	0.244	3.799	0.014	5.568	227	14.43
71	890817	4	0.266	4.282	0.014	6.019	234.5	14.35
72	890817	18.3	0.188	3.705	0.018	5.35	239.1	17.27
73	890817	21.3	0.173	2.78	0.014	4.117	205.2	13.72
74	890819	1	0.215	3.022	3.563	4.215	104.7	13.43
75	890819	3	0.203	2.887	3.39	4.094	100.7	12.81
76	890819	3.3	0.207	3.034	3.489	4.198	103.7	12.78
77	890819	23	0.185	2.172	2.745	4.001	83.7	17.07

	day	time (UT)	U* (m/s)	FF5 (m/s)	FF10 (m/s)	FF20 (m/s)	D10 (degrees)	T0.6 (Celc.)
78	890819	23.3	0.190	2.594	3.166	4.28	85	17.59
79	890823	22.3	0.155	2.901	3.356	4.229	190.6	11.61
80	890825	18	0.110	1.664	1.969	2.705	345.1	14.42
81	890827	1.3	0.230	3.418	3.747	4.214	211.9	15.78
82	890827	2	0.253	4.183	4.618	5.33	221.7	16.01
83	890827	2.3	0.346	5.396	5.973	6.653	221.3	15.94
84	890827	3	0.362	5.242	5.775	6.546	228.3	15.9
85	890827	16.3	0.365	4.406	4.868	5.594	320.1	14.46
86	890827	21.3	0.261	3.463	3.93	4.854	301.3	11.26
87	890827	22	0.196	2.956	3.345	4.073	299.2	11.3
88	890827	22.3	0.233	3.071	3.517	4.462	304.5	11.14
89	890827	23	0.218	3.165	3.656	4.574	305.2	11.08
90	890827	23.3	0.218	3.026	3.45	4.449	306.8	10.79
91	890828	0	0.220	2.751	3.246	4.123	322.5	11.12
92	890828	1.3	0.395	4.304	4.831	5.858	328	11.63
93	890828	2	0.271	3.474	3.938	4.818	321.9	11.11
94	890828	2.3	0.266	3.334	3.785	4.62	322.7	11.12
95	890828	3	0.274	3.514	3.946	4.753	318.5	11.1
96	890828	3.3	0.325	3.801	4.309	5.276	325.9	11.28
97	890828	4	0.344	3.988	4.617	5.732	329.8	11.18
98	890828	4.3	0.324	4.073	4.764	5.895	328.6	11.29
99	890828	5	0.336	4.503	5.085	5.947	322	11.75
100	890828	6	0.432	5.283	5.818	6.567	328.2	12.99
101	890828	16.3	0.520	5.649	6.131	6.991	347	15.75
102	890828	17	0.498	5.295	5.77	6.617	341.5	15.09
103	890828	18	0.229	3.275	3.748	4.509	336.6	13.81
104	890828	18.3	0.186	2.503	2.995	3.938	332.4	13.2
105	890828	19	0.169	2.176	2.589	3.289	317.1	13.24
106	890828	19.3	0.203	2.351	2.783	3.524	326.2	13.05
107	890828	20	0.195	2.328	2.755	3.636	322	13.07
108	890828	20.3	0.176	2.424	2.769	3.455	306	13.08
109	890828	21	0.172	2.312	2.61	3.187	309.9	13.08
110	890828	21.3	0.151	2.483	2.831	3.512	302.2	13.05
111	890828	22	0.212	2.451	2.789	3.486	305.9	13.22
112	890828	22.3	0.162	2.242	2.536	3.181	313.7	13.21
113	890828	23	0.125	1.998	2.314	3.01	301.7	12.89
114	890902	17.3	0.295	3.091	3.52	4.351	4.9	13.5
115	890902	18.3	0.210	2.205	2.621	3.582	356.2	11.21
116	890908	17.3	0.204	3.119	3.513	4.359	21.7	18.68
117	890910	18.3	0.260	2.385	2.758	3.544	54.5	17.72
118	890910	19	0.275	2.707	3.038	3.754	58.6	17.9
119	890910	20	0.315	2.936	3.24	3.998	59.1	17.61
120	890910	20.3	0.337	3.398	3.661	4.53	60.5	17.78
121	890910	21	0.457	4.014	4.414	5.207	62.5	17.92
122	890912	5.3	0.347	2.909	3.116	3.508	81.2	13.56
123	890914	17	0.127	2.578	3.144	3.928	239.7	12.74
124	890914	17.3	0.145	2.993	3.388	4.086	218.5	12.67
125	890914	18	0.162	2.341	2.671	3.217	214.3	12.48
126	890914	18.3	0.156	2.533	2.858	3.403	200.8	12.42
127	890914	19	0.148	2.452	2.734	3.25	183.6	12.26
128	890914	19.3	0.205	2.548	2.903	3.421	187.1	12.39
129	890915	15.3	0.326	4.459	4.847	5.426	247.4	16.84
130	890917	3	0.231	3.47	3.885	4.488	184	17.08
131	890917	17.3	0.171	2.4	2.806	3.333	274.4	18.28
132	890917	21.3	0.103	2.157	2.459	3.167	189.2	14.11
133	890918	2	0.124	2.05	2.497	3.282	144.1	14.36
134	890918	2.3	0.133	2.664	3.168	3.926	147.9	14.63
135	890918	3	0.164	2.056	2.425	2.972	334.5	14.64
136	890918	3.3	0.144	2.255	2.74	3.473	161.6	14.76
137	890918	4	0.247	2.663	3.146	3.914	262.3	15.17
138	890918	4.3	0.199	2.347	2.756	3.349	332.3	15.05
139	890918	18	0.100	1.714	2.266	3.383	272.8	20.53
140	890918	18.3	0.116	1.981	2.478	3.473	293.4	20.63
141	890918	19	0.113	1.909	2.467	3.304	318.5	20.39
142	890918	19.3	0.157	2.553	3.196	4.097	330.8	20.66
143	890918	20	0.231	3.408	4.117	5.069	152.4	21.03
144	890918	20.3	0.196	3.425	4.036	5.26	154.5	20.65
145	890918	21	0.149	2.864	3.411	4.57	154.2	20.14
146	890918	21.3	0.131	2.845	3.409	4.505	149.1	19.51
147	890918	22	0.137	2.991	3.609	4.449	145.8	19.31
148	890918	22.3	0.206	3.436	4.019	5.129	149.3	19.76
149	890918	23	0.199	3.499	4.068	5.3	153	19.96
150	890918	23.3	0.277	3.884	4.395	5.413	158.5	19.91
151	890919	0	0.279	3.186	3.633	4.32	217.5	19.06
152	890919	2.3	0.110	2.547	3.094	3.907	171.7	16.67
153	890919	3	0.143	2.657	3.104	3.869	179.6	16.76
154	890919	3.3	0.233	3.337	3.818	4.62	184.1	17.15

	day	time (UT)	U* (m/s)	FF5 (m/s)	FF10 (m/s)	FF20 (m/s)	D10 (degrees)	T0.6 (Celc.)
155	890919	16.3	0.198	2.967	3.223	3.762	273.7	17.69
156	890919	17	0.145	2.413	2.811	3.407	273	16.32
157	890919	23	0.116	2.478	2.965	3.738	178.4	11.41
158	890919	23.3	0.107	2.493	2.879	3.605	179	10.99
159	890920	0.3	0.107	2.672	3.104	3.804	181	10.98
160	890920	1	0.142	2.507	2.957	3.778	184.5	10.85
161	890920	1.3	0.118	2.579	2.95	3.667	183.7	10.34
162	890920	6	0.125	2.228	2.641	3.491	157.4	10.56
163	890921	21.3	0.209	2.463	2.959	3.515	68.1	19.16
164	890921	22	0.201	2.898	3.37	3.92	55.1	19.08
165	890922	14.3	0.298	5.475	5.948	6.512	276.6	23.14
166	890922	16	0.283	4.094	4.464	5	281	21.05
167	890922	18.3	0.325	3.864	4.299	5.077	274.8	17.35
168	890922	21.3	0.165	2.687	3.27	3.993	240.3	15.47
169	890922	22	0.166	2.958	3.438	4.013	250.3	14.89
170	890922	22.3	0.131	2.565	3.222	4.083	237.8	14.34
171	890922	23	0.189	2.737	3.211	3.846	249.5	14.91
172	890922	23.3	0.171	2.53	2.917	3.474	242	14.3
173	890923	0	0.114	2.284	2.905	3.573	246.3	14.45
174	890923	0.3	0.224	2.672	2.915	3.395	252	15.38
175	890923	1	0.247	3.04	3.357	3.838	257.7	15.43
176	890923	1.3	0.235	3.152	3.554	4.113	253.7	14.87
177	890923	3	0.164	2.638	3.083	3.734	219.2	14.76
178	891004	16	0.198	2.21	2.529	3.101	88.2	12.89
179	891004	16.3	0.161	2.172	2.547	3.162	80.2	11.49
180	891004	19.3	0.180	2.405	2.866	3.699	91.5	8.74
181	891004	20	0.241	2.847	3.286	4.157	92.8	8.98
182	891004	20.3	0.244	3.173	3.642	4.454	99.8	9.06
183	891004	21	0.276	3.184	3.597	4.263	97.7	8.7
184	891004	21.3	0.259	3.176	3.651	4.34	102.3	8.28
185	891004	22	0.233	3.259	3.789	4.376	103	7.94
186	891004	22.3	0.308	3.253	3.75	4.343	87.9	7.87
187	891004	23	0.249	3.348	3.835	4.228	96	7.71
188	891004	23.3	0.232	3.293	3.833	4.403	98.3	7.44
189	891005	0	0.182	2.626	3.185	3.533	93.6	6.926
190	891005	1	0.233	2.924	3.498	3.949	94	6.615
191	891005	1.3	0.219	2.721	3.274	3.708	91.8	6.269
192	891005	3	0.222	3.133	3.691	4.136	96.7	5.759
193	891005	3.3	0.222	2.805	3.32	3.791	61.5	5.433
194	891005	4	0.201	2.56	3.113	3.599	74.4	5.069
195	891005	4.3	0.250	3.031	3.598	4.095	69.3	5.178
196	891005	5	0.224	2.711	3.224	3.612	54.6	4.891
197	891005	5.3	0.241	2.561	3.097	3.653	348.2	4.755
198	891006	3.3	0.150	2.245	2.679	3.484	302.1	12.18
199	891006	4	0.171	2.397	2.876	3.762	291.3	11.5
200	891006	4.3	0.210	3.014	3.524	4.368	275.6	11.27
201	891006	5	0.176	2.768	3.287	4.049	276.6	10.11
202	891006	5.3	0.158	2.892	3.503	4.462	267.9	9.26
203	891006	6	0.148	2.75	3.363	4.19	262.4	9.46
204	891006	6.3	0.214	2.856	3.284	4.091	259.9	10.06
205	891007	1.3	0.245	2.933	3.39	4.213	323.4	10.86
206	891008	3	0.419	4.868	5.465	6.486	340.1	10.47
207	891008	3.3	0.636	6.077	6.588	7.69	351.5	10.54
208	891008	4	0.654	7.4	8.11	9.31	7.5	10.79

	day	time (UT)	Td2-0.6	Td10-2	Td20-10	z/L	Phi-M	Phi-H
1	890721	18.3	0.747	0.455	0.125	0.216	1.308	1.201
2	890721	19.0	0.752	0.375	0.118	0.162	1.301	1.240
3	890721	19.3	0.983	0.558	0.187	0.337	1.667	1.489
4	890721	20.0	1.015	0.644	0.297	0.310	2.421	2.119
5	890721	20.3	0.723	0.428	0.177	0.268	1.790	1.116
6	890721	21.0	0.678	0.411	0.150	0.243	1.765	1.235
7	890721	21.3	0.656	0.379	0.153	0.256	1.778	1.109
8	890721	22.0	0.576	0.304	0.109	0.197	1.740	1.097
9	890721	22.3	0.554	0.305	0.071	0.236	1.829	0.983
10	890721	23.0	0.514	0.295	0.073	0.162	1.463	1.087
11	890721	23.3	0.505	0.306	0.094	0.155	1.165	1.177
12	890722	0.0	0.474	0.281	0.084	0.140	1.197	1.407
13	890722	0.3	0.497	0.279	0.102	0.225	1.550	1.494
14	890722	1.0	0.372	0.221	0.079	0.161	1.233	1.204
15	890722	1.3	0.375	0.237	0.053	0.129	1.030	1.241
16	890722	3.0	0.317	0.189	0.058	0.105	1.181	1.581
17	890722	18.0	0.940	0.614	0.207	0.250	1.551	2.285
18	890722	18.3	1.075	0.720	0.221	0.312	2.053	1.917
19	890722	19.0	1.114	0.769	0.249	0.402	2.034	1.576
20	890722	19.3	1.058	0.742	0.252	0.315	1.901	1.676
21	890722	20.0	1.089	0.841	0.338	0.435	2.423	1.803
22	890722	20.3	0.822	0.631	0.284	0.190	1.718	1.780
23	890722	21.0	0.842	0.617	0.271	0.252	1.885	1.705
24	890722	21.3	0.972	0.726	0.330	0.359	2.034	2.250
25	890722	22.0	1.073	0.799	0.318	0.441	2.606	2.248
26	890722	22.3	1.050	0.761	0.318	0.398	2.434	2.251
27	890722	23.0	1.057	1.222	0.489	1.773	3.065	2.096
28	890730	19.3	0.262	0.204	0.073	0.029	0.953	1.135
29	890730	20.3	0.294	0.223	0.068	0.037	1.059	1.109
30	890730	21.0	0.276	0.240	0.085	0.036	1.186	1.426
31	890730	21.3	0.244	0.205	0.060	0.029	1.047	1.431
32	890731	0.0	0.249	0.242	0.067	0.067	1.061	1.003
33	890731	3.0	0.218	0.273	0.078	0.104	1.241	1.159
34	890731	3.3	0.219	0.259	0.097	0.071	1.078	1.393
35	890731	4.0	0.235	0.307	0.084	0.133	1.356	1.262
36	890731	4.3	0.173	0.239	0.071	0.103	1.368	1.395
37	890801	19.0	0.304	0.128	0.074	0.077	1.264	1.630
38	890801	19.3	0.182	0.174	0.079	0.071	1.211	1.517
39	890801	20.0	0.218	0.309	0.133	0.240	2.040	1.519
40	890801	21.0	0.277	0.481	0.108	0.220	1.610	1.625
41	890801	22.3	0.485	0.703	0.231	0.376	2.196	1.826
42	890802	0.3	0.311	0.601	0.202	0.253	1.792	2.194
43	890802	2.0	0.259	0.391	0.155	0.221	1.667	1.773
44	890802	4.3	0.186	0.287	0.103	0.165	1.626	1.610
45	890806	5.3	0.232	0.222	0.163	0.238	1.609	1.584
46	890814	20.3	0.526	0.743	0.250	0.536	3.934	1.880
47	890814	21.0	0.490	0.629	0.213	0.224	2.194	1.416
48	890814	21.3	0.442	0.501	0.160	0.150	1.848	1.423
49	890814	22.0	0.460	0.552	0.165	0.238	2.235	1.427
50	890814	22.3	0.447	0.569	0.183	0.244	2.418	1.412
51	890814	23.0	0.411	0.484	0.141	0.179	1.850	1.203
52	890814	23.3	0.380	0.409	0.136	0.156	1.517	1.303
53	890815	0.0	0.369	0.382	0.105	0.132	1.766	1.135
54	890815	0.3	0.375	0.391	0.111	0.111	1.427	1.275
55	890815	1.0	0.388	0.454	0.144	0.168	1.350	1.453
56	890815	1.3	0.396	0.481	0.144	0.175	1.173	1.187
57	890815	2.0	0.400	0.387	0.117	0.107	1.191	1.149
58	890815	2.3	0.391	0.349	0.090	0.117	1.136	1.225
59	890815	3.0	0.375	0.385	0.088	0.132	1.371	1.357
60	890815	3.3	0.384	0.389	0.106	0.141	1.269	1.339
61	890815	4.0	0.398	0.425	0.126	0.187	1.449	1.352
62	890816	22.0	0.228	0.303	0.118	0.216	2.058	1.670
63	890816	22.3	0.265	0.287	0.073	0.082	1.153	1.883
64	890816	23.0	0.337	0.462	0.206	0.264	2.463	2.299
65	890817	0.0	0.338	0.321	0.097	0.279	2.638	1.392
66	890817	1.0	0.330	0.365	0.119	0.265	12.206	1.579
67	890817	2.0	0.385	0.358	0.069	0.282	11.375	1.196
68	890817	2.3	0.289	0.323	0.116	0.217	13.089	1.650
69	890817	3.0	0.262	0.228	0.077	0.170	12.592	1.389
70	890817	3.3	0.271	0.273	0.102	0.197	13.124	1.522
71	890817	4.0	0.237	0.270	0.151	0.164	13.026	1.920
72	890817	18.3	0.474	0.669	0.262	0.390	16.397	2.312
73	890817	21.3	0.844	1.121	0.394	0.582	13.711	2.509
74	890819	1.0	0.857	0.592	0.139	0.355	1.750	1.282
75	890819	3.0	0.779	0.497	0.152	0.536	2.006	1.014
76	890819	3.3	0.768	0.554	0.172	0.380	1.973	1.478
77	890819	23.0	1.480	1.105	0.787	0.572	3.918	4.016

	day	time (UT)	Td2-0.6	Td10-2	Td20-10	z/L	Phi-M	Phi-H
78	890819	23.3	1.212	0.979	0.592	0.553	3.383	3.073
79	890823	22.3	1.044	1.322	0.344	0.720	3.250	2.265
80	890825	18.0	0.364	0.389	0.092	0.714	3.878	1.949
81	890827	1.3	0.322	0.156	-0.297	0.101	1.170	-3.325
82	890827	2.0	0.665	0.054	-0.344	0.101	1.627	-3.413
83	890827	2.3	0.514	0.312	-0.081	0.066	1.135	0.180
84	890827	3.0	0.082	0.728	-0.122	0.062	1.229	-0.275
85	890827	16.3	0.048	0.090	-0.051	0.042	1.147	0.727
86	890827	21.3	0.151	0.239	0.145	0.194	2.042	1.627
87	890827	22.0	0.114	0.206	0.110	0.339	2.139	1.407
88	890827	22.3	0.196	0.334	0.185	0.233	2.345	1.990
89	890827	23.0	0.192	0.356	0.207	0.328	2.434	1.743
90	890827	23.3	0.187	0.382	0.240	0.311	2.646	2.031
91	890828	0.0	0.174	0.387	0.219	0.303	2.304	1.926
92	890828	1.3	0.201	0.296	0.165	0.100	1.500	1.494
93	890828	2.0	0.174	0.295	0.155	0.223	1.877	1.379
94	890828	2.3	0.203	0.317	0.184	0.234	1.811	1.519
95	890828	3.0	0.160	0.316	0.161	0.231	1.701	1.334
96	890828	3.3	0.177	0.252	0.156	0.160	1.716	1.342
97	890828	4.0	0.197	0.300	0.185	0.145	1.873	1.476
98	890828	4.3	0.176	0.265	0.176	0.154	2.013	1.518
99	890828	5.0	0.141	0.204	0.089	0.128	1.483	1.162
100	890828	6.0	-0.069	0.087	-0.126	0.022	1.001	-0.622
101	890828	16.3	0.087	0.011	-0.103	0.009	0.955	-0.213
102	890828	17.0	0.115	0.040	-0.060	0.022	0.982	0.611
103	890828	18.0	0.214	0.238	0.074	0.269	1.920	1.073
104	890828	18.3	0.198	0.347	0.164	0.349	2.933	1.920
105	890828	19.0	0.131	0.292	0.124	0.361	2.389	1.893
106	890828	19.3	0.172	0.392	0.149	0.324	2.109	1.635
107	890828	20.0	0.107	0.313	0.147	0.259	2.606	2.187
108	890828	20.3	0.075	0.210	0.097	0.265	2.245	2.087
109	890828	21.0	0.136	0.237	0.086	0.313	1.933	1.748
110	890828	21.3	0.106	0.255	0.142	0.418	2.603	2.228
111	890828	22.0	0.078	0.172	0.084	0.189	1.898	1.897
112	890828	22.3	0.104	0.234	0.075	0.300	2.291	1.929
113	890828	23.0	0.131	0.296	0.131	0.490	3.214	2.653
114	890902	17.3	0.467	0.333	0.131	0.153	1.625	1.515
115	890902	18.3	0.858	0.702	0.291	0.358	2.641	2.176
116	890908	17.3	0.644	0.452	0.184	0.393	2.393	1.520
117	890910	18.3	0.530	0.361	0.179	0.209	1.745	1.728
118	890910	19.0	0.472	0.299	0.088	0.171	1.503	1.265
119	890910	20.0	0.422	0.286	0.113	0.141	1.389	1.330
120	890910	20.3	0.397	0.257	0.075	0.121	1.489	1.106
121	890910	21.0	0.376	0.179	0.066	0.067	1.001	1.030
122	890912	5.3	0.089	0.001	-0.065	0.030	0.652	0.806
123	890914	17.0	0.361	0.536	0.254	0.691	3.560	2.776
124	890914	17.3	0.375	0.397	0.118	0.369	2.774	2.443
125	890914	18.0	0.390	0.354	0.071	0.371	1.940	1.517
126	890914	18.3	0.387	0.400	0.075	0.340	2.022	1.848
127	890914	19.0	0.311	0.399	0.080	0.440	2.011	1.623
128	890914	19.3	0.299	0.372	0.066	0.206	1.455	1.657
129	890915	15.3	0.089	0.061	-0.064	0.029	1.024	0.935
130	890917	3.0	0.244	0.303	0.063	0.189	1.505	1.416
131	890917	17.3	0.302	0.545	0.101	0.289	1.778	2.072
132	890917	21.3	1.185	1.150	0.277	1.002	3.964	3.118
133	890918	2.0	0.377	0.332	0.074	0.592	3.667	1.693
134	890918	2.3	0.332	0.266	0.118	0.481	3.289	2.263
135	890918	3.0	0.484	0.314	0.081	0.294	1.925	2.019
136	890918	3.3	0.361	0.302	0.122	0.585	2.933	1.615
137	890918	4.0	0.277	0.217	0.067	0.196	1.792	1.231
138	890918	4.3	0.310	0.238	0.052	0.229	1.720	1.477
139	890918	18.0	1.637	1.199	0.499	1.397	6.447	3.771
140	890918	18.3	1.338	1.039	0.421	1.196	4.951	2.847
141	890918	19.0	1.136	0.995	0.351	1.075	4.269	2.877
142	890918	19.3	0.797	0.782	0.327	0.686	3.305	2.210
143	890918	20.0	0.574	0.644	0.254	0.389	2.381	1.502
144	890918	20.3	0.519	0.814	0.282	0.463	3.597	1.882
145	890918	21.0	0.579	0.948	0.304	0.676	4.501	2.384
146	890918	21.3	0.588	1.007	0.280	0.986	4.839	1.987
147	890918	22.0	0.513	0.808	0.252	0.739	3.537	2.234
148	890918	22.3	0.352	0.504	0.188	0.333	3.108	1.793
149	890918	23.0	0.374	0.504	0.169	0.312	3.580	1.922
150	890918	23.3	0.420	0.524	0.156	0.217	2.124	1.355
151	890919	0.0	0.493	0.639	0.193	0.157	1.420	2.110
152	890919	2.3	0.609	0.962	0.301	0.849	4.284	3.499
153	890919	3.0	0.400	0.676	0.257	0.551	3.092	2.823
154	890919	3.3	0.301	0.365	0.123	0.210	1.988	1.731

	day	time (UT)	Td2-0.6	Td10-2	Td20-10	z/L	Phi-M	Phi-H
155	890919	16.3	0.165	0.243	-0.052	0.152	1.573	0.669
156	890919	17.0	0.353	0.623	0.086	0.368	2.374	2.093
157	890919	23.0	0.848	1.007	0.325	0.621	3.863	4.531
158	890919	23.3	0.923	1.088	0.314	0.910	3.924	3.531
159	890920	0.3	0.829	1.135	0.355	1.040	3.784	3.403
160	890920	1.0	0.958	1.204	0.344	0.775	3.340	2.523
161	890920	1.3	0.998	1.319	0.375	0.679	3.507	4.456
162	890920	6.0	0.227	0.325	0.149	0.500	3.938	2.842
163	890921	21.3	0.635	0.529	0.175	0.380	1.533	1.448
164	890921	22.0	0.537	0.450	0.146	0.432	1.581	1.239
165	890922	14.3	-0.030	0.005	-0.166	0.129	1.091	-0.526
166	890922	16.0	0.138	0.181	-0.051	0.059	1.093	0.853
167	890922	18.3	0.234	0.262	0.078	0.086	1.380	1.691
168	890922	21.3	0.393	0.574	0.263	0.428	2.532	2.748
169	890922	22.0	0.517	0.847	0.260	0.489	2.001	2.360
170	890922	22.3	0.497	0.869	0.354	0.848	3.802	2.767
171	890922	23.0	0.375	0.567	0.207	0.311	1.939	2.439
172	890922	23.3	0.595	0.786	0.193	0.355	1.883	2.496
173	890923	0.0	0.311	0.914	0.315	0.748	3.377	3.769
174	890923	0.3	0.262	0.314	0.087	0.177	1.239	1.857
175	890923	1.0	0.302	0.307	0.054	0.123	1.123	1.787
176	890923	1.3	0.414	0.486	0.122	0.203	1.372	1.746
177	890923	3.0	0.225	0.262	0.071	0.225	2.286	2.474
178	891004	16.0	0.633	0.407	0.062	0.287	1.669	1.249
179	891004	16.3	1.075	0.555	0.197	0.524	2.201	1.907
180	891004	19.3	1.301	0.785	0.288	0.516	2.677	2.048
181	891004	20.0	1.025	0.696	0.245	0.339	2.085	1.535
182	891004	20.3	0.826	0.565	0.125	0.297	1.920	1.112
183	891004	21.0	0.841	0.537	0.135	0.246	1.395	1.104
184	891004	21.3	0.731	0.494	0.121	0.252	1.538	1.150
185	891004	22.0	0.700	0.495	0.134	0.344	1.457	1.104
186	891004	22.3	0.667	0.461	0.131	0.190	1.113	1.127
187	891004	23.0	0.643	0.436	0.119	0.291	0.909	1.062
188	891004	23.3	0.637	0.472	0.120	0.321	1.415	1.116
189	891005	0.0	0.783	0.588	0.121	0.524	1.101	1.116
190	891005	1.0	0.665	0.488	0.107	0.307	1.118	1.096
191	891005	1.3	0.626	0.475	0.092	0.336	1.143	1.046
192	891005	3.0	0.536	0.378	0.073	0.299	1.159	1.037
193	891005	3.3	0.574	0.401	0.077	0.340	1.226	0.932
194	891005	4.0	0.630	0.443	0.119	0.438	1.399	1.102
195	891005	4.3	0.500	0.351	0.084	0.232	1.148	1.125
196	891005	5.0	0.584	0.397	0.085	0.343	0.998	0.947
197	891005	5.3	0.549	0.375	0.086	0.290	1.333	0.980
198	891006	3.3	0.262	0.381	0.159	0.477	3.100	2.143
199	891006	4.0	0.241	0.539	0.253	0.451	2.992	2.388
200	891006	4.3	0.319	0.537	0.193	0.281	2.315	2.093
201	891006	5.0	0.481	0.829	0.269	0.415	2.497	2.560
202	891006	5.3	0.594	0.939	0.304	0.686	3.495	2.098
203	891006	6.0	0.490	0.727	0.241	0.590	3.217	2.336
204	891006	6.3	0.338	0.545	0.171	0.331	2.179	1.588
205	891007	1.3	0.210	0.340	0.141	0.191	1.942	1.858
206	891008	3.0	0.267	0.245	0.098	0.085	1.408	1.177
207	891008	3.3	0.310	0.206	0.082	0.030	1.001	1.321
208	891008	4.0	0.326	0.200	0.080	0.032	1.060	1.162

	day	time (UT)	<wT>(Km/s)	<wTv>(Km/s)	<ws>(Km/s)	Qnet(W/m2)	Zo (m)	Hprof. (W/m2)
1	890721	18.3	-0.027	-0.024	-0.029	-21	0.150	-44
2	890721	19	-0.030	-0.024	-0.031	-35	0.150	-46
3	890721	19.3	-0.023	-0.015	-0.025	-41	0.150	-17
4	890721	20	-0.021	-0.016	-0.025	-33	0.150	-24
5	890721	20.3	-0.036	-0.027	-0.040	-39	0.150	-37
6	890721	21	-0.026	-0.020	-0.031	-40	0.150	-35
7	890721	21.3	-0.032	-0.024	-0.036	-40	0.150	-38
8	890721	22	-0.025	-0.018	-0.032	-38	0.150	-40
9	890721	22.3	-0.020	-0.016	-0.025	-29	0.150	-34
10	890721	23	-0.023	-0.018	-0.027	-34	0.150	-39
11	890721	23.3	-0.025	-0.018	-0.029	-33	0.150	-35
12	890722	0	-0.017	-0.014	-0.021	-23	0.150	-28
13	890722	0.3	-0.014	-0.011	-0.018	-23	0.150	-24
14	890722	1	-0.019	-0.016	-0.024	-13	0.150	-21
15	890722	1.3	-0.018	-0.016	-0.020	-16	0.150	-25
16	890722	3	-0.013	-0.011	-0.016	-16	0.150	-27
17	890722	18	-0.015		-0.017	23	0.150	
18	890722	18.3	-0.020		-0.021	-9	0.150	
19	890722	19	-0.024		-0.028	-16	0.150	
20	890722	19.3	-0.027		-0.029	-20	0.150	
21	890722	20	-0.027		-0.031	-15	0.150	-45
22	890722	20.3	-0.036		-0.039	-14	0.150	-53
23	890722	21	-0.031		-0.034	-14	0.150	
24	890722	21.3	-0.019		-0.024	-16	0.150	
25	890722	22	-0.017		-0.021	-13	0.150	
26	890722	22.3	-0.019		-0.022	-12	0.150	
27	890722	23	-0.015		-0.019	-5	0.041	
28	890730	19.3	-0.042	-0.039	-0.059	-26	0.066	-62
29	890730	20.3	-0.036	-0.031	-0.051	-60	0.061	-69
30	890730	21	-0.029	-0.025	-0.042	-55	0.061	-61
31	890730	21.3	-0.029	-0.025	-0.037	-45	0.061	-53
32	890731	0	-0.032	-0.026	-0.044	-56	0.061	-47
33	890731	3	-0.022	-0.017	-0.031	-56	0.061	-32
34	890731	3.3	-0.022	-0.015	-0.034	-54	0.061	-35
35	890731	4	-0.015	-0.011	-0.026	-47	0.061	-33
36	890731	4.3	-0.015	-0.012	-0.022	-33	0.061	-22
37	890801	19	-0.020	-0.019	-0.021	-26	0.062	-28
38	890801	19.3	-0.022	-0.020	-0.026	-32	0.062	-25
39	890801	20	-0.016	-0.014	-0.021	-48	0.062	-22
40	890801	21	-0.012	0.007	-0.016	-58	0.061	-18
41	890801	22.3	-0.014	0.002	-0.021	-56	0.066	-26
42	890802	0.3	-0.013	-0.010	-0.017	-29	0.061	-15
43	890802	2	-0.013	-0.011	-0.020	-30	0.061	-27
44	890802	4.3	-0.012	-0.011	-0.019	-5	0.061	-20
45	890806	5.3	-0.018	-0.017	-0.024	40	0.150	-22
46	890814	20.3	-0.011	-0.010	-0.019	-23	0.110	-55
47	890814	21	-0.026	-0.023	-0.037	-22	0.110	-72
48	890814	21.3	-0.021	-0.019	-0.034	-21	0.110	-73
49	890814	22	-0.016	-0.014	-0.028	-25	0.110	-63
50	890814	22.3	-0.017	-0.015	-0.031	-23	0.110	-66
51	890814	23	-0.022	-0.019	-0.036	-23	0.041	-54
52	890814	23.3	-0.020	-0.018	-0.033	-23	0.041	-54
53	890815	0	-0.020	-0.018	-0.036	-19	0.041	-53
54	890815	0.3	-0.021	-0.019	-0.034	-21	0.041	-53
55	890815	1	-0.016	-0.014	-0.028	-22	0.041	-49
56	890815	1.3	-0.025	-0.022	-0.038	-22	0.041	-47
57	890815	2	-0.027	-0.024	-0.042	-23	0.040	-48
58	890815	2.3	-0.019	-0.017	-0.030	-20	0.040	-42
59	890815	3	-0.013	-0.012	-0.024	-17	0.040	-29
60	890815	3.3	-0.014	-0.012	-0.027	-21	0.040	-31
61	890815	4	-0.014	-0.012	-0.027	-24	0.040	-35
62	890816	22	-0.013	-0.011	-0.017	-19	0.037	-21
63	890816	22.3	-0.015	-0.013	-0.016	-28	0.066	-33
64	890816	23	-0.012	-0.003	-0.016	-43	0.037	-33
65	890817	0	-0.011	-0.024	-0.017	-47	0.037	-28
66	890817	1	-0.011	-0.013	-0.017	-49	0.037	
67	890817	2	-0.012	-0.014	-0.017	-51	0.037	
68	890817	2.3	-0.011	-0.013	-0.017	-53	0.037	
69	890817	3	-0.012	-0.014	-0.019	-53	0.037	
70	890817	3.3	-0.012	-0.013	-0.018	-52	0.037	
71	890817	4	-0.013	-0.014	-0.020	-54	0.037	
72	890817	18.3	-0.011	-0.010	-0.017	-37	0.037	
73	890817	21.3	-0.011	-0.019	-0.020	-50	0.040	
74	890819	1	-0.016	-0.012	-0.023	-49	0.150	-40
75	890819	3	-0.019	-0.011	-0.029	-50	0.150	-37
76	890819	3.3	-0.015	-0.008	-0.022	-50	0.150	-42
77	890819	23	-0.017		-0.024	-38	0.150	

	day	time (UT)	<wT>(Km/s)	<wTv>(Km/s)	<ws>(Km/s)	Qnet(W/m2)	Zo (m)	Hprof. (W/m2)
78	890819	23.3	-0.020		-0.025	-41	0.150	
79	890823	22.3	-0.012		-0.017		0.040	
80	890825	18			-0.006	-19	0.045	-5
81	890827	1.3			-0.008	-8	0.037	
82	890827	2			-0.011	-7	0.037	
83	890827	2.3			-0.018	-6	0.037	
84	890827	3			-0.019	-12	0.037	
85	890827	16.3			-0.013	-4	0.062	-13
86	890827	21.3			-0.022	-47	0.062	-21
87	890827	22			-0.017	-36	0.061	-14
88	890827	22.3			-0.019	-55	0.062	-21
89	890827	23			-0.022	-53	0.062	-22
90	890827	23.3			-0.021	-56	0.062	-20
91	890828	0			-0.021	-36	0.062	-18
92	890828	1.3			-0.040	-48	0.062	-32
93	890828	2			-0.029	-52	0.062	-23
94	890828	2.3			-0.028	-55	0.062	-23
95	890828	3			-0.031	-54	0.062	-24
96	890828	3.3			-0.035	-59	0.062	-25
97	890828	4			-0.038	-59	0.045	-28
98	890828	4.3			-0.034	-55	0.062	-29
99	890828	5			-0.031	-40	0.062	-26
100	890828	6			-0.012	53	0.062	-7
101	890828	16.3			-0.008	29	0.045	
102	890828	17			-0.017	10	0.045	
103	890828	18			-0.021	-34	0.045	-19
104	890828	18.3			-0.015	-34	0.045	-14
105	890828	19			-0.011	-24	0.062	-10
106	890828	19.3			-0.018	-35	0.062	-14
107	890828	20			-0.013	-14	0.062	-12
108	890828	20.3			-0.009	-14	0.062	-10
109	890828	21			-0.010	-22	0.062	-10
110	890828	21.3			-0.009	-15	0.062	-12
111	890828	22			-0.012	-12	0.062	-9
112	890828	22.3			-0.008	-17	0.062	-9
113	890828	23			-0.006	-18	0.062	-8
114	890902	17.3	-0.015	-0.014	-0.026	-36	0.059	-25
115	890902	18.3	-0.011	-0.006	-0.022	-55	0.045	-11
116	890908	17.3	-0.011	-0.008	-0.022	-42	0.059	-29
117	890910	18.3	-0.014		-0.024	-29	0.100	-18
118	890910	19	-0.012		-0.023	-34	0.150	-25
119	890910	20	-0.014		-0.029	-33	0.150	-28
120	890910	20.3	-0.014	-0.000	-0.030	-34	0.150	-33
121	890910	21	-0.023		-0.042	-37	0.150	-38
122	890912	5.3			-0.008	6	0.150	
123	890914	17			-0.009	-18	0.037	-18
124	890914	17.3			-0.007	-24	0.037	-20
125	890914	18			-0.010	-21	0.037	-11
126	890914	18.3			-0.008	-19	0.040	-14
127	890914	19			-0.009	-18	0.040	-12
128	890914	19.3			-0.012	-19	0.040	-14
129	890915	15.3			-0.007	19	0.066	-14
130	890917	3			-0.015	-42	0.040	-22
131	890917	17.3			-0.009	-38	0.061	-16
132	890917	21.3			-0.007	-37	0.040	-8
133	890918	2			-0.007	-37	0.110	-13
134	890918	2.3			-0.007	-39	0.110	-20
135	890918	3			-0.008	-38	0.150	-15
136	890918	3.3			-0.011	-39	0.110	-18
137	890918	4			-0.019	-40	0.110	-22
138	890918	4.3			-0.012	-39	0.110	-17
139	890918	18			-0.009	-31	0.110	
140	890918	18.3			-0.012	-32	0.110	
141	890918	19			-0.010	-32	0.110	
142	890918	19.3			-0.017	-34	0.110	
143	890918	20			-0.031	-37	0.110	
144	890918	20.3			-0.023	-37	0.110	
145	890918	21			-0.014	-36	0.110	
146	890918	21.3			-0.014	-37	0.110	
147	890918	22			-0.012	-31	0.110	-43
148	890918	22.3			-0.019	-16	0.110	-47
149	890918	23			-0.016	-19	0.110	-51
150	890918	23.3			-0.030	-23	0.041	
151	890919	0			-0.022	-36	0.037	
152	890919	2.3			-0.007	-36	0.041	
153	890919	3			-0.010	-21	0.041	
154	890919	3.3			-0.017	-27	0.040	

	day	time (UT)	<wT>(Km/s)	<wTv>(Km/s)	<ws>(Km/s)	Qnet(W/m2)	Zo (m)	Hprof. (W/m2)
155	890919	16.3			-0.008	-7	0.061	-15
156	890919	17			-0.007	-41	0.061	-17
157	890919	23			-0.006	-49	0.041	-17
158	890919	23.3			-0.007	-50	0.041	-15
159	890920	0.3			-0.008	-49	0.040	-20
160	890920	1			-0.014	-50	0.040	-16
161	890920	1.3			-0.007	-52	0.040	-16
162	890920	6			-0.006	-5	0.110	-17
163	890921	21.3	-0.012	-0.016	-0.023	-39	0.150	-25
164	890921	22	-0.011	-0.014	-0.023	-40	0.150	-35
165	890922	14.3			-0.023	98	0.061	-4
166	890922	16			-0.009			
167	890922	18.3			-0.019			
168	890922	21.3			-0.012			
169	890922	22			-0.014			
170	890922	22.3			-0.012			
171	890922	23			-0.014			
172	890922	23.3			-0.011			
173	890923	0			-0.007	-10	0.066	-19
174	890923	0.3			-0.013	-8	0.066	-16
175	890923	1			-0.012	-19	0.066	-20
176	890923	1.3			-0.017	-29	0.066	-29
177	890923	3			-0.006	-9	0.037	-14
178	891004	16	-0.012	-0.011	-0.015	-31	0.150	-16
179	891004	16.3	-0.011	-0.009	-0.014	-52	0.150	-17
180	891004	19.3	-0.014	-0.009	-0.019	-56	0.150	-21
181	891004	20	-0.022	-0.015	-0.031	-58	0.150	-38
182	891004	20.3	-0.020	-0.015	-0.028	-59	0.150	-47
183	891004	21	-0.023	-0.016	-0.033	-58	0.150	-38
184	891004	21.3	-0.020	-0.012	-0.028	-59	0.150	-44
185	891004	22	-0.017	-0.008	-0.028	-58	0.150	-43
186	891004	22.3	-0.022	-0.005	-0.036	-58	0.150	-40
187	891004	23	-0.018	-0.005	-0.029	-59	0.150	-41
188	891004	23.3	-0.013	-0.003	-0.026	-59	0.150	-42
189	891005	0	-0.011		-0.021	-57	0.150	-28
190	891005	1	-0.013	0.008	-0.025	-58	0.150	-39
191	891005	1.3	-0.013		-0.023	-57	0.150	-34
192	891005	3	-0.012		-0.021	-58	0.150	-38
193	891005	3.3	-0.013		-0.024	-57	0.150	-34
194	891005	4	-0.012	-0.030	-0.023	-57	0.150	-29
195	891005	4.3	-0.014		-0.023	-57	0.150	-36
196	891005	5	-0.014	-0.023	-0.025	-56	0.150	-31
197	891005	5.3	-0.016	-0.037	-0.026	-53	0.110	-28
198	891006	3.3			-0.010	-51	0.062	-13
199	891006	4			-0.014	-26	0.061	-16
200	891006	4.3			-0.017	-38	0.061	-27
201	891006	5			-0.015	-57	0.061	-26
202	891006	5.3			-0.017	-55	0.066	-32
203	891006	6			-0.012	-31	0.066	-27
204	891006	6.3			-0.021	-13	0.066	-24
205	891007	1.3	-0.014	-0.012	-0.018	-32	0.062	-19
206	891008	3	-0.026	-0.038	-0.040	-53	0.045	-36
207	891008	3.3	-0.037		-0.050	-58	0.045	-46
208	891008	4	-0.041	-0.030	-0.057	-54	0.059	-64

B.4 Calibrations and accuracies KNMI instruments

K.N.M.I.

Instrumentele Afdeling

juni 1985

Termijnen van ijkingen	NAUWKEURIGHEID (±)	IJKTERMIJN
MAXIMUMTHERMOMETER	0.1 °C	2 JAAR
MINIMUMTHERMOMETER	0.1 °C	2 JAAR
STATIONSTHERMOMETER	0.1 °C	2 JAAR
ZEEWATERTHERMOMETER	0.1 °C	2 JAAR
KOELHUISTHERMOMETER	0.1 °C	2 JAAR
GRONDTHERMOMETER	0.1 °C	2 JAAR
PSYCHROTHERMOMETER	0.2 °C	2 JAAR
THERMOGRAAF	0.5 °C	1 JAAR
GRONDTHERMOGRAAF	0.5 °C	1 JAAR
HYGROGRAAF	6 % R.V	1 JAAR
ELEKTRISCHE HAARHYGROMETER	6 % R.V	1 JAAR
BAROGRAAF	1.0 mBar	2 JAAR
KWIKBAROMETER	0.2 mBar	3 JAAR
ANEROIDEBAROMETER	0.5 mBar	2 JAAR
DIGITALE ANEROIDEBAROMETER	0.3 mBar	1 JAAR
DIGITALE ANEROIDEBAROMETER (type noordzee)	0.3 mBar	1/2 JAAR
PLATINA WEERSTAND	0.1 °C	3 JAAR
CUP-ANEMOMETER	0.5 M/S	1 JAAR
PROPVAAN	W S 0.2 M/S, WR 0.5°	1/2 JAAR
REGENMETER	0.3 mm regen	1 JAAR
ROTRONIC VOCHTSENSOR	3 % R.V	1/2 JAAR
SOLARIMETER	1 % van de meetwaarde	2 JAAR
DIGITALE WINDVAAN	3 graden	1 JAAR
WINDVAAN		

De opgegeven nauwkeurigheden betreffen alléén het instrument zelf. Dit is dus niet de nauwkeurigheid van het totale meetsysteem. Fouten veroorzaakt door de opstelling (b.v. straling (bij temperatuur), wind (bij regen), cosinus (bij straling) of versterkers c.q. omzetters kunnen vele malen groter zijn.

Direct na ijking is de nauwkeurigheid van het instrument minimaal een faktor twee beter dan de opgegeven nauwkeurigheid. De ijktermijn is zo vastgesteld dat het instrument (bij gebruik van voorgeschreven opstelling en onderhoud) aan het eind van de ijktermijn nog aan de nauwkeurigheid voldoet.

Na verloop van de ijktermijn mag het instrument niet meer gebruikt worden.

HET HOOFD VAN HET IJKLABORATORIUM

(A. van Londen)

B.5 Official specifications sonic anemometer

SPECIFICATIONS

MODEL DA(T)-310 —— Probe TR-61A ——

ITEM		
Measuring Method		Time-sharing transmission/reception switchover type ultrasonic pulse emission.
Measuring Range		A, B, W axis 0 ~ ± 30 m/s
		Temperature* T : -10 ~ +40°C Fluctuation Temp.* T′: T_0 ~ ± 5°C (T_0 : Central Temperature)
Resolution		Wind speed 0.005 m/s Temperture* 0.025 °C
Accuracy		within ± 1 %
Number of Measurement Repetitions		approx. 20 /sec
Response		10 Hz
Coordinates Conversion	Input	Wind Speed Conponents A, B
	Operational Equation	$X = \frac{1}{\sqrt{3}}(A-B)$ $Y = A + B$
	Accuracy	within ± 1 %
Wind Speed Components Output	OUT 1	A, B, W 0 ~ ± 10m/s / 0 ~ ± 1V (Max. 8V)
	OUT 2	0 ~ ± F·S / 0 ~ ± 1V (Max. 10V)
	F·S	A, B : ± 5, ± 10, ± 25, ± 50 m/s
		W : ± 1, ± 2, ± 5, ± 10 m/s
Vector Synthesizer Circuit	Input	X, Y Wind Speed Conponents
	Operational Equation	U : $U = \sqrt{X^2+Y^2}$
		θ : $\theta = \tan^{-1}(X/Y)$
	Accuracy	U : within ± 1 % (for F·S)
		θ : within ± 5°
	Output	$U(\bar{U})$: 0 ~ F·S / 0 ~ 1V , F·S : 5, 10, 25, 50 m/s
		$\theta(\bar{\theta})$: 0 ~ 540° / 0 ~ 1V
Thermometer* Output	OUT 1	T -10 ~ +40°C / -0.2 ~ 0.8V
	OUT 2	T′ T_0 ~ ± 5°C / 0 ~ ± 1V
Output Impedance		Max. 1Ω or below (Max. 5mA)
Output Indicator		DC Voltmeter, Class 2.5 (±1V and 1V)
Output Connector		Front Panel: BNC connector, OUT1 and OUT2 (for X, Y, W, T), U($\bar{U}$), θ($\bar{\theta}$) Rear Panel : RM21TR-155, OUT1 (for X, Y, W, T), U($\bar{U}$), θ($\bar{\theta}$)
Caliblation Signal		-1V, 0V, +1V : OUT2, U, θ
Probe / Junction Box		TR-61A (Span 20cm) / QA-60A
Operating Temperature Range		Main Unit : 0 ~ 40°C / Probe, Junction Box : -10 ~ 50°C
Operating Humidity Range		40 ~ 85 %
Power Supply		AC 100/115/230V ± 10%, 50/60Hz

* DAT-310 only.

(NOTE) If a surface of Probe Head is covered with ice, It is not able to measure wind speed and temperature.

C.1 Literature

Batchelor, G.K., 1967, Introduction to fluid dynamics, Cambridge Univ.Press, U.K.

Beljaars, A.C.M., 1982, The derivation of fluxes from profiles in perturbed areas, Bound. Lay. Met., **24**, 35-55.

Beljaars, A.C.M., Schotanus, P., Nieuwstadt, F.T.M., 1983, Surface layer similarity under non-uniform fetch conditions, J.Clim. Appl. Met., **22**, 1800-1810.

Beljaars, A.C.M., Walmsley, J.L., Taylor, P.A., 1987, A mixed spectral finite-difference model for neutrally stratified boundary layer flow over roughness changes and topography, Bound. Lay. Met., **38**, 273-303.

Beljaars, A.C.M. 1988, The measurement of gustiness at routine wind stations. KNMI Scientific Report WR-88-05.

Bergström, H., 1988, A study of wind speed modification and internal boundary layer heights in a coastal region, Bound. Lay. Met., **42**, 313-335.

Bosveld F., Beljaars, A.C.M. 1987, Complex terrain effect on dry deposition. 16th Intern. Meeting on Air pollution modelling and its applications April 1987, Lindau. Also KNMI, FM-87-10.

Businger, J.A.,Wyngaard, J.C.,Izumi, Y.,Bradley, E.F. 1971, Flux profile relationships in the atmospheric boundary layer, J. Atm. Sci., **28**,181-189.

Businger, J.A.1973, Turbulent transfer in the atmospheric surface layer, Workshop on Micrometeorology, ed. D.A. Haugen, Am. Met. Soc., pp 67-100.

Businger,J.A. 1982, Equations and concepts. Chapt 1 in Atmospheric turbulence and air pollution modelling, (Nieuwstadt and van Dop, editors), Reidel Publ. Comp.

Carson, D.J., Richards, P.J.R. 1977, Modelling surface turbulent fluxes in stable conditions. Bound. Lay. Met., **14**, 67-81.

Cuijpers J.W.M. 1987, Vertical profiles of the structure parameter of refractive index and the structure parameter of temperature in the earth's atmosphere, KNMI Scientific Report WR 87-13.

Duchêne-Marrullaz, P., 1977, Full-scale measurements of atmospheric turbulence in a suburban area, Proc. 4th Int. Conf. on Wind effects on buildings and structures, Heathrow 1975,K.J. Eaton, ed.,Cambr. Univ. Pr. UK, pp 23-31

Dyer, A.J., 1974, A review of flux profile relationships. Bound. Lay. Met.,**7**, 363-372.

Finnigan, J.J., Einaudi, F. and Fua, D. 1984, The interaction between an internal gravity wave and turbulence in the stably stratified nocturnal boundary layer, J.Atm. Sc., **36**, 1041-1052.

Hanna, S.R., 1983, Lateral turbulence intensity and plume meandering during stable conditions, J. Clim. Appl. Met., **22**, 1424-1430.

Hicks, B.B., 1976, Wind profile relationships from the Wangara experiment, Quart. J. Roy. Met. Soc.,**102**, 535-551.

Hicks, B.B., 1981, An examination of turbulence statistics in the surface boundary

layer, Bound. Lay. Met., **21**, 389-402.

Högström, U. 1987, Non-dimensional wind and temperature profiles in the atmospheric surface layer: a re-evaluation, Bound. Lay. Met, **42**, 45-72

Holtslag, A.A.M., 1984, Estimates of diabatic windprofiles from near-surface weather observations, Bound. Lay. Met.,**29**, 225-250.

Horst, T.W., 1975, Spectral transfer for a three component sonic anemometer, Journ. Appl. Met., **12**,1072-1075.

Kaimal, J.C., Haugen, D.A., 1969, Some errors in the measurement of Reynolds stress, J.Appl. Met.,**8**, 460-462.

Kaimal, J.C., Wyngaard, J.C.,Izumi, Y., Coté, O.R., 1972 Spectral characteristics of surface-layer turbulence, Quart. J. Roy. Met. Soc., **98**, 590-603.

Kaimal, J.C., 1975, Sensors and techniques for direct measurement of turbulent fluxes and profiles in the surface layer. Atmospheric Technology **7**, 7-14.

Mackey, S., Ko, P.K.L., Spatial configuration of gusts, Proc. 4th Int. Conf. on Wind effects on buildings and structures, Heathrow 1975, 41-52.

Mason, P.J ., Derbyshire,S.H., 1990, Large eddy simulation of the stably stratified atmospheric boundary layer, Meteorological Office Bracknell, UK, unpublished document.

Monna, W.A.A., Driedonks, A.G.M., 1979, Experimental data on the dynamic properties of several propeller vanes, J.Appl. Met., **18**, 699-702.

Monna, W.A.A., Van der Vliet, J.G.,1987, Facilities for research and weather observations on the 213m tower at Cabauw and at remote locations, KNMI Scientific Report WR-87-5.

Monin, A.S.,Obukhov, A.M., 1954, Basic laws of turbulent mixing in the ground layer of the atmosphere, Trudy Geophys. Inst. Ak. Nauk SSSR, **24**, 163-187.

Nieuwstadt, F.T.M. 1984, The turbulent structure of the stable, nocturnal boundary layer, J. Atm. Sci., **41**, 2202-2216.

Obukhov, A.M. 1946, Turbulence in an atmosphere with inhomogeneous temperature, Trudy Ak. Nauk SSSR, **1**, 95-115. Translation: Bound. Lay. Met.,1971, **2**, 7-29.

Parry, H.D.,Sanders,M.J.,Jensen,H.P.1975, Operational applications of a pure acoustic sounding system, Journ. Atm. Phy., **14**, 67-77.

Peterson, E.W., 1969a, Modification of mean flow and turbulent energy by a change in surface roughness under conditions of neutral stability. Quart. J. Roy. Met. Soc.,**95**, 561-575.

Peterson, E.W., 1969b, On the relation between the shear stress and the velocity profile after a change in surface roughness, Journ. Atm. Sci., **26**,773-774, including comments by Bradshaw, P. and reply by Peterson, pp 1353-1355.

Pons, J.C., Pages, J.P. 1976, Utilisation d'un anémomètre sonique pour la mesure des fluxs turbulents dans l'atmosphère, La Météorologie, **sér. 6, no. 7**, 5-10.

Rayment, R., Readings,C.J.,1971, The importance of instrumental tilt on measurements of atmospheric turbulence, Quart. J. Roy. Met. Soc., **97**, 124-131.

Schotanus, P., 1982, Turbulente fluxen in inhomogene omstandigheden, KNMI,

W.R.82-3.

Slob,W., 1978,The accuracy of aspiration thermometers. KNMI Scientific Report WR-78-1.

Sorbjan, Z., 1986, On similarity in the atmospheric boundary layer, Bound. Lay. Met., **25**, 377-397.

Stull, R.B., 1988, An introduction to boundary layer meteorology, Kluwer Ac. Publishers, Dordrecht, The Netherlands.

Tatarski, V.I.,1961, Wave propagation in a turbulent medium, Dover Publications, New York.

Tennekes, H.,Lumley, J.L., 1972, A first course in turbulence, MIT-Press.USA.

Thorpe, A.J., Guymer, T.H., 1977, The nocturnal jet, Quart. J. Roy. Met. Soc., **103**, 633-653

Vliet, J.G. van der, 1981, De invloed van de mast en de uithouders op de windmeting in Cabauw, KNMI Scientific Report WR-81-4.

Wessels, H.R.A., 1984, Distortion of the wind field by the Cabauw meteorological tower, WMO Instruments and observing methods Report no.15, WMO Technical Conference, Noordwijkerhout, Netherlands , pp. 251-256.

Wieringa, J., 1973, Gust factors over open waters and built-up country. Bound. Lay. Met., **3**, 424-441.

Wieringa, J., 1980, A revaluation of the Kansas mast influence on measurements of stress and cup anemometer overspeeding, Bound. Lay. Met., **18**, 411-430.

Wieringa, J., 1982, Reply, Bound. Lay. Met., **22**, 251-255.

Wyngaard, J.C., 1973, On surface layer turbulence, Workshop on Micrometeorology, (ed. D.A. Haugen), Am. Met. Soc.,101-149.

Wyngaard, J.C., Businger, J.A., Larsen, S.E., 1982, Comments on "A revaluation of the Kansas mast influence on measurements of stress and cup anemometer overspeeding", Bound. Lay. Met., **22**, 245-250.

Zhang, S.F., Oncley, S. P., Businger, J.A., 1988, A critical evaluation of the von Karman constant from a new atmospheric layer experiment, 8th AMS Symposium on Turbulence and diffusion, San Diego, April 1988, prepr. pp. 148-150.

Zilitinkevitch, S.S. , Chalikov, D.V. 1968, Determining the universal wind-velocity and temperature profiles in the atmospheric boundary layer, Izv. Atm. & Oc. Physics, **4**, 294-302.